HELSINKI UNIVERSITY OF TECHNOLOGY
Department of Electrical and Communications Engineering
Laboratory of Acoustics and Audio Signal Processing

Janne Hautsalo

Study of Aurora Related Sound and Electric Field Effects

Master's Thesis submitted in partial fulfillment of the requirements for the degree of Master of Science in Technology.

Espoo, June 9, 2005

Supervisor:	Professor Unto K. Laine
Instructors:	Professor Unto K. Laine

HELSINKI UNIVERSITY OF TECHNOLOGY

ABSTRACT OF THE MASTER'S THESIS

Author:	Janne Hautsalo
Name of the thesis:	Study of Aurora Related Sound and Electric Field Effects
Date:	June 9, 2005 **Number of pages:** 99
Department:	Electrical and Communications Engineering
Professorship:	S-89
Supervisor:	Prof. Unto K. Laine
Instructor:	Prof. Unto K. Laine

Sounds that accompany intense auroral displays have been reported throughout history. Because there has been no instrumental evidence of the sounds, the idea that these sounds are the result of auroral processes has been questioned. At the same time, the research done on the observational material of the sounds has suggested that these sounds are real physical effects.

Infrasound produced by aurora has been registered by a number of research teams. However, the few attempts to record audible aurora related sounds have failed. The biggest reason for the failure is that a healthy human ear has been a more sensitive instrument for the detection of faint sounds than the recording technology of the past.

This thesis gives a review of the previous studies of aurora related sounds, which almost entirely deals with the observational reports. The results of the survey of aurora related sound reports by the public in Finland are presented, arranged as a co-operation between the Sodankylä Geophysical Observatory and Helsinki University of Technology. A measurement system for aurora related sound and electric field effects is introduced. The data collected by the introduced measurement set up is analyzed with the aid of statistical analyses.

The correlation results lend support to the previous findings on auroral infrasounds. In addition, in the geomagnetically most active part of the most interesting measurement, a correlation is found between the geomagnetic activity and acoustic power in audible frequencies when the geomagnetic data is delayed about 0–70 seconds with respect to the acoustic data.

Keywords: aurora related sounds, auroral sounds, geomagnetism, space weather, statistical data analysis, correlation, time series

TEKNILLINEN KORKEAKOULU DIPLOMITYÖN TIIVISTELMÄ

Tekijä:	Janne Hautsalo
Työn nimi:	Tutkielma revontuliin liittyvistä ääni- ja sähkökenttäilmiöistä
Päivämäärä:	9.6.2005 **Sivuja:** 99
Osasto:	Sähkö- ja tietoliikennetekniikka
Professuuri:	S-89
Työn valvoja:	Prof. Unto K. Laine
Työn ohjaaja:	Prof. Unto K. Laine

Voimakkaiden revontulimyrskyjen aikana on kautta historian tehty havaintoja ääni-ilmiöistä. Koska näitä ääniä ei ole kyetty tallentamaan, on ilmiön todenperäisyys kyseenalaistettu. Toisaalta ääni-ilmiöiden kuulijahavaintoja käsittelevä tutkimus on tullut siihen lopputulokseen, että kyseessä on luultavasti todellinen, fysikaalinen ilmiö.

Useat tutkimusryhmät ovat mitanneet revontulten aiheuttamia infraääniä, joita ihmiskorva ei kykene erottamaan. Harvat yritykset tallentaa kuultavaa ääntä ovat sen sijaan epäonnistuneet. Suurin yksittäinen syy epäonnistumisiin on se, että terve ihmiskorva on ollut yksinkertaisesti parempi väline hyvin heikkojen äänien rekisteröintiin kuin menneiden aikojen teknologia.

Tämä diplomityö luo katsauksen aikaisempaan revontuliin liittyvien ääni-ilmiöiden tutkimukseen, joka on lähes täysin perustunut kuulijahavaintoihin. Työssä käsitellään myös Sodankylän geofysiikan observatorion ja Teknillisen korkeakoulun yhteistyössä järjestämän kuulijahavaintotutkimuksen tuloksia. Lisäksi revontuliin liittyvien ääni- ja sähkökenttäilmiöiden mittaamista varten kehitetty laitteisto esitellään. Mittalaitteiston avulla mitattuja datoja tutkitaan tilastollisten analyysimenetelmien avulla.

Korrelaatiotulokset tukevat aikaisemmin mitattuja revontuliin liittyviä infraäänihavaintoja. Lisäksi mielenkiintoisimman äänitteen geomagneettisesti aktiivisimmassa jaksossa geomagneettinen aktiviteetti ja audiotaajuuksien ääniteho korreloivat, kun geomagneettista dataa on viivästetty suhteessa akustiseen dataan noin 0–70 sekuntia.

Avainsanat: revontuliin liittyvät ääni-ilmiöt, revontulten äänet, geomagnetismi, avaruussää, tilastollinen analyysi, korrelaatio, aikasarjat

Acknowledgements

This Master's thesis has been done for the Auroral Acoustics project in the Laboratory of Acoustics and Audio Signal Processing, Helsinki University of Technology. This thesis has been funded by the Research Foundation of Helsinki University of Technology and the Academy of Finland.

I want express my gratitude to Professor Unto K. Laine for his guidance and support throughout the work. Without his inspiration and enthusiasm for aurora related sounds, this thesis and the whole project would never have come into being. I especially want to thank him for providing me with all the data he has collected in his numerous measurements.

I wish to thank Professor Lauri Tarkkonen for giving some backup support with the statistical analyses. I would also like thank Ph.D. Esa Turunen and Mr. Antti Kero for their important co-operation.

The Finnish Meteorological Institute has provided the project team with vital weather and geomagnetic data. I especially want to thank Mr. Kari Pajunpää for his co-operation in terms of the geomagnetic field data.

Thanks are also addressed to Mr. Klaus A. J. Riederer who helped to measure the directivity pattern of the acoustic reflector. Special thanks belong to Ms. Delia Berrouard for giving me advice on writing in English.

I also want to thank my parents and whole family. Their support has been very important throughout my studies.

Finally, I would like to thank my beloved Laura for all the support and encouragement she has given me.

Otaniemi, June 9, 2005

Janne Hautsalo

Contents

Abbreviations

B & K	Brüel & Kjær
CME	Coronal Mass Ejection
DAT	Digital Audio Tape
DSP	Digital Signal Processing
ELF	Extremely Low Frequency
FMI	Finnish Meteorological Institute
FFT	Fast Fourier Transformation
HL	Hearing Level
HRTF	Head-Related Transfer Function
HUT	Helsinki University of Technology
LT	Local Time
RF	Radio Frequency
SGO	Sodankylä Geophysical Observatory
SD	Standard Deviation
SNR	Signal-to-Noise Ratio
SPL	Sound Pressure Level
UT	Universal Time
VLF	Very Low Frequency
WWW	World-Wide Web

List of Figures

List of Tables

Chapter 1

Introduction

Sounds that accompany intense auroral displays have been reported throughout history. Generally, these sounds have been described as hissing, swishing, rustling or crackling that rises and falls with the intensity of the aurora. Because there has been no instrumental evidence of the sounds, nor any decent analysis, the idea that the aurora related sounds are the result of auroral processes has always been questioned. It has been suggested that the neural system controlling human senses and consciousness could, for some reason or other, act misconceived during a geomagnetic storm, and thus produce these observations while, in the objective sense, there was no sound.

An attempt to record aurora related sound was made in Alaska in the 1960's. The inconclusive outcome of this study may have been one of the reasons why many auroral researchers have totally disclaimed the potential existence of aurora related sounds. The sounds have been considered as mere folklore or a perceptual artifact where one connects the sounds to the colours and visual movements of the aurora. The lack of time delay between the visual and auditory effects has led many scientist to doubt the physical reality of the sounds and to consider them psychological effects. On the other hand, there are some internationally respected auroral researchers among the large group of people who have made observations of aurora related sounds. Many scientists have remained convinced of the validity of reports on auroral sounds, rationalizing that they are rare and localized occurences.

While the attempts to record audible sound have failed, infrasounds (frequencies below 20 Hz, which are generally inaudible to the human ear) produced by aurorae have been registered by a number of research teams [14, 54, 68, 69]. The attenuation of sound caused by the atmosphere is considerably lower for low frequencies than for high frequencies. Therefore, the infrasonic packages sent by the aurora may travel to the ground level.

The mechanism producing aurora related sounds, i.e. the sound source, has remained a

mystery. In the literature there has been speculation of, e.g., brush discharges as potential sound sources [62]. This hypothesis is, however, insufficient to explain the phenomenon extensively. In the event that the sound is proven to be a real physical effect, the sound source should also be found.

During the last few decades, the measurement, storage and analysis methods of digital audio have developed enormously. In addition, portable computers and the development of the World-Wide Web (WWW) have enabled ever-increasing possibilities for real-time supervision of (tropospheric) weather, geomagnetic activity and space weather. For these reasons it was time to make a new attempt to store and analyze these aurora related sounds. Starting from this basis, a series of audio and electric field measurements were carried out during the years 2000–2004 by the Laboratory of Acoustics and Audio Signal Processing of Helsinki University of Technology (HUT), aiming at the successful recording of aurora related sounds.

This thesis introduces measurement and analysis procedures for aurora related sounds. Results obtained with the analysis procedures are presented. The measurement set up for recording aurora related acoustic and electric field signals is presented. In addition, the thesis makes a review of the previous studies on the topic. A look at the survey of aurora related sound reports carried out by the Sodankylä Geophysical Observatory (SGO) is also taken. This thesis does not commit itself to the possible production mechanisms of the sounds.

With the help of the obtained results, it is desired to gain preliminary knowledge as to whether the measured acoustic power correlates with geomagnetic disturbances.

In this thesis the term “aurora related sounds” is used instead of “auroral sounds”, the latter of which has generally been used in auroral research. It is somewhat clear that the sound source producing the audible sounds cannot be high in the altitudes of the visual aurora (80–300 km). With the power levels that exist in those heights, it is most unlikely that sound audible at ground level could be produced. The term “aurora related sounds” is used to emphasize the fact that we are dealing with sounds that exist during geomagnetic storms, but most likely do not originate from the visual aurora.

This thesis has ten chapters. Chapter 1 introduces the topic and takes a look at the aurora and aurora related sound in mythology, literature and the arts. A brief look at the previous studies and the short history of the Auroral Acoustics project of HUT is presented. Chapter 2 gives an overview of the characteristics of the observed aurora related sound events. Chapter 3 deals with the hypotheses that have been presented on aurora related sounds. Chapter 4 considers the different problems of this research. An overview of aurora and space weather is given in Chapter 5. Chapter 6 gives a review of some essentials of atmospheric acoustics and psychoacoustics. The results of the survey of aurora related sound

reports are presented in Chapter 7. Chapter 8 introduces the developed measurement system and Chapter 9 analyzes the measurement data. The thesis is finally concluded in Chapter 10.

1.1 Historical Perspective and Previous Studies

Northern lights have been a source of myths and folklore that originate from ancient times. Actually, the Finnish word for the aurora, *revontuli* (i.e. fox fire), has its origin in a myth which explains that northern lights are given birth by a fire fox striking fire with its tail.

Aurorae have usually been associated with the supernatural and they have awakened strong emotions, even fear, among people. Often the aurorae have been considered as a bad omen, predicting war, disaster or plague.

Inhabitants of the west coast of Norway used to believe that the northern lights were "old maids" dancing and waving white gloved hands. Connections between the aurora and old women were common in Finland, too, where it was believed that the northern lights were "old women of the North hovering in the air". [13]

Among the Inuit in Greenland and the Hudson Bay area, the northern lights were the realm of the dead. The Greenlander Inuit believed that a flickering northern light signified that their dead friends were trying to contact surviving relatives. The Greenlanders respected the northern lights deeply and therefore avoided making fun of them. The same kind of connections between aurora and unborn and departed souls are found in ancient China and some Siberian tribes. Another widespread belief among the Inuit tribes was that the aurorae were spirits playing football with a walrus skull. [13, 20, 22]

There exist attempts to explain aurora with more scientific basis, such as the interpretations that the aurorae were reflections from far-off locations. E.g. in Norway it was believed that the aurorae were reflections of shoals of silver herring in distant oceans, or icebergs in the North Atlantic. Some Sámi people believed that the aurorae were simply "thunderstorms" of the winter [20]. This is interesting, for this characterization could also refer to the presence of an elecric type of sound.

The aurora seems to have inspired many of the wise men of history. Even Aristotle (384–322 BC) most likely witnessed some auroral displays, although they are very rare in Mediterranean countries. Aristotle's science had four elements: fire, air, water, and earth. He described in his *Meterologica* how a vapor caused by the sun rises from the earth and collides with the element fire, which then bursts into flames producing an aurora. [20, 22]

In older times it was a fairly world-wide belief that the aurora was some kind of fire. Our ancestors in Nordic countries believed that the northern lights were active volcanoes in the far north placed there by the God to light up and heat the dark and cold parts of the country.

Even the world-famous scientist Anders Celsius noted in his diary on September 24$^{\text{th}}$, 1732 that the aurora was caused by active volcanoes close to the North Pole. [13]

Though the present scientific knowledge of the aurora is able to explain the phenomenon, some myths still live among the residents of the Arctic. One of these myths is that one can communicate with the aurora by whistling. It is believed that by whistling to the aurora, one could accelerate its motion. The Greenlander Inuit believed that one could even receive a rustling sound from an aurora, meaning that contact had been established with their dead friends. This brings the aspect of aurora related sound to the picture. In the survey of aurora related sound observations arranged by SGO (further discussed in Chapter 7) eight people reported that whistling had affected the aurora [37]. Though the real scientific validity of observations like this may not be high, the folklore and myths of the aurora form an interesting foundation of material for the study of cultures and people throughout history.

1.1.1 Aurora Related Sounds in Literature and Arts

International literature provides many potential references to aurora related sounds. It has been suggested that the earliest reference to aurora related sound is found in *Germania*, written by the Roman historian Tacitus (55-117 AD):

> Beyond them is another sea, calm even to stagnation by which the circle of the earth is believed to be surrounded and confined; because the last gleam of the setting sun lingers till he rises again, and so brightly that it dims the stars. It is believed too that a sound is heard, that the forms of gods and rays from a head are seen. [13]

Eather [20] says that a number of references in Norwegian sagas to the song of the Valkyries could be interpreted as referring to auroral sounds. The aurora was explained as a flickering light from their armor as they rode through the skies.

Perhaps the best known assumed biblical description of aurora is found in The Old Testament's Book of Ezekiel (1:22-24), which also has a potential reference to aurora related sounds. The sound is compared to the "noise of great waters":

> 22. And the likeness of the firmament upon the heads of the living creature was as the colour of the terrible crystal, stretched forth over their heads above. 23. And under the firmament were their wings straight, the one toward the other: every one had two, which covered on this side, and every one had two, which covered on that side, their bodies. 24. And when they went, I heard the noise of their wings, like the noise of great waters, as the voice of the Almighty, the voice of speech, as the noise of an host: when they stood, they let down their wings. [11]

A number of poets have expressed the sounds of aurora. The British poet William Wordsworth (1770–1850) describes the aurora and its sound in his poem *The Complaint of a Forsaken Indian Woman*, composed in 1798:

> In sleep I heard the northern gleams;
> The stars, they were among my dreams;
> In rustling conflict through the skies,
> I heard, I saw the flashes drive,
> And yet they are upon my eyes,
> And yet I am alive;
> Before I see another day,
> Oh let my body die away! [62]

Those who are interested may find more poetry where aurora related sounds have been described, for example in [20] and [62].

1.1.2 Previous Studies of Aurora Related Sounds

One of the most eager pioneers of the research of aurora related sounds was Dr. C. A. Chant, Professor of Astronomy at the University of Toronto. Chant wrote a number of articles on aurora related sound (some of which are used as reference for this work) mostly to the Journal of Royal Astronomical Society of Canada. Keay has written a biographical article [30] on Chant's work. Chant concluded that probably the best evidence in favor of aurora related sounds was that practically all observers who had heard them described them in the same way.

The most comprehensive document on the topic has been written by Silverman and Tuan [62]. Their work, *Auroral Audibility*, was published in *Advances of Geophysics* in 1973. Auroral Audibility includes almost 200 anecdotal reports of aurora related sounds collected from different sources around the world. The observation reports typically came from people who spent much of their time outdoors. The range of people giving the reports varied from native people to internationally respected auroral researchers. With the help of the reports, Silverman and Tuan presented some hypotheses considering potential sound production mechanisms, concluding that the most likely source is brush discharge.

The research of aurora related sounds has been almost entirely based on observational reports. An exception to this was a series of experiments that were carried out at the Geographical Institute, University of Alaska in 1962–1964 in order to record aurora related sounds. However, the attempts failed to provide conclusive results which may have been due to the fact that the experiments were carried out too close to a sunspot minimum [62]. In addition, the analog audio technology used in the experiment was of much lower quality

than the present-day digital technology.

While the attempts to record audible aurora related sound have failed, the measurements of infrasound have resulted in positive evidence. In 1969, Wilson [69] reported regular arctic observations of infrasounds recorded with low-frequency microbarographs (0.001–1 Hz). In 1971, Procunier [54] showed that acoustic events in the frequency range of 1–16 Hz are correlated with disturbed geomagnetic conditions and optical aurora. These observations of acoustic events were made with the aid of Helmholtz resonators.

The lack of scientific literature in the field of auroral acoustics gives a good picture of the difficulties of the research. These difficulties are considered in detail in Chapter 4. It is also worth noting that the nature of the research is interdisciplinary, which makes it difficult for a scientist specializing in a certain field to master all the available tools of research. Very few of the researchers dealing with the topic have had a background in acoustics, psychoacoustics, electroacoustics, or Digital Signal Processing (DSP). This may have led to some unrealistic conclusions regarding this potentially objective phenomenon [41].

1.2 The Auroral Acoustics Project at HUT

The Auroral Acoustics Project kicked off on December 1999 as researchers of the SGO were contacted by Professor Unto K. Laine. This led to active co-operation between HUT and the SGO. The development of methodology and instrumentation as well as the active collection of sound material was started. On February 21–25, 2000 a series of preliminary recordings were carried out in the Sodankylä region of Finland. Parallel to acoustic measurements, Very Low Frequency (VLF) radio signals were recorded.

As another preliminary step, a survey of observations of aurora related sounds was started at the SGO in order to gain background information for acoustic measurements.

An unpredictably strong geomagnetic storm took place on April 6–7, 2000 as the measurement system was still under development. Due to lack of preparation time, audio recordings had to be performed with a non-professional *ad hoc* setup. The results were encouraging and gave motivation to develop a better measurement system and further study the phenomenon. One of the references [41] takes a closer look at this particular measurement.

The developed measurement set up included a highly sensitive, low-noise microphone that was placed to the focus of a parabolic reflector, and a simple VLF receiver. With the help of simultaneously digitized acoustic and VLF signals it was desired to gain knowledge of possible connections between sounds and local fluctuations of electric field.

A large amount of data was collected with the measurement system in Finland during geomagnetic storms as well as in geomagnetically normal conditions since 2000. The years

2000–2002 fall into a maximum of the solar cycle where the possibility of strong geomagnetic disturbances is highest. Because this cycle is approximately 11 years long, with the exception of some isolated events, we will have to wait until 2011 for the next maximum.

It should be remarked that the work has not only included the analyses, but also the development of the methodology. Because the phenomenon is unknown, it is not perfectly clear what should be searched for and what is the best way to do this.

According to the present knowledge the most interesting measurement up to the date of this thesis was made on April 11–12, 2001. The place of measurement was at Lake Pielinen in Eastern Finland, close to Koli hill. This measurement resulted in the first international report written under the project [42].

Generally speaking, it is very difficult to get scientifically valid proof of the connections between acoustic phenomena and simultaneous geomagnetic processes or atmospheric electricity. As we are dealing with an occasional phenomenon which is dependent on sunspot cycles and all the weather parameters, it is clear that sheer luck (as it is commented in Chapter 4) is also a factor in achieving measurements of good quality.

More information of the Auroral Acoustics project can be found on the project web page [1].

Chapter 2

Characteristics of Aurora Related Sounds

This chapter summarizes some characteristics of observed aurora related sounds. The chapter is mostly based on the work of Silverman and Tuan [62] where observation reports from various sources around the world are considered.

2.1 General Descriptions of Aurora Related Sounds

Aurora related sounds have usually been described as faint hissing, swishing, rustling or crackling, i.e. the descriptions have been *onomatopoetic*[1]. Often the sounds have been compared to some well-known sound source. E.g. characterizations such as "swishing of silk" [9], “wrinkling of aluminium foil” and “rippling of a distant river or waterfall” [13] have been used. Though the range of different descriptions is wide, they have often been very similar in terms of the nature of the sound. About 38% of the observations gathered by Silverman and Tuan [62] fell into the category of hissing and swishing, 30% into rustling and crackling, and the remaining 32% to the other types of sounds [37].

Typically, aurora related sounds are heard simultaneously with the visual observation of the aurorae [43, 62]. Many researchers have used the adjective “anomalous” when speaking of aurora related sounds. Particularly, the impression that there seems to be no delay between the visual observation and the sound has led to the usage of this adjective.

[1] The term “onomatopoetic” refers to the formation or use of words such as “buzz” or “murmur” that imitate the sounds associated with the objects or actions they refer to [2].

2.2 Characteristics of the Audible Aurora

A common feature that can be found in many observation reports is that the sounds are associated with rapidly moving forms of aurora. In almost all cases considered by Silverman and Tuan [62] the visual movements of the aurora and the sounds were said to occur simultaneously.

Often the sound was associated with the localized aspects of the aurora: streamers, flashes or rays. Many descriptions also associated the sounds with either the intensity variation or general movement of the aurora. [62]

2.3 Frequency of Occurrence

It seems rather obvious that aurora related sounds are heard only rarely. A number of logical reasons for this can be deduced.

The first consideration is that all auroral activity is dependent upon the activity of the sun. This activity goes in cycles of 11 years. The hearing of aurora related sounds is also dependent on this 11-year sunspot cycle experiencing periods of low and high activity.

The second consideration is that it has been estimated that only a fraction of the brilliant displays give rise to audible sounds [62]. This is natural because the weather conditions at the moment of auroral activity and type of the location where the observation is made play a dominant role in determining whether there is, in general, a possibility to hear faint sounds. A still environment with a minimal amount of natural and man-made noise is a prerequisite.

The third consideration deals with the possible differences in acuteness of hearing. There is a considerable range in the ability of persons with "normal" hearing to detect faint sounds of high pitch (see Chapter 6). It might be, therefore, that an observer with normal hearing would be incapable of hearing the sound produced by aurora on ordinary occasions, but could hear it when it was unusually intense. [7]

2.4 Weather

Silverman and Tuan [62] summarized that the most common condition for auroral sounds seemed to be that of a still, clear night. The most common statements in the reports were that the night was still or calm, with only one report mentioning a breeze.

Another common statement was that the night was clear or bright. The most common observation other than these was that the night was cold with temperatures ranging to as low as $-45°$C. However, there were a number of observations on summer nights or otherwise mild nights. [62]

2.5 Localization of the Phenomenon

Localization, or the spacial extent, of the phenomenon is not known. Silverman and Tuan [62] reported, based on very scarce information, that there seemed to be some indication that the effect occurs on a scale of kilometers or less. However, this estimate should be treated with great caution.

2.6 Association with Odor

According to Silverman and Tuan [62], a few reports noted the presence of an odor at the time of an auroral display, described as either a strong smell of sulphur or ozone. They mentioned that it seemed an odor could accompany an auroral display, possibly even when sounds are not present. Odors of sulphur and ozone have also been reported by Lamar and Romig at meteor entries [45] (see section 2.7).

2.7 Sounds from Lightning and Meteors

Sound similar to aurora related sounds have been reported as an instantaneous accompaniment of both lightning and meteors. For instance, Lamar and Romig [45] have reported observations of sounds and electromagnetic effects associated with meteors.

A distinctive characteristic of both lightning and meteor sound reports is that the lag between the visual observation and the sound has been reported to be remarkably shorter than what it should be in the case of direct transmission of sound. [62]

According to Keay's hypothesis [31, 32, 33, 34], light given off by a meteor's trail is accompanied by VLF radio waves. These waves can then be transformed into acoustic vibration via objects around the listener, acting as "transducers". This hypothesis, called "electrophonics", is studied in more detail in section 3.2 of Chapter 3. Additionally, Keay refers to measured ELF/VLF emissions associated with earthquakes and proposes electrophonics could also explain why many animals become unusually upset before an earthquake [32, 33].

2.8 Miscellaneous

Silverman and Tuan [62] leave open the question of the effects of altitude and terrain on the audibility of the aurora, though a number of their reports gave an impression that audibility may be more prevalent at higher altitudes.

Sometimes aurora related sound have been reported to accompany a phenomenon called

”low aurora”. Low aurora refers to an aurora that is seen exceptionally low, from ground level to perhaps cloud heights. In at least twenty reports gathered by Silverman and Tuan [62] low aurora was mentioned. The low aurora is a controversial phenomenon and a number of explanations for it have been presented. The references [7], [8] and [9] deal with aurora related sound and low aurora more closely.

Some reports of Silverman and Tuan [62] note effects on dogs. The reactions of dogs in all of the cases were related to emotions of fear and uneasiness. None of the reports noted effects on other animals.

Chapter 3

Hypotheses of Aurora Related Sounds

A number of hypotheses on the sound production mechanism of aurora related sounds have been presented, many of which have been covered by Silverman and Tuan [62]. This chapter gives a review of the most important hypotheses.

3.1 Brush Discharge

Silverman and Tuan [62] concluded that the most likely source of aurora related sounds seems to be brush discharge, and that these are generated by aurorally associated electric fields. They also stated that the quality of the sounds suggests some kind of electrostatic discharge and, therefore, supports this hypothesis.

Brush discharge is the occurrence of discharge from point electrodes where very sharp potential gradient exist. The local potential gradient can be increased by an irregularity on the Earth's surface such as an isolated tree or a mountain, by lowered air density as the altitude is increased, by dust, by fog, and by induction from clouds with active internal circulation. [62]

The brush discharge can produce a rustling or hissing sound, light (generally purple in color) near the ground, and can make light, slender objects such as hair stand on end [62]. The smell of ozone or sulphur that has been reported to accompany the sounds on rare occasions seems to support the brush discharge hypothesis. Lamar and Romig [45] also note that an occasional smell of ozone as well as electromagnetic disturbances associated with meteor entries suggest that a local corona discharge is responsible for hissing noises.

There are some references from as early as the 1930's [7, 8, 9, 15] that suggested brush discharges as sound production mechanisms. However, it was not until 1946 electric field

measurements indicating sufficiently large values for production of brush discharges were first reported by Olson [52].

The normal average electric field on the Earth's surface over open ground is about 100 V/m which is insufficient to cause discharge. Silverman and Tuan refer to the work of Olson [52] where it has been shown that during auroral corona (i.e. a spectacular form of aurora where all rays of aurora seem to converge to a point) this field can rise to very high values (close to 10 kV/m) which are sufficient to cause discharge.

According to Silverman and Tuan [62], aurorally associated electric fields are most likely produced by a space charge possibly resulting from ionization by hard X-rays which have themselves been produced at higher altitudes by the impact of energetic particles.

3.2 Electrophonics

A hypothesis called "electrophonics" has been proposed by Keay [30, 31, 32, 34]. Most of his work deals with meteor sounds but he says aurora related sounds are produced the same way. This hypothesis is based on objects in close proximity to the observer, acting as "transducers" to make the conversion of electromagnetic radiation into acoustic waves. These transducers are objects that act as loudspeakers, converting electromagnetic signals into audible vibrations. According to Keay, e.g. aluminium foil, thin wires, pine needles or dry, frizzy hair all respond to a VLF field. The radio waves induce small charges in such objects, and these charges force the object to vibrate in time with the oscillating waves, effectively making them act like the diaphragm in a loudspeaker.

Keay says that the plasma trail of a large fireball, or bolide, generates the required ELF or VLF emissions. He notes it has been shown that large fireballs generate radiation in the ELF/VLF region [31]. Similarly, very low-frequency hissing from aurora has been registered by a number of research groups [48, 60].

Keay [30] suggests that if the VLF amplitude is sufficient, the combination of a high electric field modulated by a substantial audio frequency component would have the required properties to excite an acoustic response from naturally present objects by a straightforward transduction process. Keay notes that a brush discharge could explain the crackling and some of the higher frequency components of the auroral sounds, but the hissing and swishing sounds are more akin to the VLF hiss associated with aurora.

The electrophonics hypothesis has been criticized because a meteor or aurora can hardly produce electromagnetic power of the scope needed to produce audible sound. Keay's work inspired Silverman and Tuan to further study this particular hypothesis. They conclude with D. Y. Wang [67] that the intensity of VLF emission required for the production of anomalous sounds necessitates unreasonably high currents.

3.3 Psychological Explanation

A psychological explanation is based on the assumption that people tend to hear what they expect to hear, even when the sound is absent in reality. It has been argued that the close connection between the senses of hearing and seeing would lead to an expectation of sound in a vivid auroral display, and the mind would then provide this. The involuntary physical experience of a cross-modal association is generally called *synesthesia* [17]. Silverman and Tuan [62] state that if the psychological explanation were real, one would expect a greater frequency of reports. Furthermore, most observers have noted sound only rarely. If the psychological explanation were correct, it would be expected that these observers would have heard the sounds almost always.

A number of instances have been reported where the aurora was not visible at the moment of hearing the sounds [7, 9, 38, 62]. Naturally, the psychological theory is in contradiction with these reports.

3.4 Direct Transmission of Audible Sound

Almost all auroras occur at heights greater than 80 km, typically around 100 km [23]. An altitude of 60 km can be considered the lowest possible for occurence of aurora [62]. Attenuation of high-frequency sounds is in general much higher than that of low-frequency sounds. Silverman and Tuan [62] refer to the work of Procunier and Sharp [55], saying that even if the inverse square attenuation of sound is neglected, the highest frequency which will allow 0.1% of the initial energy to be transmitted to the ground level from a height of about 60 km is only about 40 Hz.

Also, if the sound were in fact produced at heights of 60 km or higher, then a lag of several minutes would occur between sight and sound. Because almost all observers have reported that the visual movements and the sound occur simultaneously, this explanation appears unlikely.

3.5 Human Auditory Response to Electromagnetic Radiation

It has been reported by Frey [24] that the human auditory system could respond directly to electromagnetic radiation in the frequency range from at least 425 to about 3000 MHz. The sound has been described as a buzz, clicking, hiss, or knocking.

It is known that aurorae occasionally produce radio noise in the radio frequency (RF) region. According to Frey [24], the minimal average power density that could lead to auditory response is 400 μW/cm^2. However, the example considered by Silverman and Tuan

[62] led to a conclusion that the energy density caused by the aurorae could only be of the order of 10^{-17} W/cm^2 at its extreme.

Response of the human auditory system to electromagnetic radiation is linked to a phenomenon called the "Hum", described as unidentified low-frequency humming. The Hum has been described as "an idling Diesel" engine or "the drone of a distant aircraft". It is believed that the Hum is caused by pulsed radio waves. It is reported that approximately 5% of the population "hear" the Hum. Almost all are aged 50 or over, and 70% of these are women. It is claimed that there is a positive link between the pulsed signals and the perceived Hum. [10, 19]

3.6 Catalyzation by Infrasounds

Wind higher up in the atmosphere is approximately laminar and it does not produce much noise. The constant velocity layers are parallel to the ground. Laine [41] has proposed that a strong infrasound package "shooting" through these layers might cause "noisy" turbulence. Thus, the sound source could be purely flow mechanical.

Another hypothesis related to infrasound put forward by Laine [41] states that there might be a possibility that a strong geomagnetic field could ionize the air. Through this or some other mechanism, ionized clouds of opposite charges in the atmosphere could form. A strong infrasound wave package shooting through these clouds might activate discharging mechanisms, and acoustic noise would be produced.

3.7 Miscellaneous

The sudden presence of an electric field in the atmosphere polarizes the air molecules. Work done on the molecules by the electric field produces an increase in pressure which can be detected if the field is sufficiently strong. Silverman and Tuan [62] considered whether this could produce audible sound. They said that the electric field change required to produce audible sound is something like 1.9×10^6 V/m which is far too large when compared with most observed values at distances of a few kilometers.

Silverman and Tuan [62] additionally considered the possibility that the VLF hiss produced by aurora could be converted into pressure variation at the ear. They concluded that the average electric field intensities (recorded by Martin *et al.* [48]) are not large enough to produce audible sound.

Chapter 4

The Problem

The work of Silverman and Tuan [62] led to a conclusion that observational evidence speaks for the reality of aurora related sound, and that the most probable sound production mechanism is brush discharge.

The primary goal of the Auroral Acoustics project of HUT and the SGO is to determine whether further evidence for the existence of aurora related sounds can be found by means of recorded acoustic, electric field and geomagnetic field signals.

The aim of this chapter is to present the goals of the project and to give an overview of the methodological problems that have been faced.

4.1 The Goals of the Project

The basic research problem of Auroral Acoustics project at HUT has been presented by Laine [41]. The primary question is: "Are aurora related sounds a real physical effect or are they just perceptual artifacts or malfunctions?" If current and new evidence speaks for true physical sounds, the next question is: "What is their nature and how are they produced?"

It is known that the structure of sound may reveal its production mechanism. This is another motivation for us to try to capture these sounds for closer analysis. [41]

The aim of this thesis is essentially to study the first question. Because there are already some instrumental observations of the aurora related sound effects in the infrasound region, our primary interest is focused on audible sound.

4.2 Methodological Problems

Since there is a lack of previous work using recorded audio data in the field of this study, the development of the whole methodology has been an essential part of the research. These

methodological problems are now considered. This section is mostly cited from [40].

In general terms the problems that have been faced during the development of the methodology may be listed as follows:

- Forecasting nights with auroral activity.
- Forecasting weather conditions (e.g. wind and cloudiness) close to the location of the measurement.
- Search of locations with least amount of ambient noise (as high signal-to-noise ratio (SNR) as possible).
- Development of portable measurement equipment with high sensitivity and low noise level.
- Synchronization of acoustic and electric field measurements to geomagnetic measurements.
- Simultaneous measurement of local electric field signals.
- Analysis of the measurements. [40]

Since we are dealing with a phenomenon that is totally dependent on the aurora, we need to have ways to find out the timing of possible aurora occurrences. Forecasting the aurora is based on the follow-up of sunspots and the flares in their vicinity, coronal mass ejections (CMEs), and coronal holes. Real time satellite data of these processes is collected by several satellites located between the Earth and the Sun and it is provided on the WWW. When an Earth-directed CME shockwave is observed in a coronagraph, it takes from one to four days before the wave can be measured by a satellite traveling in the vicinity of the point of minimum gravity of the Earth and Sun. From this specific location the wave reaches the Earth in less than an hour. However, it is very difficult to forecast which of the CMEs are truly geoeffective. [40]

One might consider the possibility of recording sound constantly but this has a number of drawbacks. Firstly, this would result in measureless amounts of data. Secondly, the automatic recording of audio data has the problem that some events may be difficult to identify from the data afterwards, unless the recording session has been under human supervision. Particularly at the beginning of the research project, it is important for a scientist to become familiar with the soundscapes of the recordings. Also, maintenance of this kind of system would be difficult, and undoubtedly the system would be unfavourable in terms of the expenses. Constant recording of sound could, however, be used in future work if there are more resources.

Besides the space weather, we are interested in the weather on the Earth. It is desirable that the wind is still and the sky is clear. The supervision of weather can most easily be performed via the WWW.

Finding a silent location for the measurement is difficult, especially in Southern Finland where ambient noise is a big problem. It is difficult to foretell just by relying on a map whether a certain location is silent. Motorboats in the summer, and snowmobiles in the winter, often cause undesirable noise. Air traffic is a problem year-round, and nature and animals are sound sources. Therefore, merely the avoidance of places with dense human settlement is not a solution to this problem. Additionally, the place should be on open ground where there are no trees in the vicinity. The tops of pine and spruce trees produce sound even when the wind is only light, as well as deciduous forest in the summer. [40]

One of the mysteries of aurora related sounds is that, although there is a large amount of observations, no one has ever managed to record these sounds objectively. If we compare recording techniques of past decades with human hearing we notice that this is not at all surprising. The scale for measuring the sound pressure level (SPL) is such that 0 dB corresponds to the hearing threshold (around 1 kHz) of a person with normal hearing. With a studio-microphone of good quality, the sensitivity is about 17–20 dB. Even with many typical measurement microphones, the sensitivity is not better than 12–20 dB. Thus, a healthy human ear is able to detect sounds that a microphone of a fairly good quality cannot register. Furthermore, it should be noted that the technology used in earlier attempts to record aurora related sounds has mostly been analog. This has increased the amount of white noise even more [40]. During the last couple of decades electronics and digital audio technology have developed enormously, giving us better abilities to record and store faint sounds. The measurement system developed for this project is presented in Chapter 8.

Considering we have managed to capture aurora related sound material on a DAT tape, the next problem is to find a procedure for the analysis of the data. It is very difficult to point out events that are the best candidates for aurora related sounds from the large amount of data and identify the proper scientific methods to show or even prove that these particular sounds cannot belong to any of the known ambient sounds. Nevertheless, it may be thought that such pinpointing of sound events is of secondary interest and, instead, utilize the whole data by performing basic statistical analyses. The analyses of the measurements are covered in Chapter 9.

To summarize, the hunt for aurora related sounds is anything but an easy task. First, the measurements have to be focused on the high-activity part of a sunspot cycle. The reseacher is required to constantly keep an eye on solar forecasts and be ready for a measurement trip whenever there is a possibility for a geomagnetic storm to arise. Next, the weather conditions need to be checked. If it is clear and calm, the conditions are favorable. In

the event of rainy or windy weather the measurements must either be given up entirely or carried out despite the fact that the recorded sound material may become mostly useless due to the excessive noise of wind and rain. Finally, we have to move to the site of the measurement (which has been selected beforehand) and set up the measurement system. A typical measurement by HUT has lasted from three to six hours and it has been timed to take place somewhere between 9 PM and 3 AM local time (LT). This means unenviable working hours for the researcher performing the measurements.

Chapter 5

Aurora and Space Weather

Aurora is a consequence of strong geomagnetic disturbances called *geomagnetic storms*. These perturbations are caused by bursts of particles carried by the *solar wind*. As these particles collide with molecules in the Earth's higher atmosphere, a visual phenomenon that we call aurora or "northern lights" is born.

The origin of the aurora is 149 million kilometers from Earth at the Sun. In addition to electromagnetic radiation, the Sun gives off particles. These energetic charged particles are carried out into space along with the solar wind. This wind sweeps toward Earth through interplanetary space at speeds ranging from 300 to 1000 kilometers per second, carrying with it the solar magnetic field. The solar wind is not a stable flow of particles — it has major fluctuations. The greatest factor affecting the amount and durations of these fluctuations is variation in the activity of the Sun. [16, 23]

The magnetic field, extending into space as the magnetosphere, acts as a barrier protecting the Earth from the energetic particles and radiation of the hot solar wind. Electrons are deflected around the Earth by the magnetosphere, but some get trapped. Part of these trapped electrons are accelerated along the magnetic field lines towards the polar regions and then strike the atmosphere to form the aurora. Figure 5.1 illustrates the interaction of the solar wind and the Earth's magnetosphere. The electrons, which stream down the magnetic field of the Earth, reach the neutral atmosphere in a rough circle called the *auroral oval*. This circle is centered over the magnetic pole and is around 3000 kilometers in diameter during quiet times. The circle grows larger when the magnetosphere is disturbed. The location of the auroral oval is generally found between 60 and 70 degrees north and south latitude. [16]

The visual aurora is caused by the interaction of high-energy particles (usually electrons) with atoms and molecules in the Earth's upper atmosphere. Through collision, these high-energy particles can "excite" valence electrons that are bound to neutral atoms. The excited

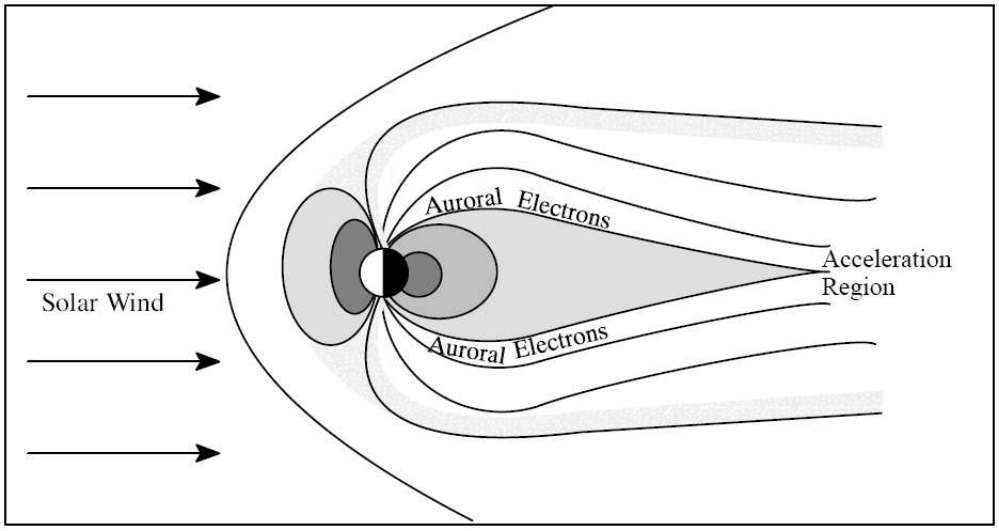

Figure 5.1: Some of the important regions of the magnetosphere. [16]

electrons can then return to their initial, lower energy state, and in the process release photons (light particles). Different colours are due to the electrons of different atoms, and different energy states within the atoms being excited. [16]

Auroral features come in many shapes and sizes. Tall arcs and rays start 100 kilometers above the Earth's surface and extend upward along its magnetic field for hundreds of kilometers. Most of the aurora features are greenish yellow but sometimes tall rays will turn red at their tops and along the lower edges. [16]

The Sun is a highly active star that changes on time scales of hours to hundreds of years. The interplanetary magnetic field direction as well as solar wind speed and density are affected by the activity of the Sun. They can change drastically and influence the geomagnetic activity. As geomagnetic activity increases, the southern edge of the aurora borealis moves to lower latitudes. Similarly, solar mass ejections coincide with larger auroral ovals. If the interplanetary magnetic field is in the opposite direction of the Earth's magnetic field, there can be increased energy flow into the magnetosphere and thus, increased energy flow into the polar regions of the Earth. This will result in an intensification of the auroral displays. [16]

Geomagnetic activity can be divided into two main categories: storms and substorms. The storms are most directly related to specific solar wind events, while the substorm activity is more complicated because of the temporal storing of energy in the magnetotail. The magnetic storms are known to be due to two main reasons: the coronal mass ejections (CMEs) and coronal holes that cause fast solar wind streams. These storms are typically

non-reoccurrent and transient. The largest storms are related to CMEs. The development of a geomagnetic storm can be monitored by an hourly Dst index. [51]

The substorm is the most common cause of auroral displays in auroral latitudes. The substorm process has its origin in the Earth's magnetosphere and, thus, it is often called a *magnetopheric substorm*. A magnetospheric substorm is a very complicated phenomenon that is not yet fully understood. [51]

5.1 Geomagnetic Field and Its Measurement

The Earth has a magnetic field, which to a large extent, can be described as a dipole. The geomagnetic field is a vector quantity and it is presented in X-, Y-, and Z-components. The X-component points to the true geographic North, Y to East and Z down to the center of the Earth. In Finland the field is directed almost perpendicularly downwards and thus the Z-component is much larger that the X- and Y-components. The geomagnetic field can be measured with instruments called magnetometers. Data from many magnetometers allow observers to track the current state of the geomagnetic conditions. The strength of the geomagnetic field in Finland is about 51 000 nT. Figure 5.2 gives an example of geomagnetic field data measured in Nurmijärvi, Finland. [3]

Electric currents flowing in the upper atmosphere cause continuous variability in the geomagnetic field. During auroral periods, the strongest currents flow in the east-west direction causing variation. This is especially so in the geomagnetic X-component which typically decreases. At its strongest, the aurora may cause disturbances of over 1000 nT in the magnetic field. [3]

The disturbed state of the magnetic field is often described by converting the magnetometer data into the form of three hourly indices which give a quantitative measure of the level of geomagnetic activity. One such index is the K-index. The K-index value ranges from 0 to 9. It is directly related to the amount of fluctuation, relative to a quiet day, in the geomagnetic field over a three-hour interval. The higher the K-index value, the more likely it is that an aurora will occur. The relationship between the maximum fluctuation of the geomagnetic field and the K-index is nonlinear. At low K-index values, a smaller amount of increase in the maximum fluctuation is needed to raise the K-index by one than at high K-index values. The K-index is tied to a specific observatory location. For locations where there are no observatories, one can only estimate what the local K-index would be by looking at data from the nearest observatory. A global average of magnetic activity is converted to the planetary K-index, Kp. This index is available on a daily basis over the WWW. [4, 16]

The A-index depicts the daily average level of geomagnetic activity. Because of the non-

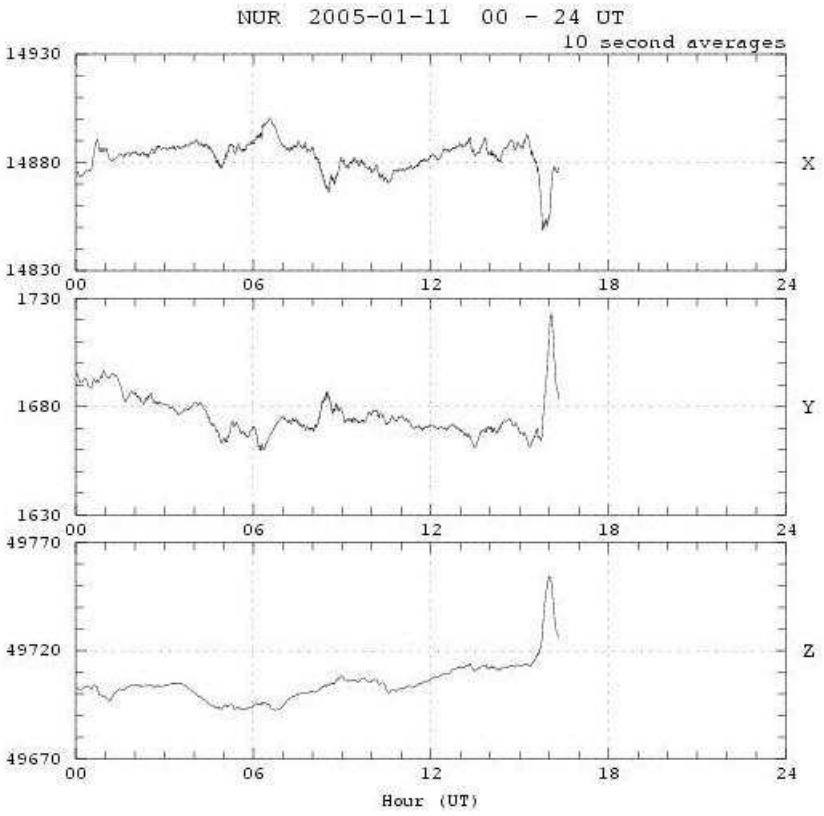

Figure 5.2: X-, Y-, and Z-components of the geomagnetic field (in nT scale) measured by FMI in Nurmijärvi, Finland, January 11^{th}, 2005. [3]

linear relationship of the K-scale with the magnetometer fluctuations, it is not meaningful to take averages of a set of K-indices. Therefore, each K is converted back to a linear scale called the "equivalent three hourly range" a-index. The daily A-index is the average of eight a-indices. [5]

5.2 Sunspots and the Activity of the Sun

The Sun goes through cycles of high and low activity that repeat approximately every eleven years. Areas exist on the Sun which are about $1000°\text{C}$ cooler than their surroundings and appear darker. These areas, known as sunspots, are created by strong magnetic fields on the Sun. Flares, the most violent events in the solar system, occur in the vicinity of large and active sunspots. In a matter of minutes, a large flare releases a million times more energy than the largest earthquake. The official sunspot number is R. Usually this number is given as a daily value or as a monthly or annual average [53]. Figure 5.3 shows the connection

between sunspot number and geomagnetic activity from 1940 to 2000.

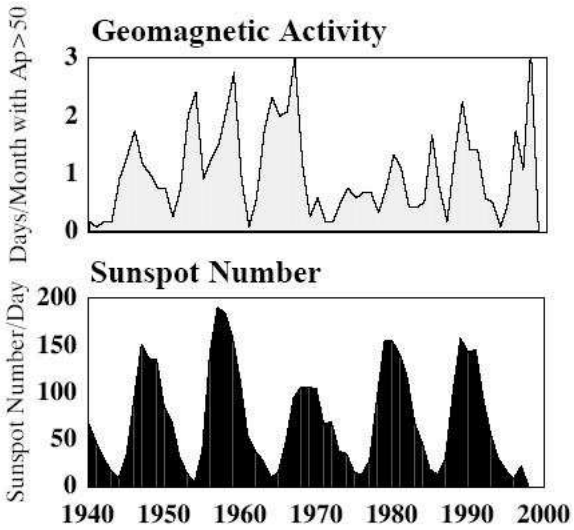

Figure 5.3: The yearly averages for geomagnetic activity and sunspot numbers show the correlation of these two measures of space environment disturbances. [28]

A coronal mass ejection (CME) is a large cloud of magnetized coronal plasma which is injected into interplanetary space, some in association with a solar flare. CMEs create disturbances in the background solar wind which can lead to geomagnetic storms when they reach the Earth. CMEs are best observed using a type of telescope called a coronagraph. [21]

Chapter 6

Review on Acoustics

This chapter gives a short review of the fundamentals of atmospheric and psychological acoustics. The aim is to give the reader a basic understanding of the concepts that are most essential for this study.

6.1 Atmospheric Acoustics

Outdoor sound propagation is affected by many mechanisms, including

a) source geometry and type;

b) meteorological conditions;

c) atmospheric absorption of sound;

d) terrain type and contour. [44]

In this section a look at these mechanisms is taken and their influence on sound propagation in the atmosphere is estimated. Since there is no unanimous notion of where the sound source of this study might be located, the approach is to present only the basics of outdoor sound propagation. Therefore, primarily the approximate attenuation of the sound is considered and the more sophisticated models are excluded.

Atmospheric attenuation, normally a positive quantity, is typically expressed as the sum of three nominally independent terms:

$$A_t = A_s + A_a + A_e \tag{6.1}$$

where A_s is the attenuation due to geometric spreading, A_a is the attenuation due to atmospheric absorption, and A_e is the excess attenuation due to all other effects [64].

6.1.1 Attenuation of Sound Due to Geometric Spreading

A general expression for the spreading loss A_s, in decibels, between any two points at distances r_1 and r_2 from an acoustic source can be given in the form

$$A_s = 20g \log r_2/r_1 \tag{6.2}$$

where r_2 and r_1 are the distances between the acoustic center of the source and the farthest and closest positions, respectively. g = 0 for plane-wave propagation such as within a uniform pipe (i.e. no spreading loss), $g = 1/2$ for cylindrical propagation from a line source, and g = 1 for spherical wave propagation from a point source [64]. The latter two conditions correspond respectively to the commonly specified condition of 3 and 6 dB loss per doubling of distance from the source.

6.1.2 Attenuation of Sound By Atmospheric Absorption

Sound energy is dissipated in air by two major mechanisms:

- Viscous loss due to friction between air molecules which results in heat generation (*classical absorption*).
- Relaxational processes - sound energy is momentarily absorbed in the air molecules and causes the molecules to vibrate and rotate. These molecules can then re-radiate sound at a later instant which can partially interfere with the incoming sound. [44]

The attenuation A_a, in decibels, over a path length r, in meters, due only to atmospheric absorption can be expressed by

$$A_a = -20log\left(\frac{p(r)}{p(0)}\right) = -20\log exp(-\alpha r) = ar, \tag{6.3}$$

where $p(r)$ is the sound pressure after traveling the distance r, $p(0)$ is the initial sound pressure at $r = 0$, α is the attenuation coefficient in Nepers per meter, and a is the attenuation coefficient in decibels per meter ($= 8.686\alpha$) [64].

While spreading losses are independent of frequency and weather, atmospheric absorption losses are strongly dependent on these parameters. At long distances and for high frequencies, atmospheric absorption is usually much greater than spreading losses for sound propagation outdoors. This means that the attenuation of sound in the atmosphere is greatly dependent upon location and weather conditions.

The sound absorption coefficient in air versus the frequency/pressure ratio for various percentages of relative humidity at $20°$C is shown in Figure 6.1. The attenuation by absorption is constant for a given difference in propagation path lengths, unlike geometrical

spreading where it is constant for a given ratio of propagation path lengths. This is assuming the weather parameters do not change considerably along the propagation path. Thus, atmospheric absorption tends to become more important with increasing distance between the source and receiver.

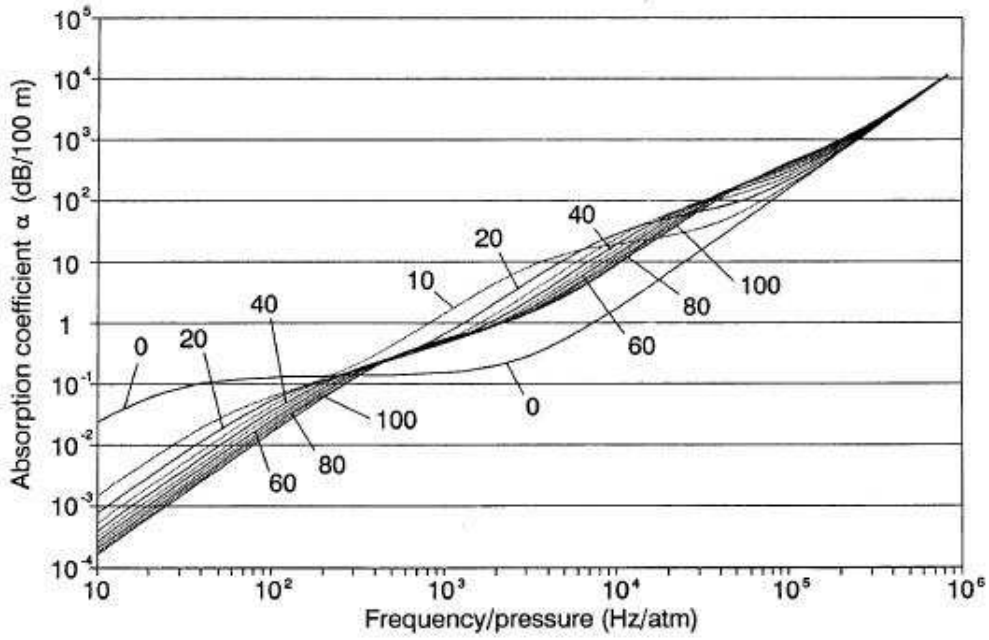

Figure 6.1: Sound absorption coefficient in air (dB/100 m) versus frequency/pressure ratio for various percents of relative humidity at 20° C. [6]

Interestingly, the attenuation due to absorption decreases with increasing humidity. An exception to this is totally dry air, which has the least absorption above the frequency of about 300 Hz. Below the temperatures of -20°C the humidity of air decreases rapidly and the air becomes acoustically transparent [39].

6.1.3 Excess Attenuation

Excess attenuation, A_e, is a combination of all effects excluding geometrical spreading and absorption:

$A_e = A_{wind} + A_{temperature} + A_{ground} + A_{vegetation} + A_{barrier}+$ any other effects...

Effect of Wind and Turbulence

Over open ground, vertical wind velocity gradients commonly exist due to friction between moving air and the ground. The wind speed, in the absence of turbulence, typically varies

logarithmically up to a height of 30 to 100 meters, then negligibly thereafter. As a result of this velocity gradient and the resulting change in sound velocity, a sound wave propagating in the direction of the wind will be bent downward. In the upwind direction the sound speed decreases with altitude. Sound waves are directed upward, away from the ground, forming a "shadow zone" into which no direct sound propagates. This process is called refraction, whereby the path of the sound waves curves in the direction of the lower sound velocity. [44, 64]

Wind is generally somewhat “gusty”, i.e. turbulent, and the gustiness increases usually with wind velocity. As a result, the received sound will also fluctuate. The turbulence also causes considerable attenuation of sound in the atmosphere. [58]

Temperature Effects

Besides wind, refraction results from vertical temperature gradients. The speed of sound in air is proportional to the square root of absolute temperature. In the presence of a temperature gradient, the effect is to refract sound waves in the direction of lower sound velocity; in this case, the lower temperature. If the temperature decreases upwards, as is usually the case during the daytime, the sound rays will be refracted upwards and an observer at some distance may be left in a shadow zone. At night there is generally an inversion of the temperature gradient, and the sound rays will be bent downwards. [44, 58]

Effect of Ground and Vegetation

Typical soil surfaces with or without vegetation tend to absorb energy from incident acoustic waves. Accurate prediction of ground effects requires knowledge of the absorptive and reflective properties, i.e. the acoustic impedance, of the surface. [44]

Vegetation and foliage provides a small amount of attenuation, but only if it is sufficiently dense to fully block the view along the propagation path. The attenuation may be due to vegetation close to the source, close to the receiver, or both. [44]

6.2 Psychoacoustics

Psychoacoustics, or *psychological acoustics*, studies the human auditory system using indirect methods with experimental paradigms and acoustic stimuli. The aim of psychoacoustics is to provide a functional description of the hearing process. [25, 29]

The objective of psychoacoustic tests is to form a delineation of the *psychophysical function* $h = f(s)$, with the help of the description or reaction function $b = g(h)$, using measurable stimulus s. Alternatively, we may try to find out the stimulus s given the description

b, using the known properties of f and g. This is typically the case when dealing with the observation reports represented in Chapter 7.

Figure 6.2 represents a setting of a typical psychoacoustic measurement. An external, objective *sound event* s arriving at the listener's ear induces an internal psychological response, i.e. the subjective *auditory event* h, which cannot be measured directly. The test subjects may describe this auditory event introspectively, i.e. by observing themselves. An external observer may gain information of the auditory event only via the description b or the reaction of the test subject. The blocks of the schematic diagram may be highly nonlinear and complex, and often they include dependencies that can only be modeled statistically. [29]

In a psychoacoustical measurement, the precision and reliability of the results are mainly determined by the precision of the parameters of the sound event, external disturbances, internal disturbances, and the precision of the description or the reaction. The functions f and g may vary remarkably between different test subjects.

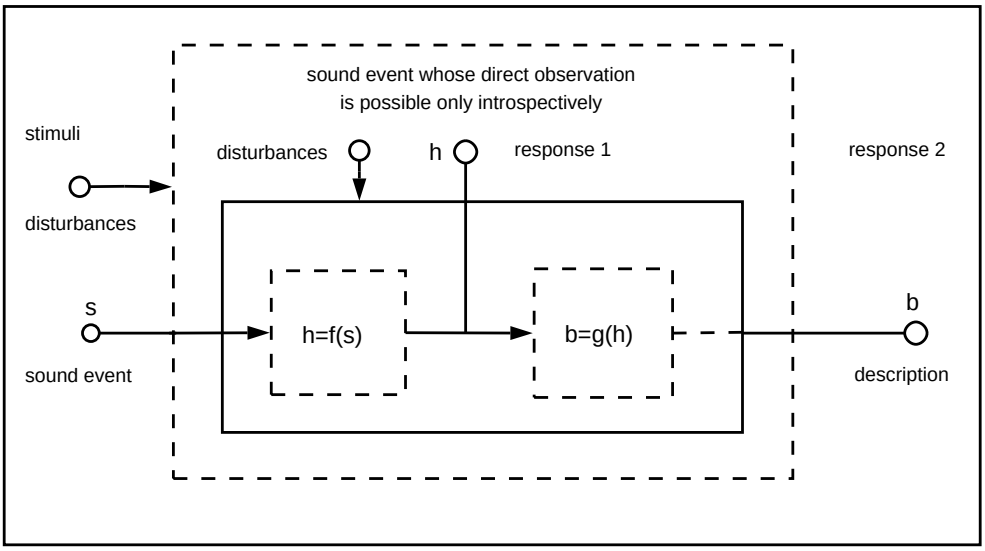

Figure 6.2: Schematic diagram corresponding to a psychoacoutic measurement in which the stimulus is the sound event s and the result is the description b of the auditory event h. [29]

6.2.1 Sensitivity of the Ear

Intensive Thresholds

Intensive thresholds of hearing define the lowest possible sound levels that a listener can detect as well as the highest sound levels that a listener can tolerate. These thresholds are

used to describe hearing sensitivity and the dynamic range of hearing, i.e. the difference between the highest and lowest sound pressure level (SPL) that can be detected [26].

Absolute hearing thresholds are the lowest SPLs required for listeners to detect sound. *0 dB HL* (hearing level) represents the zero reference level, which is based on the average hearing level of a large number of young adults considered to be otologically normal. The 0 dB level is fixed to the standardized pressure of 20μPa. The ear is maximally sensitive to frequencies from 2 kHz to 5 kHz. These are the most important frequencies for human speech. [26, 70]

There is some variability in absolute thresholds even for persons with healthy auditory systems. For example, it has been noticed that threshold values for a 1 kHz tone may vary over a range of 20 dB. [26]

The upper limits of the SPLs that a listener can tolerate, the *terminal thresholds*, are typically 130 to 140 dB at all frequencies [26].

Frequency Thresholds

The frequency range of hearing is generally stated to be between 20 Hz and 20 kHz for normal young human ears. The frequency range of hearing is linked to the intensity of the sound. The higher the intensity, the higher the upper frequency limit. At moderate intensities (80 dB) the limit is often no higher than 18 kHz, but it cannot be extended indefinitely because there is a final practical limit imposed by pain. [26]

Below 20 Hz, in the infrasound range, the sound may arouse an auditory sensation, described as “flutter”, down to about 10 Hz [26]. Strong infrasounds may produce sensations of uneasiness or even fear.

6.2.2 Auditory Masking

In hearing, masking is generally defined as the interference with the perception of one sound, the signal, by another sound, the masker. The interference may decrease the loudness of the signal, may make a given change in the signal less discernable, or may make the signal inaudible. The change in audibility, the *amount of masking* is defined as the SPL at which the signal is just audible in the presence of the masker minus the SPL at which the signal is just audible in the quiet. [59]

Simultaneous masking is the increase in threshold caused by a masker that is present throughout the signal [59]. Experiments on masking by white noise provide important information about the effects of masker level and signal frequency. The noise power density of white noise is independent of frequency. Masking due to white noise with fixed SPL is approximately constant up to about 500 Hz and begins to rise 3 dB/octave with increasing

frequency after this [29]. Measurements with white noise have also shown that the masked threshold increases 10 dB for every 10-dB increase in masker level. This relationship is also true for narrowband maskers whose passbands encompass the signal frequency [59].

Auditory masking may also be considered in time domain. *Nonsimultaneous masking* is the increase in threshold caused by a masker presented before a signal (*premasking*) or after it (*postmasking*) [29, 59]. Premasking has an effective range of only 5–10 ms before the masker whereas postmasking affects about 150–200 ms after the masker [29].

Chapter 7

Survey of Aurora Related Sound Reports by SGO

The aim of this chapter is to present the essential results of the survey of aurora related sound reports collected by the SGO. This chapter is mostly based on the essay written by Kero [37].

Two questionnaire-type surveys on aurora related sounds had been carried out previously, one by Tromholt [65] in Norway and the other by Beals [9] in Canada. Approximately one in five people replied to the surveys, and these were naturally those who were most interested in the phenomenon. About 80% of the respondents of both surveys claimed to have heard aurora related sounds. [62]

The co-operation of HUT and the SGO on aurora related sound research was launched in spring 2000. Soon after this, collection of aurora related sound observations made by the public in Finland was started. The SGO announced a telephone number that people willing to give a report could call, and meanwhile HUT introduced a WWW form that people could fill out and send to the project personnel. During their telephone interviews the personnel of the SGO filled out forms similar to the WWW form of HUT. Thus, the telephone interviews and the WWW forms could be combined to create uniform material. This combination of materials was done by the SGO. Detailed analysis of the observation reports has not yet been published.

By the end of 2002, 237 reports had been received. 56% of the respondents were male and 44% female. The oldest observation dates back to 1925 and, as expected, the number of reports per year correlated with the sunspot number indicating the auroral activity [37]. Some results of this survey were presented by Laine *et al.* [43]. The results lend support to the earlier surveys: auroral sounds are heard only when the aurorae are very bright and active, clear rays are visible and in most observations the auroral corona is above the head

of the observer. The sound is weak and dissimilar to other natural sounds of the observation environment but it is, however, distinct and clearly recognizable. [43]

The distribution of number of reports per year showed no major differences between the 1940's and today. However, two slights peaks were found: in the 1940's and 1950's, and the beginning of the 21st century. During the 1960's, vast migration from rural areas to cities took place in Finland. It is clear that in a city hearing faint sounds is practically impossible outdoors. It is also likely that people living in the countryside spend more time outside than city dwellers. This acts as an explanation as to why the amount of observations dropped slightly after the 1950's. The second peak (after the year 2000) may have to do with the publicity that the ongoing project has gained in Finnish media, which has increased peoples' awareness of the phenomenon. [37]

7.1 Age Distribution of the Observers

One of the new findings of the survey was that the age distribution of the observers at the moment of observation showed a peak for an age below 15 years, with a decreasing tail for increasing age. Similar distributions were found for men and women. The age distribution is presented in Figure 7.1. The median of the distribution is 20 years. [43]

A natural explanation to this discovery is that it is known that human hearing is at its best between the ages of 14 and 18 years. After this, both the ear's sensitivity and ability to detect high frequencies become weaker. Another explanation might be that young people will spend their evenings outside more often than older people. [43]

7.2 Weather

The average temperature for a sound observation was $-20°\mathrm{C}$. This result may however be somewhat biased by the generally adapted language to describe and recall temperatures [43]. It is worth noting that below the temperature of $-20°\mathrm{C}$ the humidity of air decreases rapidly and the air becomes acoustically transparent which makes the attenuation of sound very weak as it was noted in Chapter 6. On the other hand, very low temperatures are rare and people often prefer to stay inside during very cold nights.

The temperature distribution is presented in Figure 7.2.

7.3 Latitudinal Dependency

A surprising discovery was made revealing that there was no latitudinal dependency in the distribution of observations. They were evenly distributed from the southernmost tip

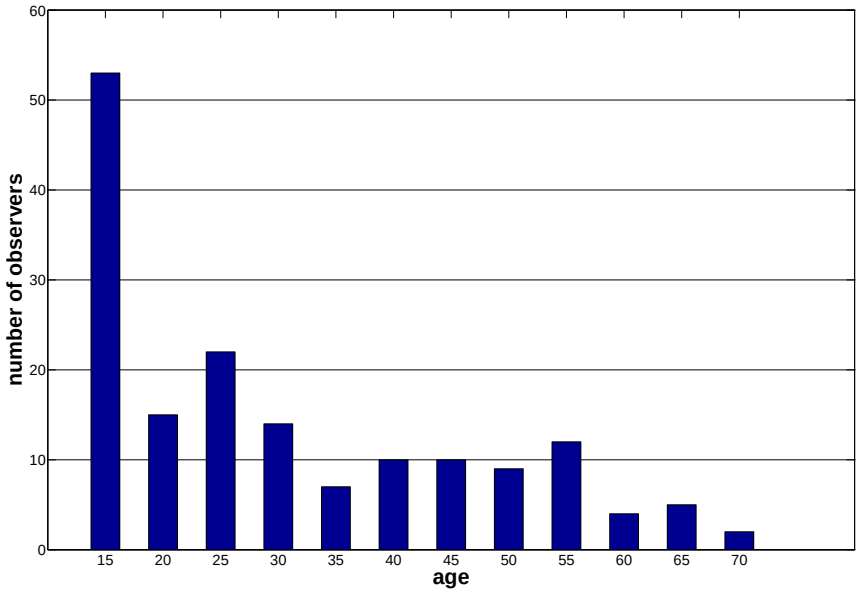

Figure 7.1: Number of observers in different age groups. [66]

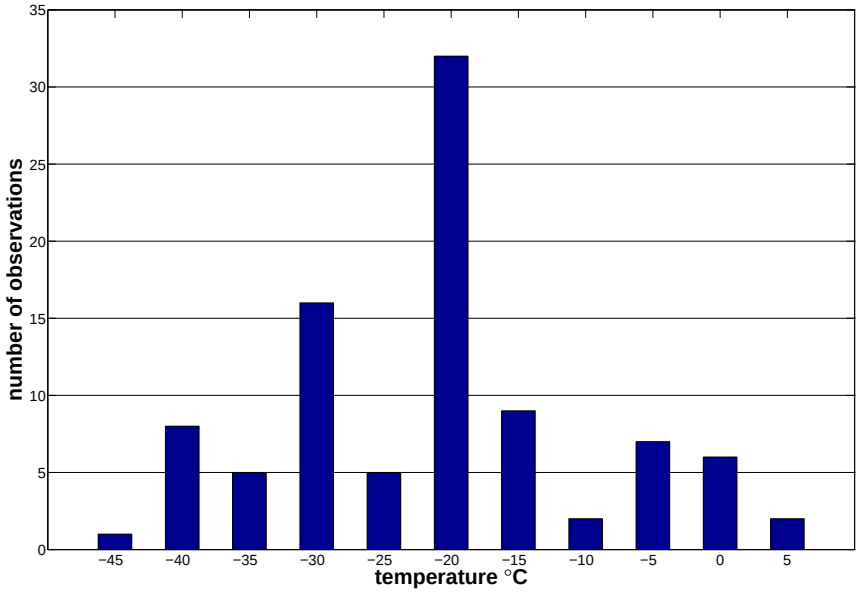

Figure 7.2: Number of observations in different temperatures. [66]

of Finland up to the northernmost point, i.e. from about 60° to 70° north. The probable explanation for this is that the population density becomes larger the further south we go in Finland. Also, during strong geomagnetic storms aurora are seen equally well in Southern Finland as in Lapland. [43]

7.4 Characteristics of Observed Sound Events

In the study of Silverman and Tuan [62], hissing and swishing formed the biggest category of descriptions (38%), the second biggest category being crackling and rustling (32%), and other types of sounds forming the remaining category (30%). In the survey by the SGO the biggest difference compared to the study of Silverman and Tuan was that the category "other types of sounds" was considerably smaller (9%). The proportion of hisses and swishes was now 47% and that of crackling and rustling 44%. [37]

In the survey by the SGO it was found that 33% of the descriptions were associated with electricity, forming the biggest group of sound associated with some known phenomenon. Most of these descriptions were related to electric discharge, such as "the sound of welding". Another group of descriptions reflected sounds of a continuous type, such as "the sound of an electric line" and "the sound of an electric power house". [37]

The association with electricity is particularly interesting because the existence of electric types of sounds in nature are rare. It is most likely that if the connection between aurora and the observed sound exists it is electrophysical. On the other hand, people today are generally fairly aware of the fact that the aurora is an electrical phenomenon. Therefore, it remains to consider whether the large amount of observations associated with electricity reflect peoples' tendency to classify sounds according to the electric nature of the phenomenon, or if the sound source is indeed electrical. [37]

The second biggest group of sounds associated with some known phenomenon were the sounds related to fire (23%). Often the sound was associated with intensively burning wood. The verbal descriptions of fire are very rich in their characteristics. They may contain humming, popping, crackling, and even whistling sounds. Descriptions such as "burning juniper" refer to rapid but irregular burning. As the third group of sounds there were eleven descriptions related to water. These included a wide range of sounds, such as sounds of rain, running water, and the breaking of thin ice and soap bubbles. Some other associations were related to sounds made by man and sounds of machines or items made by man. [37]

Detailed analysis of the characteristics of the observations is not carried out in this thesis. Considering this, it is noted that only a rough classification is given to the sound events. The sounds can be divided into two major categories depending on their nature: continuous (such as hissing) and discrete (such as pops or cracks). Both categories are further divided into two classes: tonal and atonal.

This division is not strict, and a third category could be placed between continuous and discrete events. It would be a mixture of these two and would contain events such as a series of cracks. Also, it may sometimes be difficult to classify a sound strictly within tonal or atonal classes.

Chapter 8

Measurement System

The measurement system of aurora related sound and electric field effects is now introduced. The measurement set up is able to record audio and electric field signals in the frequency range of about 5 Hz – 24 kHz. 5 Hz refers to the -3-dB lower limiting frequency of the microphone, and thus it is, in practice, possible to record signals even below it. With the aim of simultaneously digitized acoustic and electric field signals it was desired to gain knowledge of a possible connection between the acoustic signal and local fluctuation of the electric field. The system is fully battery-operated and can easily be carried to places where the ambient noise and weather conditions are favorable.

The system used for most measurements is presented in Figure 8.1. The main components of the system are:

- Brüel & Kjær 4179 condenser microphone
- Brüel & Kjær 2660 microphone preamplifier
- acoustic reflector
- Brüel & Kjær 2804 battery driven power supply
- Sony TCD-D3 DAT recorder
- VLF antenna
- Sennheiser HD580 headphones for monitoring
- passive high-pass filter (not used in most recordings)

The DAT recorder is inside the car where the measurement is monitored with headphones.

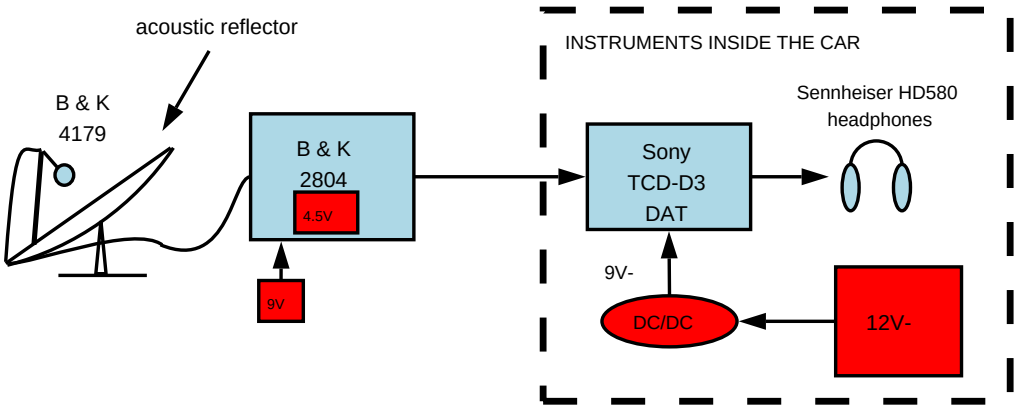

Figure 8.1: The measurement system. [1]

8.1 Description of the Set Up

This section gives an overview of the most essential components of the set up. There were no (acoustic) specifications available for the acoustic reflector. Hence, some extra attention had to be paid to defining the amplification and directivity pattern of the reflector.

8.1.1 Microphone and Preamplifier

The microphone B & K 4179 forms a combined system with the B & K 2660 preamplifier. It is specially designed for very low-level sound measurements. The microphone is mounted to the focus of the parabolic reflector. The microphone and its preamplifier are mounted in metal tubes and permanently connected with a wire of one meter. The system is able to measure SPL down to 0 dB in the frequency band 7 Hz - 12.5 kHz. The lower limiting frequency (-3 dB) of the microphone is about 5 Hz. The 1/3-octave bandwidth inherent noise floor of the complete system at 1 kHz is typically -16 dB. The output impedance of the preamplifier is 50Ω. The specifications of the combined system are presented in [57].

According to the specifications provided by B & K [57], the operating temperature range for the preamplifier is from -20 to +60°C and from -10 to +50°C for the microphone. Only a few recordings have been carried out in temperatures below -10°C.

In [43] it has been shown that the microphone and its preamplifier are insensitive to variations in the ambient magnetic field.

8.1.2 The Acoustic Reflector

In order to improve the acoustic sensitivity, the microphone was mounted in the focus of a parabolic satellite antenna with 78 cm of maximum diameter. The idea to apply a relatively

cheap commercial reflector designed for satellite receivers was originally given by Ph.D. Esa Turunen.

Parabolic dishes have been used for many years as sound concentrators without any accurate knowledge of their acoustic properties. Most of these reflectors were manufactured for microwave transmission applications, for which theoretical treatments and practical characteristics may be readily available. However, it is incorrect to assume that sound waves and short electromagnetic waves behave alike. Therefore, measurements were made to find out the acoustic directivity pattern and the gain of the reflector. Some theory and practical measurements of acoustic properties of parabolic reflectors can be found, e.g. in [46] and [47].

The Measurement of the Directivity Pattern

The directivity pattern of the parabolic reflector was measured by Klaus Riederer in the anechoic chamber of the Laboratory of Acoustics and Audio Signal Processing at HUT. This was performed with a measurement set up originally designed for measurement of head related transfer functions (HRTF). Eight loudspeakers with elevations from -30° to $+90^\circ$ were used. A horizontally revolving stand made it possible to use azimuths from 0° to 350°. Thus, there were altogether 288 different possible measuring directions for an incoming acoustic signal. The average sound power of impulse response was computed for every angle of incidence. The average sound power was also computed for each 1/3-octave band.

It was desirable that the wave impinging on the reflector would be approximately a plane wave. However, due to limitations of the HRTF measurement set up, the directivity pattern could not be measured in far-field. The distances between the microphone and the loudspeakers were 1.4–2.7 m. This may have resulted in some smoothing in the measured patterns. For a plane wave, the gain of the reflector should be even larger and better focused than in the case of this close-field measurement.

The Results

Acoustic gain of the reflector as a function of the angle of incidence is presented in Figures 8.2, 8.3 and 8.4 for 1/3-octave bands with center frequencies 1 kHz, 3.15 kHz and 5 kHz, respectively. The gain is given on a relative scale where 0-dB level corresponds to the maximum gain within each band. The normal of the reflector is marked with an arrow. The angle between the normal of the reflector and the ground is 50.3°.

It is seen that the direction of maximum gain is directly upwards. Also, the increase of frequency has an effect of making the response sharper.

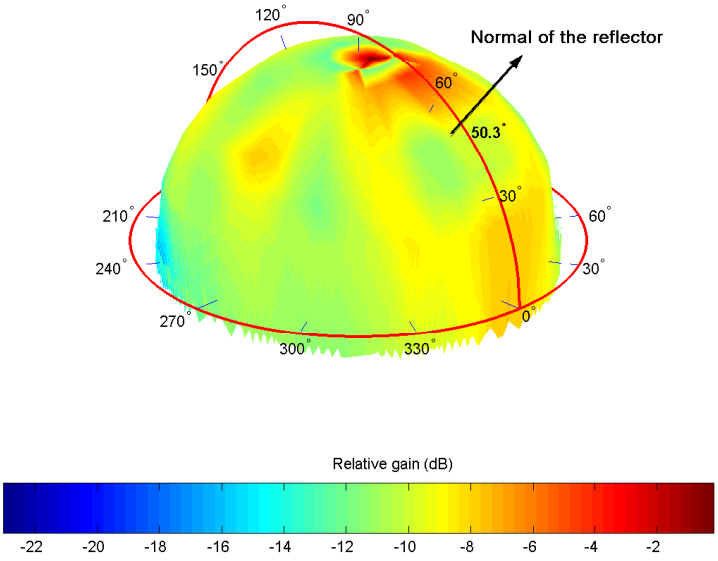

Figure 8.2: Directivity pattern of the acoustic reflector for the 1/3-octave band with center frequency 1 kHz. The gain is given on a relative scale where 0-dB level corresponds to the maximum gain within the band of 1 kHz.

The measurement of the directivity pattern should ideally have been carried out in far-field conditions. However, since the HRTF measurement system was readily available, and a measurement in far-field conditions would have taken an excessive amount of time, the approximate results obtained with the HRTF measurement system are considered to be adequate.

The directivity pattern of the reflector is favourable in the sense that the maximum gain points directly upwards. It functions according to the interests of the study: the ambient noise received from the ground level is amplified considerably less than the sound directly above from the sky.

8.1.3 Power Supply

The battery driven power supply B & K 2804 is designed for field measurements of sound and vibration. It supplies 200 V, 28 V or 0 V polarization voltage to the condenser microphone, and 28 V supply for powering the preamplifier. The microphone B & K 4179 utilizes the polarization voltage of 200 V. The power supply is driven by 3×1.5 V non-rechargeable alkaline batteries. The specifications of the power supply are given in [56].

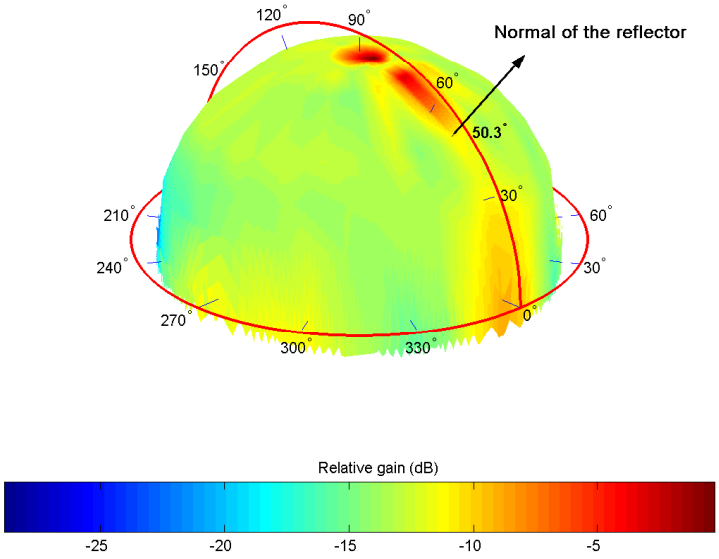

Figure 8.3: Directivity pattern of the acoustic reflector for the 1/3-octave band with center frequency 3.15 kHz.

8.1.4 DAT Recorder

The audio and electric field signals are recorded by a Sony TCD-D3 DAT recorder using sample rate of 48 kHz.

8.1.5 VLF Antenna

The measurement system is capable of recording and storing VLF signals in frequencies below 24 kHz. The VLF antenna is made of a telescope rod of glass fibre which raises a thin copper wire straight up from the earth to the height of four meters. It is mounted about six meters from the car where the measurement is monitored. A passive low-pass filter is connected between the antenna and the coaxial cable leading to the car. The filter helps to damp possible RF signals. The VLF signal is led directly to the microphone input of the DAT player without any additional active preamplifier. The VLF signal is left at a low level in order to minimize its possible leakage to the audio signal on the other channel of the DAT.

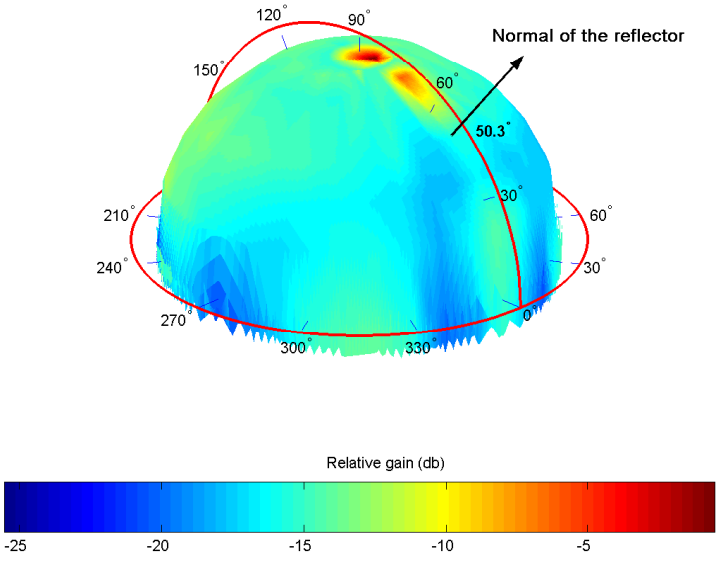

Figure 8.4: Directivity pattern of the acoustic reflector for the 1/3-octave band with center frequency 5 kHz.

8.1.6 Analog High-pass Filter

In outdoor sound, most of the energy is concentrated at the infrasound region which is not of the highest interest to this study. Therefore, a first-order analog high-pass filter with a -3 dB cut-off frequency at 500 Hz was designed and constructed in order to damp undesired low-frequency components, as well as the noise caused by the wind. The high-pass filter somewhat flattens the spectrum and allows usage of higher gain. In this way the filter helps to improve the SNR at the middle and higher audio range. The filter has been used for all measurements since the spring of 2003.

8.2 Calibration of the Measurement Set Up

The measurement set up was calibrated in the anechoic chamber of the Laboratory of Acoustics and Audio Signal Processing at HUT. The calibration was performed in two steps. The aim of the first calibration was to connect the real SPLs to the recordings carried out by the set up. In the second calibration the maximum gain of the acoustic reflector was

determined.

The measurement signal used was white noise that was fed from a loudspeaker. It was desired that, on impinging the acoustic reflector, the sound wave would be as close as possible to a plane wave. Therefore, to obtain far-field type conditions, the loudspeaker and the microphone were placed in corners of the room opposite to one another so that the distance between the loudspeaker and the microphone was 6.3 meters.

The signal was first recorded on a DAT tape without the reflector, and the SPLs were measured with a B & K 2238 Mediator sound level meter. With the help of the recorded signal and measured SPLs, the true SPLs could be combined with the acoustic measurements made outdoors.

Next the microphone was mounted to the focus of the acoustic reflector. The reflector was directed so that the direction of the maximum gain pointed to the loudspeaker. Using this direction, the test signal was recorded on a DAT tape. By comparing this signal with the signal recorded without the reflector, the maximum gain of the reflector could be determined.

The experiment showed that the maximum gain of the reflector is 21 dB in terms of the total acoustic power.

8.3 Data

The audio and electric field signals are stored with a sample rate of 48 k samples/s (16 bits). This leads to a relatively high data rate of 360 M samples/h and 1.44 G samples (2.88 GB) per night, typically four hours of recording. The data are transferred from the DAT tapes in digital form to a computer in which the analyses are performed.

Up to the spring of 2005, data of ca. 100 nights had been collected. Most of the measurements were made during high or moderate geomagnetic activity. Almost all geomagnetic events caused by large CMEs directed at the Earth that occurred during favorable weather conditions during the years 2000–2004 were recorded. Up to the date of this thesis, only a small fraction of this data has been analyzed. For reference purposes, data was also gathered during some nights of low geomagnetic activity.

Chapter 9

Analysis of the Measurements

The objective of the analyses performed in this thesis was to provide new knowledge that would lend the ability to answer the primary research problem: “Are aurora related sounds real, physical effects or are they just perceptual artifacts or malfunctions?” The possible sound production mechanisms are discussed only briefly.

There are basically two different approaches to the analysis of the measurement data. One is to point out the potential aurora related sound events and base the research on them, e.g. by studying the waveforms or spectra of these events. The other is to consider larger amounts of data (several minutes or hours at a time), and study them by performing statistical analyses.

Since the detection of sound events without any objective decision-making is very difficult, statistical analysis or, more specifically, statistical analysis of time series was introduced as the main tool of the study. Some of the statistical analyses, and the results gained with them, have already been represented to some extent in [41] and [42]. Nevertheless, the methods used in this thesis are somewhat different.

The benefit of statistical analysis is that it provides an objective tool for the analysis of data sets. It does not make assumptions on the data as human decision-making does. However, it is clear that human decision-making is used at least at the moment when a particular statistical method is selected. The method must not be “optimized” according to the data at hand to give the best possible result. It is required that the selected method is based on some knowledge, or at least a decent assumption, of the underlying phenomenon.

Considering we have results produced with a statistical method that has been chosen by following some appropriate criterion, it has to be decided what can be said according to the results, i.e. what the *significance* of the result is. Great care must be exercised at this phase, and often there is no straightforward answer to this question as we will find out in this chapter.

The aim of the statistical analyses performed in this thesis is to gain knowledge of the possible connections between acoustic and geomagnetic signals. This is done by the means of *correlation* computation. The motivation for the use of geomagnetic data comes from the fact that disturbances in geomagnetic field data reflect the activity of aurora. Primarily, it is simply intended to find out if the connection between geomagnetic and acoustic data exists. If the connection is found, in further studies it is intended to determine what kind of connection this is.

This chapter has two main parts. The methods that were used for the analysis of acoustic data and geomagnetic data are first introduced. After that the results gained with the given methods are presented. The measured VLF signals are also considered in brief.

9.1 Acoustic Power and SPLs

The *energy* of the sequence $x[n]$ over a finite interval $0 \leq n \leq N-1$ is defined by

$$\varepsilon_x = \sum_{n=0}^{N-1} |x[n]|^2. \tag{9.1}$$

The (average) power of the sequence within the same interval is gained simply by dividing the energy by the number of samples, N. [50]

The power of the acoustic signal was computed in successive, non-overlapping, segments of 1.0 s resulting in vectors of 3 600 samples per hour, each sample telling the average power in a time frame of 1.0 s. The acoustic power could then be further converted into true SPLs with the help of the results of the calibration represented in Chapter 8. Figure 9.1 shows a one-hour long example of a signal analyzed in this way. In a silent environment, the SPLs are typically 20–25 dB. However, exact SPLs were not important for most of the analyses performed in this thesis.

It should be noted that low frequencies dominate in the acoustic signals recorded outdoors without high-pass filtering, which is also the case in Figure 9.1.

Computation of acoustic power suppresses the amount of data a great deal — by a factor of 48 000. When performing the statistical analysis of data over several minutes, or even hours, resolutions finer than 1 second do not seem reasonable. Hence, by performing this kind of preprocessing on the data, we could ease the computational burden and cope with several hours of audio data.

9.2 Acoustic Power in 1/3-Octave Bands

The computation procedure of acoustic power is now repeated using 1/3-octave frequency bands. These are listed in Appendix B. For this procedure, the *Parseval's* relation and

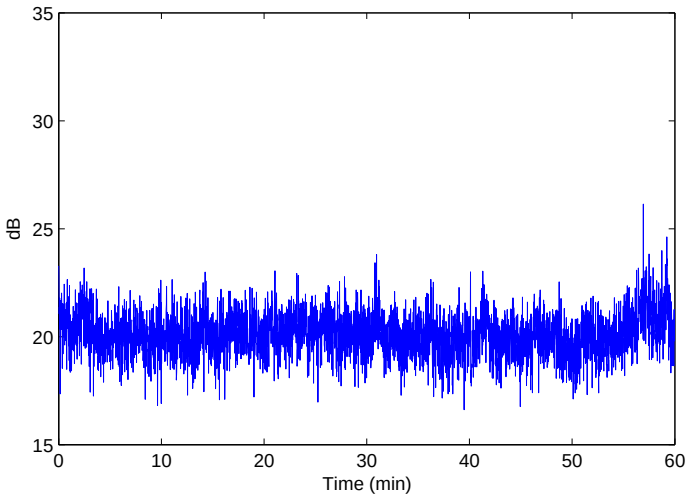

Figure 9.1: An example of SPLs from a recording in a silent environment.

windowing together with Fast Fourier Transform (FFT) are applied.

9.2.1 The Parseval's Relation

The Parseval's relation states [50]

$$\sum_{n=0}^{N-1} |x[n]|^2 = \frac{1}{N} \sum_{n=0}^{N-1} |X[n]|^2 \tag{9.2}$$

where $x[n]$ denotes the signal in time domain and $X[n]$ the same signal in frequency domain, N being the number of samples. It is seen from the lefthand side of the equation that this equals the signal energy ε_x. Therefore, the power is given by

$$P_x = \frac{\varepsilon_x}{N} = \frac{1}{N^2} \sum_{n=0}^{N-1} |X[n]|^2. \tag{9.3}$$

9.2.2 Windowing

Windowing is used in harmonic analysis to reduce the undesirable effects related to spectral leakage. If an FFT is performed with a relatively large amount of samples, the leakage is not as severe as in the event of short FFTs. However, we are now dealing with signals that may experience strong infrasound packages. If a simple rectangular window was used, leakage of the infrasound to higher frequencies might occur leading to false results. To minimize the probability of such a chance, a minimum 4-term Blackman-Harris window was applied

to the signal before the FFT. The equation of the window with a length of N is

$$w[k+1] = a_0 - a_1 \cos\left(2\pi \frac{k}{N-1}\right) + a_2 \cos\left(4\pi \frac{k}{N-1}\right) - a_3 \cos\left(6\pi \frac{k}{N-1}\right) \quad (9.4)$$

where $0 \leq k \leq (N-1)$. The coefficients are $a_0 = 0.35875$, $a_1 = 0.48829$, $a_2 = 0.14128$ and $a_3 = 0.01168$. [27]

The window used in the analyses is shown both in time and frequency domains in Figure 9.2. The minimum 4-term Blackman-Harris window with a length of $N = 24000$ provides relative sidelobe attenuation of -92 dB (i.e. the difference in height from the mainlobe to the highest sidelobe peak). The mainlobe width (-3 dB) of the window is 0.00015259π which is 3.6622 Hz with a sample frequency of 48 kHz. The mainlobe width presents some restrictions in precision in the lowest 1/3-octave bands but is, in general, satisfactory for our purposes.

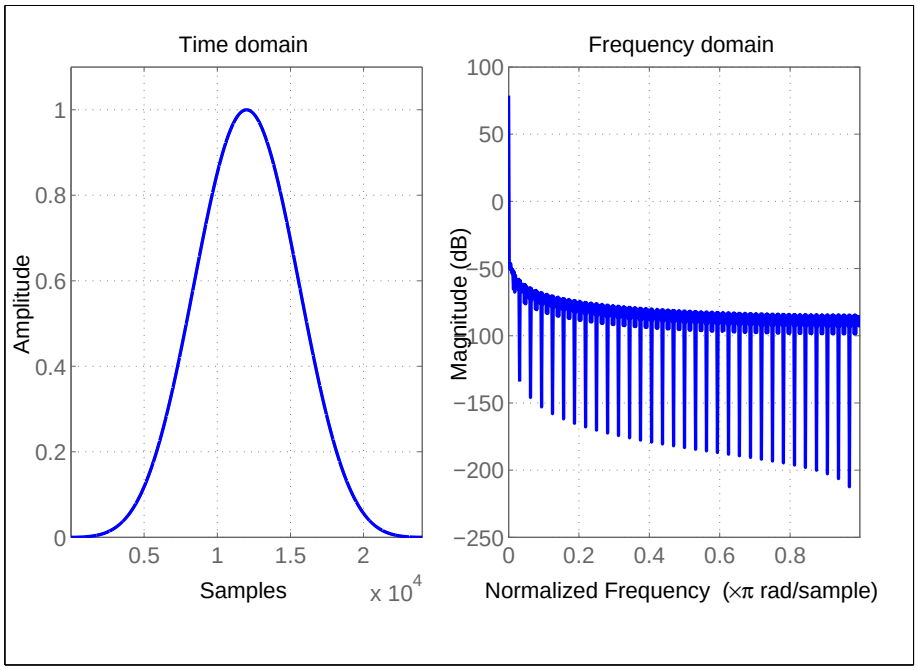

Figure 9.2: The minimum 4-term Blackman-Harris window with $N = 24000$.

9.2.3 Computation of the Acoustic Power

The signal power within each 1/3-octave band can easily be computed with the help of the equation 9.3. Figure 9.3 shows how the signal was analyzed frame by frame. In many analyses it is convenient to ignore the factor $1/N^2$ which only affects the scaling of the sequence.

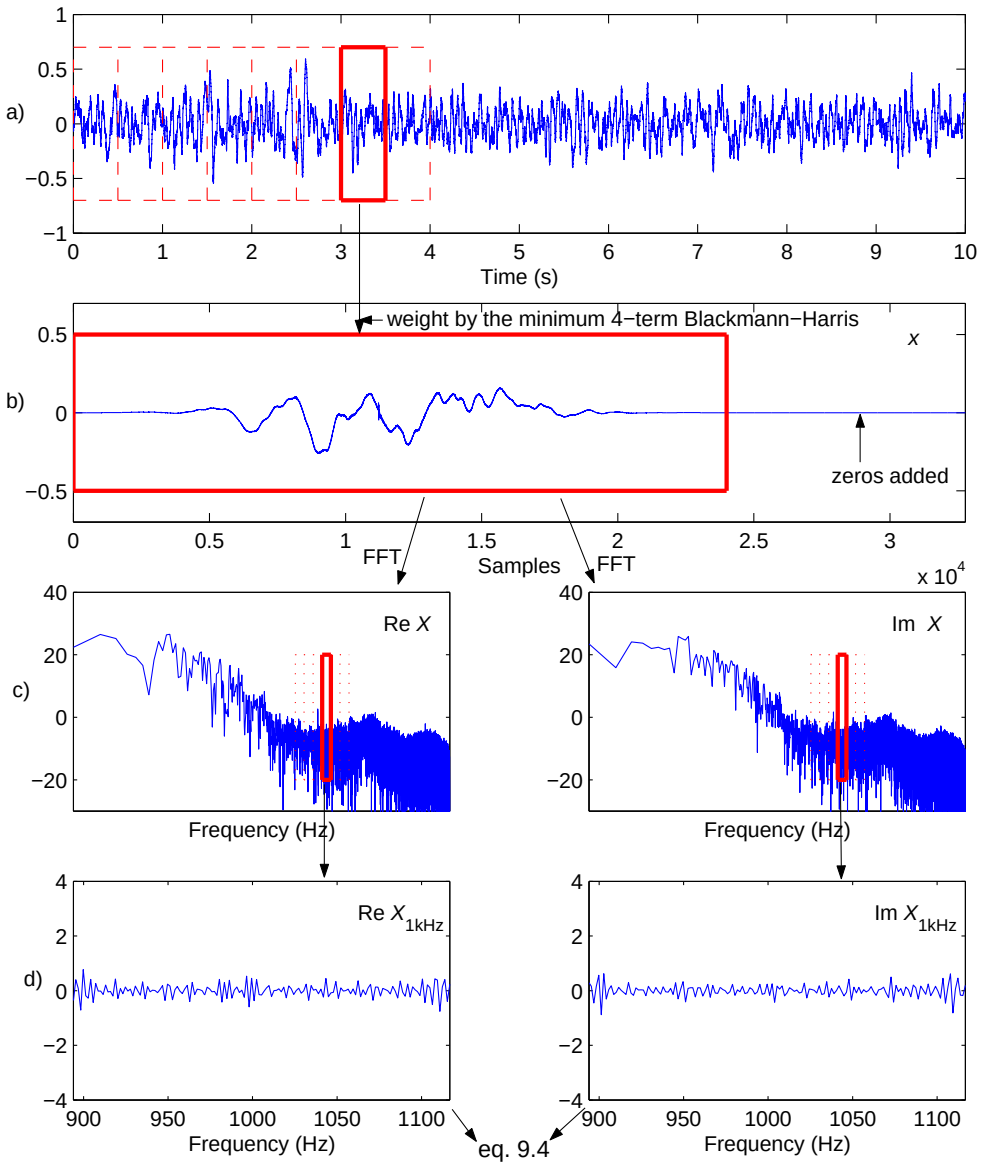

Figure 9.3: The acoustic signal in a) is read in frames of 0.5 seconds (24 000 samples) and weighted by the minimum 4-term Blackman-Harris window. The data is padded with zeros to form the vector x shown in b). The FFT is then performed to obtain X whose real and imaginary parts are presented in c). The real and imaginary parts of the spectra within the 1/3-octave band with center frequency 1 kHz are given in d).

Computation of acoustic power can be summarized as follows:

1. 0.5 seconds of data (i.e. 24 000 samples) are read from the audio file (Figure 9.3a) and weighted by a minimum 4-term Blackmann-Harris window given by equation

9.4.

2. To provide an efficient calculation of the FFT, the vector is padded with zeros so that altogether 32 768 ($= 2^{15}$) samples are gained. Denote the resulting vector by x (see Figure 9.3b).

3. FFT is performed. The resulting vector is X (see Figure 9.3c).

4. Data belonging to each 1/3-octave band are picked from X. The resulting vectors are denoted by X_{f_c}, where f_c is the center frequency of the band. Figure 9.3d shows the real and imaginary parts of X_{1kHz}.

5. Signal power P_{f_c} within each band is computed from X_{f_c} by the equation 9.3.

6. The next 0.5 seconds of data are read and steps 2–5 are performed.

Following the steps 1–6, 7 200 data points are gained per hour.

The windowing has the effect that the beginning and the end of each 0.5-second segment are given smaller weight than the center of the segment. Therefore, one might want use a more sophisticated approach by making the successive windows overlap so that each time instant is given, at least approximately, an equal weight. This is an improvement to be considered in the future work. On the other hand, this increases the serial correlations of the samples which may be undesirable on some occasions. In any case, we are dealing with large amounts of data and most likely this does not cause remarkable differences in the results that are obtained.

9.3 Geomagnetic Activity

The absolute value of time derivative of the geomagnetic field is often used as the measure of the geomagnetic activity. The magnetometer data we are dealing with has a sample rate of 1 Hz. One option for measuring the geomagnetic activity is to differentiate the signal and use the absolute value of the differentiated data as the measure. The other option, and the more practical one in many situations, is to compute the standard deviation (SD) of the signal in sequencial blocks of a fixed length.

As it was stated in Chapter 5, aurorae typically cause variations in the X-component of the geomagnetic field. Therefore, the attention might be restricted to the time derivative of the X-component. Alternatively, we may measure the variations in the total geomagnetic field by forming the resultant of the time derivatives of the X-, Y- and Z-components (or the resultant of the SDs of the components). An even more sophisticated measure may be formed by giving each component a different weight. Since we have no prior information

of the significance of the components in terms of the analyses performed, equal weights are given to the components.

9.4 Correlation between the Geomagnetic and Acoustic Data

The geomagnetic data available is sampled at a rate of 1 sample per second while the audio signal was recorded at a sample rate of 48 000 samples per second. As the rates are totally different, it is impossible to compute the correlation sample by sample. This would presumably be pointless in any event since the nature of these two signals is different. Now that the acoustic power has been computed with a resolution of 1 sample per second, it is possible to compute correlation between it and the geomagnetic activity. It is, however, more reasonable to reduce the resolution in order to diminish the interdependency of successive samples. There are a number of problems that have to be considered.

One problem is related to the type of the possible relationship of these signals. The *Pearson correlation coefficient*, or the correlation coefficient for short, is a measure of linear relationship between two variables. We cannot be sure that the hypothetical relationship between geomagnetic activity and acoustic power is linear, and thus have to take into account other types of relationships.

The lag between the two data sets is an essential aspect in this study. The geomagnetic disturbances travel at the speed of light while the acoustic signal is relatively slow (approximately 330 m/s at sea level at 0° C). The delay of the geomagnetic signal can be considered to be zero whereas the delay of the acoustic signal is greatly affected by the distance between the sound source and the receiver. Since we can only make assumptions on the amount of lag, it presents an additional degree of freedom. Nevertheless, if there is a clear indication of maximum correlation occurring at some distinctive lag, D [s], between the acoustic and geomagnetic data, this can be used to estimate the distance between the sound source and the receiver ($r = Dc$, where c [m/s] is the speed of sound). The correlation as a function of lag is generally called the *cross-correlation* function.

Assuming that the correlation exists, it is most likely that the processes do not occur at a constant lag. It could be assumed that the lag is within some limits. It is rational to think that we receive sounds from different sources at different distances, thus experiencing different delays. However, it is difficult to tell whether a geomagnetic impulse is able to trigger acoustic events immediately. It is possible that there is a time constant in this hypothetical geomagnetic-to-acoustic conversion, or the underlying processes are so complicated that connecting the lag to a physical model may be difficult.

Some preliminary correlation results of the measurement in Koli on April 11th, 2001 were presented by Laine *et al.* [42]. It was concluded that a relatively high correlation be-

tween the geomagnetic activity and acoustic energy is found in the measurement around the time of the highest geomagnetic activity. The maximum correlation was achieved when the geomagnetic data was delayed about 66–81 s. When the time resolution of both geomagnetic and acoustic data was reduced to 10 seconds by low-pass filtering and downsampling, the highest correlation found in a window of 15 minutes was 0.83. These analyses were made without trend removal. Trend removal is considered in subsection 9.4.3.

9.4.1 Pearson Correlation

The Pearson correlation coefficient ρ is a measure of the degree of linear relationship between two variables. The correlation coefficient may take on any value between minus one and plus one

$$-1.0 \leq \rho \leq +1.0. \tag{9.5}$$

The sign of the correlation coefficient defines the direction of the relationship, either positive or negative. A positive correlation coefficient means that as the value of one variable increases, the value of the other variable increases; as one decreases, the other decreases. A negative correlation coefficient indicates that as one variable increases, the other decreases, and vice-versa. [49, 63]

The absolute value of the correlation coefficient measures the strength of the relationship. For instance, a correlation coefficient of $\rho = -0.5$ indicates a stronger degree of linear relationship than one of $\rho = 0.4$. A correlation coefficient of zero ($\rho = 0.0$) indicates the absence of a linear relationship and correlation coefficients of $\rho = +1.0$ and $\rho = -1.0$ indicate a perfect linear relationship. [49, 63]

Correlation coefficient ρ for two random variables X and Y is defined as:

$$\rho = \frac{\mathrm{Cov}(X,Y)}{\sqrt{(\mathrm{Var}X)(\mathrm{Var}Y)}}. \tag{9.6}$$

$\mathrm{Cov}(X,Y)$ denotes the covariance of the two variables and $\mathrm{Var}X$ and $\mathrm{Var}Y$ variances of X and Y, respectively. [49]

The job of the researcher is to estimate ρ based on a set of observations (x_i, y_i) on the pairs of random variables (X,Y). Hence, estimates of $\mathrm{Var}X$, $\mathrm{Var}Y$ and $\mathrm{Cov}(X,Y)$ have to be created. These are given by

$$\widehat{\mathrm{Var}X} = S_{xx}/N \tag{9.7}$$

$$\widehat{\mathrm{Var}Y} = S_{yy}/N \tag{9.8}$$

$$\widehat{\mathrm{Cov}(X,Y)} = S_{xy}/N \tag{9.9}$$

where $S_{xx} = \sum_{i=1}^{N}(x_i - \bar{x})^2$, $S_{yy} = \sum_{i=1}^{N}(y_i - \bar{y})^2$, $S_{xy} = \sum_{i=1}^{N}(x_i - \bar{x})(y_i - \bar{y})$, and N is the number of samples. $\bar{x}$ and $\bar{y}$ represent the averages of x and y, respectively. Combining these gives the estimator for ρ:

$$\hat{\rho} = R = \frac{S_{xy}}{\sqrt{S_{xx}S_{yy}}}.[49] \tag{9.10}$$

The random variable R^2 represents the proportion of variability of one variable explained by the other. When this proportion is multiplied by 100%, we obtain a statistic called the *coefficient of determination*. [49]

A significant correlation coefficient between X and Y does not necessarily imply that variations in X cause variations in Y, or vice versa. I.e. it does not reveal the causality between the variables. Sometimes the correlation results simply from both X and Y being associated with a third variable that might have causal influence on both X and Y. However, if a significant R is found between X and Y so that X has been delayed with respect to Y, there is some indication that Y may have been caused by X.

The Pearson correlation coefficient has the restriction that it assumes the variables X and Y to be normally distributed. If X and Y cannot be assumed to be normally distributed, even approximately, the reliability of ρ is reduced.

9.4.2 Hypothesis Testing and Statistical Significance

Consider some population parameter, θ, for which there is some preconceived notion. The value of θ has now been approximated based on a sample. It is to be determined whether or not the sample value is in concordance with the preconceived notion. This situation is typically formulated as hypotheses. The *null hypothesis* H_0 states that the true value of θ (which has been approximated based on the sample) truly equals the preconceived value θ_0, "the null value". The *alternative* or *research* hypothesis H_1 states that the true value of θ is not equal to θ_0. The purpose of the experiment is to decide whether the evidence tends to refute the null hypothesis. [49]

The *P value* gives the probability that the difference of θ from θ_0 is due to random chance. The difference is said to be *statistically significant* if the P value is smaller than some fixed level, α. If the difference is statistically significant, we reject the null hypothesis and accept the alternative hypothesis. Often $\alpha = 0.05$ is used, i.e. there is 5% possibility that the difference is caused by chance. It is common to report the smallest fixed level at which the null hypothesis can be rejected. [49]

The null hypothesis for a correlation coefficient, $\rho = 0$, may be tested by use of the T distribution (*Student's t*) whose sample value is

$$t_{n-2} = \frac{R\sqrt{N-2}}{\sqrt{1-R^2}}, \tag{9.11}$$

R being the estimate of correlation coefficient and N the number of pairs of samples. The t-test is *two-tailed*. Given the sample value t_{N-2}, it is needed to find the p which fullfills the condition $P(|T| \geq t_{N-2}) = 2p$.

In the case of a correlation, the primary goal is often to show that significant correlation really exists between two variables. In that case, H_0 would state that there is no association between the variables ($\rho = 0$), and H_1 that the correlation exists ($\rho \neq 0$).

At the end of any study we will be forced into one of the following situations:

1. We will have rejected H_0 when it was true. (*Type I error*)
2. We will have made the correct decision of rejecting H_0 when the alternative H_1 was true.
3. We will have failed to reject H_0 when the alternative H_1 was true. (*Type II error*)
4. We will have made the correct decision of failing to reject H_0 when H_0 was true. [49]

In this study the hypotheses might be given as:

H_0: ρ between the geomagnetic activity and acoustic power is zero. If $p \leq \alpha$, reject H_0 and accept H_1.

H_1: $\rho \neq 0$.

However, since the correlations performed in this thesis are given as a function of lag, or, of lag and frequency, the formulation of the hypotheses is not a straightforward process. A separate hypothesis is given for each lag and frequency band, resulting in hundreds of different hypotheses. In this kind of a complicated situation, it is important that there is a decent assumption of the underlying physical processes. If a high correlation occurs at a lag or frequency which is in concordance with some physical model, the significance of the correlation is increased.

9.4.3 Properties of Time Series

The geomagnetic and acoustic data are time series, which makes the situation more complicated than in the case of randomly sampled data. It is possible to classify time series as being either *stationary* or *nonstationary*. In time series analysis a common practice is to divide the data into successive segments, usually of equal length, and to choose some statistical parameter, such as the mean, to characterize the data within each segment. If the expected value of the statistical parameter is the same for each section, the time series is stationary; otherwise, it is nonstationary. [18]

In general, a time series can be separated into different components. Kendall [36] suggests the following decomposition:

a) a trend, or long-term movement;

b) fluctuations about the trend of greater or less regularity;

c) a seasonal component;

d) a residual, irregular, or random effect.

In time series there is a tendency for the values to cluster, in the sense that high values tend to follow high values and low values tend to follow low values. Thus, the samples are not independently distributed in time. Often, a time series is considered to be composed of two main components: a *random element* and a *nonrandom element*. A nonrandom element is said to exist when observations separated by k time units are dependent. The nonrandom element may be composed of a trend, or a long-term movement, fluctuations about the trend, and a seasonal component. These parts need not be present in a time series. Often, the first step in analyzing a time series is to separate the nonrandom element from the random element. [18]

Since correlation assumes independence of the observations, there is a need to modify it when computing the significance of a correlation for a time series. One such modification is to replace the true sample size N by "effective" sample size N'. For very large sample sizes,

$$N' = \frac{N}{1 + 2r_{1,x}r_{1,y} + 2r_{2,x}r_{2,y} + \dots} \tag{9.12}$$

where $r_{1,x}$, $r_{2,x}$, ... are *serial correlation coefficients* for the time series x, and $r_{1,y}$, $r_{2,y}$, ... are serial correlation coefficients for the time series y [18].

The kth serial correlation coefficient or *autocorrelation* at lag k is defined as

$$r_k = \frac{\frac{1}{N-k}\sum_{i=1}^{N-k}(x_i - \bar{x})(x_{i+k} - \bar{x})}{\frac{1}{N}\sum_{i=1}^{N}(x_i - \bar{x})^2}. \tag{9.13}$$

[36]

If each of the time series is considered to be generated by a first-order *Markov process*, i.e. each sample of time series depends only on the sample preceding it (*lag*-1), the Equation 9.12 becomes

$$N' = N\frac{1 - r_{1,x}r_{1,y}}{1 + r_{1,x}r_{1,y}} \tag{9.14}$$

Clearly, if either time series is random ($r_{1,x} = 0$ or $r_{1,y} = 0$), the effective sample size equals the true sample size, $N' = N$. [18]

Trend Analysis

Trend is usually thought of as a smooth motion of a time series over a long period of time. In time series, the sequence of values follow an oscillatory pattern. If this pattern indicates a more or less steady rise or fall, it is defined as a *trend*. However, especially when the time series is short, it may be difficult to tell with certainty that an apparent trend is not part of a slow oscillation. [18]

Presence of similar trends in two variables X and Y to be correlated will frequently result in a high correlation. This is so even when the trend in X is not the cause of the trend in Y or vice versa, the two trends being due to a common third cause or pure accident. Since the trend often tends to play such a dominant role, it is often "eliminated" from the data and the remaining residuals are correlated. This is by no means the only right solution and cannot be done blindly unless we have a good understanding of the phenomenon we are studying. Sometimes it may happen that, eventually, the trends are the variables that should be studied. Some considerations of the trend removal problem have been presented by Roos [61].

In the simplest case the trend is clearly linear and it can be found by fitting a line to the data. In the event of a nonlinear trend, one possible solution is to fit a polynomial of higher order to the data. However, for the reasons discussed, e.g. by Kendall [36], a more practical way to do this is to smooth out irregularities in the time series by the use of moving averages. For observations x_1, x_2, ..., x_i, ..., x_N we may use moving averages with a length of three ($m = 3$) for example. The samples of the trend, y_i, are then given by

$$y_i = \frac{b_1 x_{i-1} + b_2 x_i + b_3 x_{i+1}}{3} \tag{9.15}$$

where

$$\sum_{i=1}^{m} b_i = m. \tag{9.16}$$

It is usually convenient to use odd numbers as the moving average length m. The case where all the weights equal 1 is called the *simple moving average*. The increase in length of the moving average has the effect of making the trend smoother. In general, there is no simple answer to the question of what the length of the moving average should be or how the weights should be chosen. Kendall [36] presents some considerations on these questions. After the trend has been established it is possible to remove it from the data by taking the deviations about the trend line as a new variable.

When using the moving-average method, consequences known as *Slutzky-Yule effect* must be taken into account. If a moving average is used to determine the trend, a long-time oscillation tends to be included as a part of the trend. Oscillations which are comparable to the length of the moving average, m, or shorter, are damped out. The moving average also

introduces an oscillatory component into the random element. The induced oscillation has a variance and average period that depend upon the weights and the length of the moving average used [18, 36]. According to Dawdy [18], the use of a weighted, instead of a simple, moving average results in a magnified Slutzky-Yule effect. When performing correlation, it is important to control that the correlation is not caused by the similar type of oscillations that have been introduced to both data by the use of moving averages.

Alternatively, moving median can be used instead of moving average. The main advantage of median as compared to moving average smoothing is that its results are less biased by outliers[1] within the smoothing window.

Kendall [36] says that any moving average is likely to distort the cyclical, short-term and random effects in a series, and that in some cases it is desirable to try several averages to see which of the results most nearly corresponds to the object of the analysis.

After the trend has been established, it can be removed from the original time series by subtraction. We are left with a fluctuating series which may, at one extreme, be purely random, or, at the other, a smooth oscillatory movement. For the most part we have something between these two. [36]

9.4.4 Rank Correlation

Rank correlation is based on arranging the data in *ranked* order, i.e. they are ordered according to some quality (size, importance, etc.). This arrangement as a whole is called a *ranking* in which each member of the data has a *rank*. [35]

A ranking may be regarded as a less accurate way of expressing the ordered relation of the members because it does not tell us how close the various members may be on the scale. However, though the ranking loses in accuracy, its generality acts as a benefit. It does not make any assumptions of the data, and thus is distribution independent.

Instead of the linear relationship, rank correlation measures the degree of *monotonic* relationship. A monotonic relationship exists when any increase in one variable is invariably associated with either an increase or a decrease in the other variable.

Spearman Correlation Coefficient

Rank correlation is usually expressed as *Spearman's* correlation coefficient. Assuming there are no ties in either data, for two variables, X and Y, the Spearman's correlation

[1] An outlier is a data point that is located far from the rest of the data. Given a mean and standard deviation, a statistical distribution expects data points to fall within a specific range. Those that do not are called outliers and should be investigated.

coefficient is given by

$$R_s = 1 - 6\frac{\sum_i d_i^2}{N(N^2-1)} = 1 - 6\frac{S(d^2)}{N(N^2-1)} \tag{9.17}$$

where N is the number of pairs of values (x, y) in the data and d_i is the difference between the ranks of x_i and y_i [12, 35]. The interpretation of the value of R_s is similar to that of the Pearson's correlation coefficient: $R_s = 0$ indicates no correlation between the data, $R_s = 1$ perfect positive correlation, and $R_s = -1$ perfect negative correlation.

The test of significance is similar to that of the Pearson correlation coefficient. If population correlation is zero, then as N increases, the distribution of

$$t_{N-2} = \frac{R_s\sqrt{N-2}}{\sqrt{1-R_s^2}} \tag{9.18}$$

approaches closer and closer to the distribution of Student's t with $N-2$ degrees of freedom [12]. For $N > 20$ it is probably accurate enough to use these expressions on the assumption of normality in the sampling distribution [35].

9.4.5 The Practical Correlation Computation between Geomagnetic Activity and Acoustic Power

For the correlation, the same number of samples of two variables per time unit are needed. The simplest way to achieve this is to correlate the acoustic power and the resultant of the differentiated geomagnetic field data, which are both given with a rate of 1 sample per second. Since there is serial dependence in samples of the time series, it is more reasonable to divide the data into longer time blocks and to take the mean or SD of the samples within each block. The segmental divisions could be performed at the magnitude of perhaps 30 seconds to several minutes. This method lessens the serial correlations of the variables and eases the computational burden.

In [42], the resolution reduction was performed by low-pass filtering and downsampling. This has, however, the drawback that most of the data is "wasted". If the data is downsampled by a factor of M, only every Mth sample of data is used. Instead, if mean or SD within a time block is taken, all the samples are used. This is why it seems more reasonable to use the latter procedure.

The variables x and y corresponding to geomagnetic activity and acoustic power, or the fluctuation of acoustic power, are now formed. SD σ of a random variable X may be estimated as

$$\hat{\sigma} = \sqrt{\frac{S_{xx}}{N-1}} \tag{9.19}$$

where $S_{xx} = \sum_{i=1}^{N}(x_i - \bar{x})^2$ and N is the number of samples. The formation of the variables to be correlated and the correlation are summarized as follows (illustrated in Figure 9.4):

1. The size of the time block, T_b, is chosen (e.g. $T_b = 1$ min).
2. SD of each component of the geomagnetic field is computed within each block. The resultant of these components is formed. Denote the resulting vector by x' (Figure 9.4c).
3. Either the mean or SD of the acoustic power is computed within each block. Denote the resulting vector by y' (Figure 9.4d). This can also be performed separately for every 1/3-octave band.
4. Trend is removed from the vectors x' and y'. Denote the resulting vectors x and y.
5. Correlation coefficient is computed between the vectors x (Figure 9.4e) and y (Figure 9.4f).

To simplify things, the detrended variables x and y shall be respectively called geomagnetic activity and acoustic power from now on. In the case that SD is used for acoustic data, y will denote the fluctuation of acoustic power. The correlation is computed with different lags between the two data. We have, in practice, an unlimited access to geomagnetic data before and after the acoustic measurement. Therefore, it is easiest to achieve different lags by fixing the acoustic sequence and shifting the geomagnetic sequence.

If we are intending to use the Pearson correlation coefficient, the distributions of the variables x and y are desired to be Gaussian (at least approximately). Figure 9.5 gives the distributions of variables x and y computed in blocks with $T_b = 60$ s for examples of geomagnetic and acoustic data. It becomes clear that the distributions of x' and y' are nonnormal. This might suggest that the Spearman correlation coefficient should be used. On the other hand, the Spearman correlation has a poorer precision which is undesirable. The solution might be to report both the Pearson and Spearman correlation coefficients.

If the trend is removed from the variables x' and y', the distributions of the resulting variables x and y are remarkably closer to normal (see Figure 9.6). Therefore, it seems reasonable to report the Pearson correlation coefficients if the trend has been eliminated.

The effect of the length of the simple moving average is illustrated in Figure 9.7 for acoustic power. The samples are given in intervals of 1 minute. It is clearly seen how the increase in the number of coefficients leads to a smoother trend.

One might still ask whether we should worry about the consequences of the Slutzky-Yule effect. This question can be answered by performing a practical permutation test.

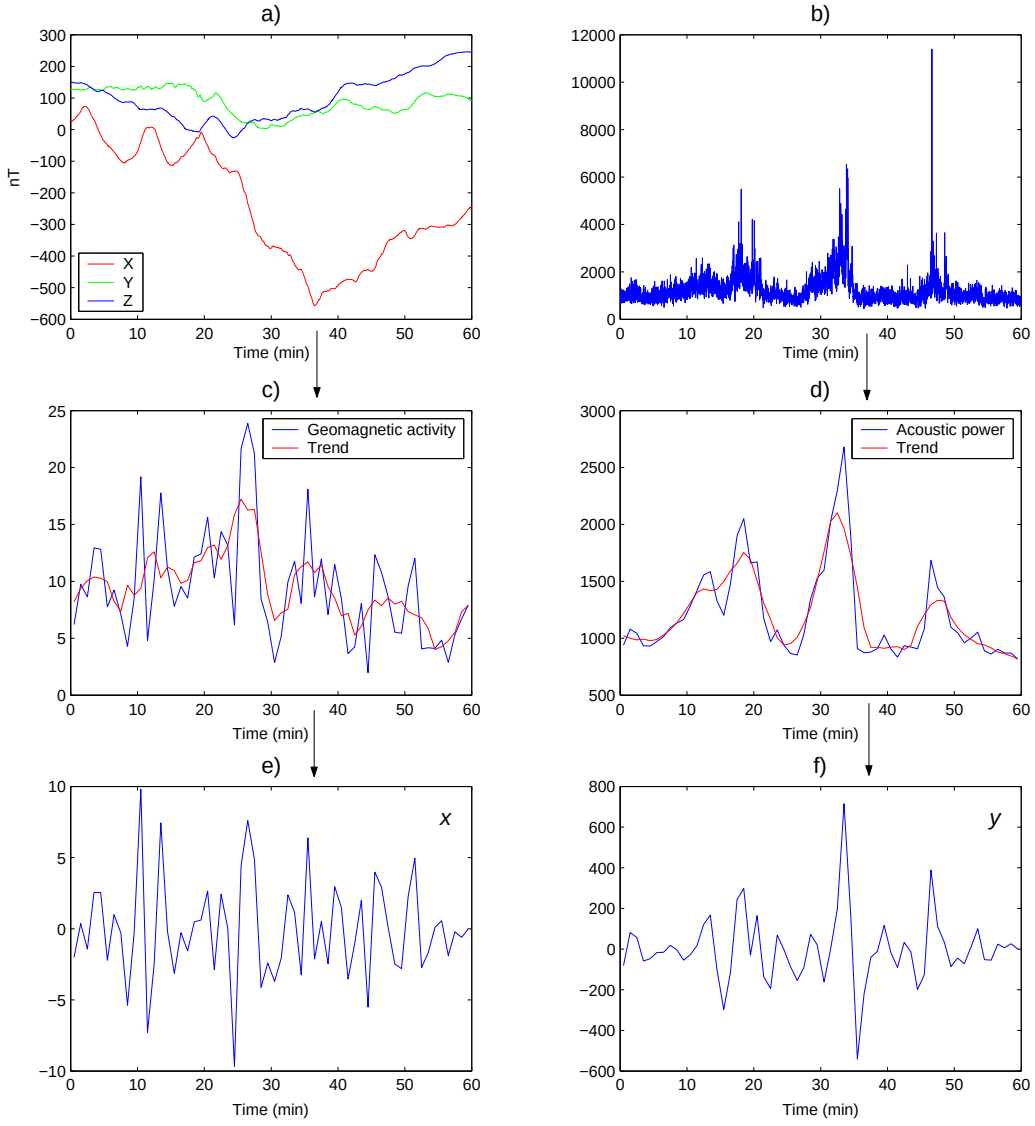

Figure 9.4: The figure illustrates the computation of the variables to be correlated. The X-, Y-, and Z-components of the geomagnetic field data are given in a) and the acoustic power in b). The variable corresponding to geomagnetic activity (c) has been computed by forming the resultant of the SDs of the different components shown in a) in sequential blocks of 2 minutes ($T_b = 2$ min). The variable corresponding to acoustic power (d) has been computed by taking the mean from b) in sequential blocks of 2 minutes ($T_b = 2$ min). The trends established with a simple moving average ($m = 5$) are also plotted in c) and d). The variables to be correlated, x and y, are given in e) and f), respectively.

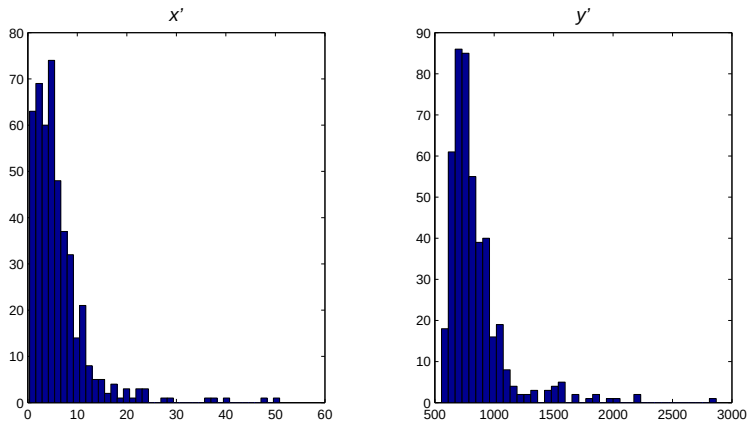

Figure 9.5: Distributions of variables corresponding to geomagnetic data, x', and acoustic data, y'.

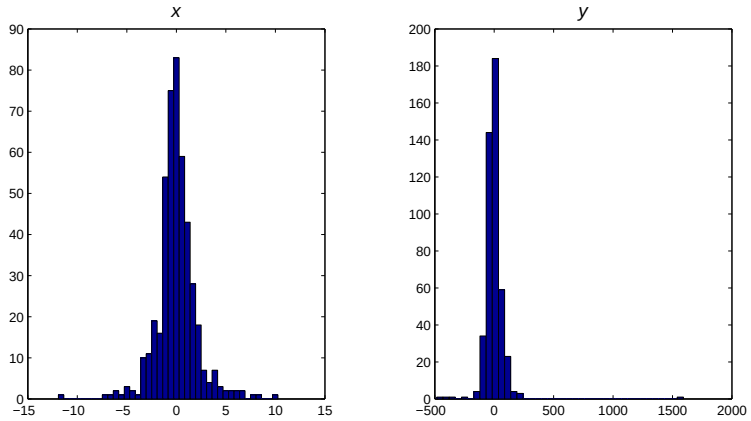

Figure 9.6: Distributions of variables corresponding to detrended geomagnetic data, x, and acoustic data, y.

100 samples of geomagnetic and acoustic data from an example measurement were taken, corresponding to variables x' and y'. The samples of the acoustic power were put into a random order, while the samples of geomagnetic activity were kept in original time order. Both data were then detrended and the resulting variables were correlated. This operation was repeated 10 000 times and the correlation coefficient was stored each time. By randomizing one data set, the resulting distribution of the coefficients should be close to normal in the absence of undesirable effects. As a reference, two random sequences, both of 100 samples, were generated and the correlation coefficient was computed between them. This was also repeated 10 000 times. The correlation coefficients computed from the random sequences approximate the normal distribution. If the distribution of correlation efficients

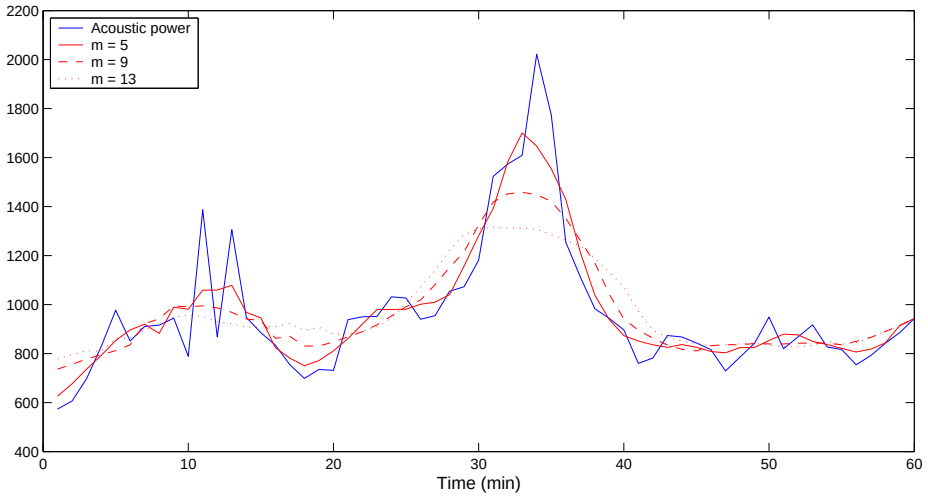

Figure 9.7: Acoustic power and trends established with simple moving averages with lengths $m = 5$, $m = 9$ and $m = 13$.

of the example data violates normality remarkably, it might indicate that the Slutzky-Yule effect has generated similar oscillations in both the geomagnetic and acoustic data, which are then "picked" by the correlation.

Figure 9.8 shows the result of this test. It is seen that the detrending has the effect of increasing the amount of higher correlations slightly while the amount of very small correlation coefficients is reduced. Nevertheless, it can be concluded that this is not too dramatic and does not prevent us from the use of the detrending operation if the Slutzky-Yule effect is kept in mind when interpreting the results. The same test was also performed using a moving median. This did not change the results noticeably.

Finally, the whole correlation procedure is concluded in Figure 9.9 as a block diagram.

9.5 The Results

The results gained with the introduced methods are now presented. Overall characteristics of the most interesting measurement are first given, after which the correlation results are presented.

9.5.1 Overall Characteristics of Acoustic and Geomagnetic Data: Measurement in Koli, April 11$^{\text{th}}$, 2001

A look is now taken at a measurement which appears to be the most interesting one up to time of this writing. The analyses of this thesis are performed using the data of this

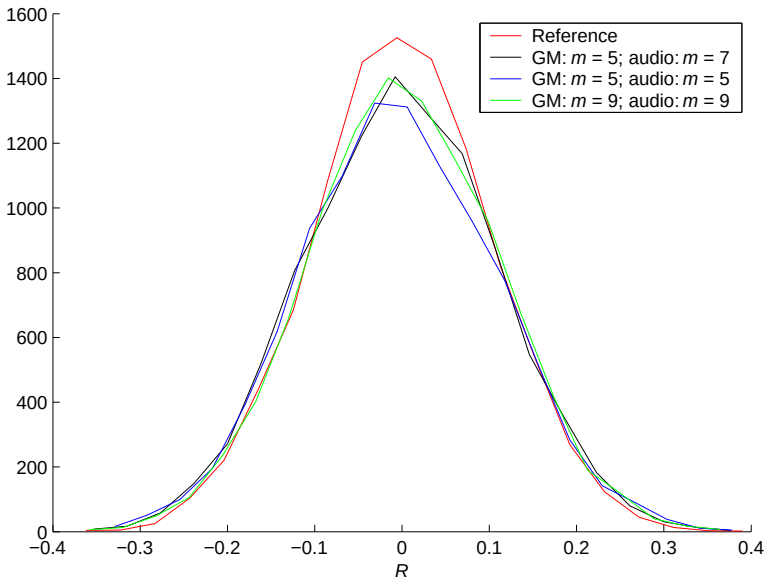

Figure 9.8: Permutation test of the effects of detrending by simple moving averages on correlations. The geomagnetic and acoustic data were detrended with simple moving averages of different lengths and then correlated. The interval $-1.0 \leq R \leq 1.0$ was divided into 20 equally spaced blocks and the number of the points falling to each block is now presented.

particular measurement.

A relatively strong geomagnetic storm (Kp = 8) took place on April 11^{th}, 2001. A measurement of acoustic and electric field signals was carried out during this storm at Lake Pielinen in Eastern Finland, close to Koli hill. The closest place for geomagnetic measurements was in Hankasalmi, about 210 km southwest from Koli. Some preliminary results from this occasion have been presented by Laine *et al.* [42].

There are basically two reasons why this measurement is particularly interesting. One reason is that the circumstances were favorable for an acoustical measurement: the weather was clear and still, and there was relatively little ambient and man-made noise during the recording session. The second and more important reason is that in the recorded audio there are many sound events which have common characteristics with the observations of aurora related sounds and whose sound sources cannot be identified. It was well-grounded to use this recording for closer analysis.

The temperature profile provided by FMI is given in Figure 9.10. At the beginning of the measurement the temperature was about $-2°$C and it decreased to $-4.7°$C. The wind speed during the measurement was 0 m/s. At 19 UT the relative humidity of air was 72% and it decreased during the measurement so that it was 87% at 23 UT.

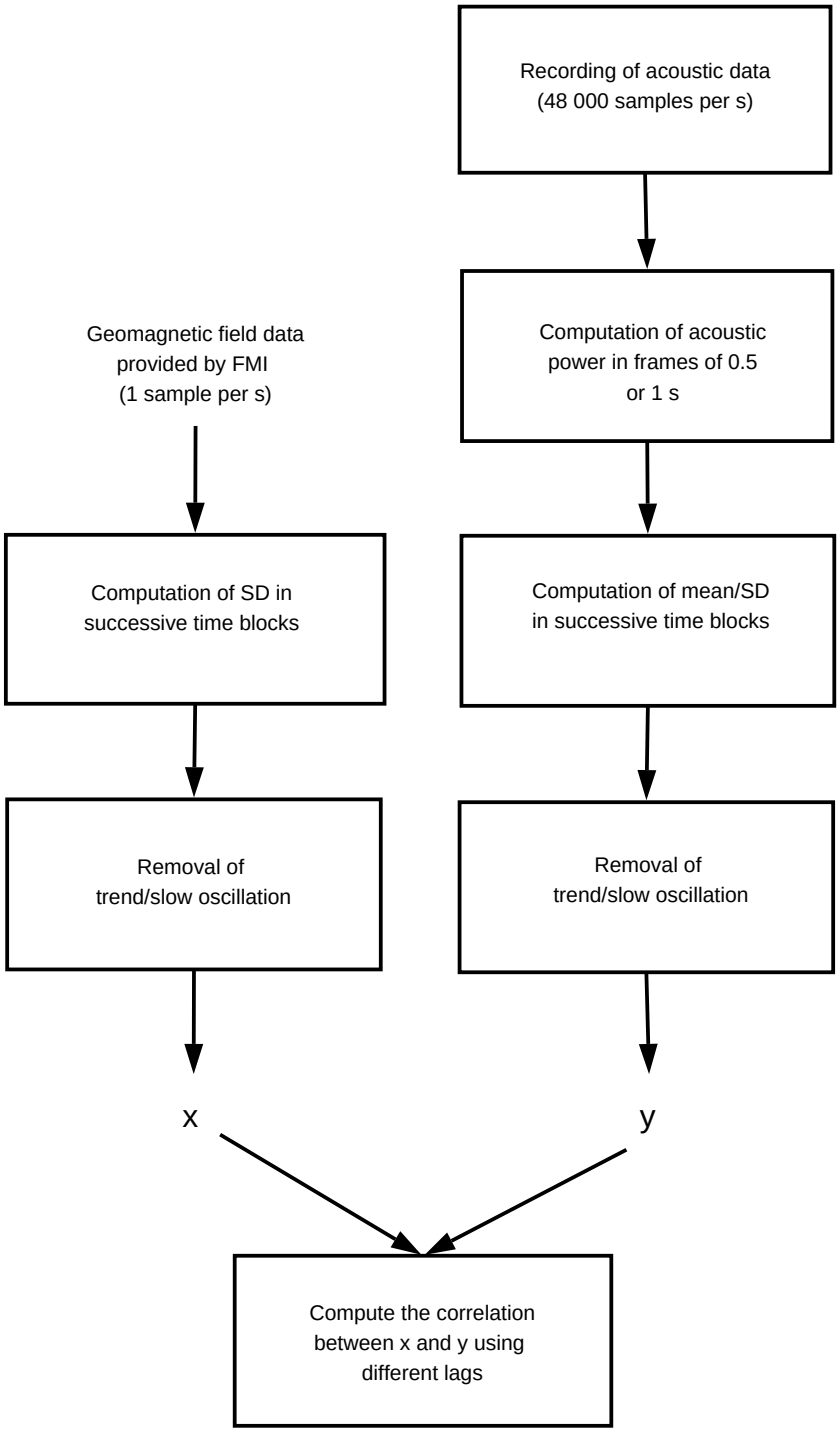

Figure 9.9: Block diagram of the correlation procedure between the geomagnetic field data and acoustic data.

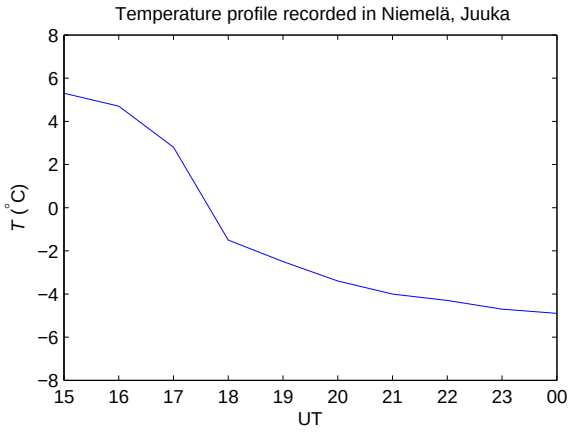

Figure 9.10: Temperature profile recorded by FMI on April 11$^{\text{th}}$, 2001, in Niemelä, Juuka about 12 km from the place of measurement of acoustic and electric field signals. The LT is UT + 3 hours.

The SD of the geomagnetic field during the hours starting at 19, 20, 21 and 22 UT is given in Figure 9.11.[2] As the figure shows, the highest geomagnetic activity was experienced during the hours starting at 21 and 22 UT.

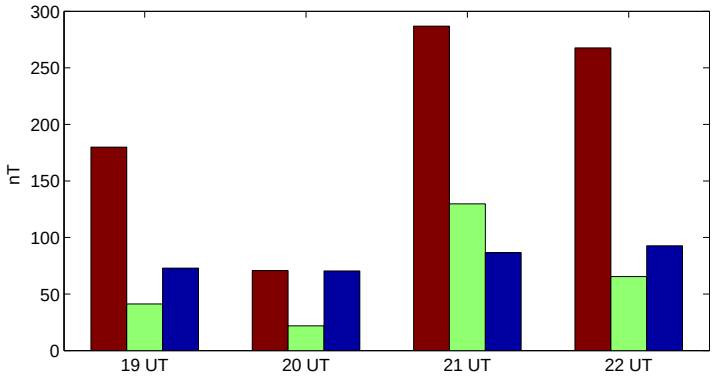

Figure 9.11: SD of the geomagnetic field recorded by FMI in Hankasalmi, April 11$^{\text{th}}$, 2001. X-component is marked with red, Y-component with green, and Z-component with blue.

Average acoustic power measured in 1/3-octave bands during these four hours are shown in Figure 9.12, where the mean acoustic power is plotted on an arbitrary dB scale together with the SD. It is seen how the infrasound region dominates the total acoustic power. It is also seen that the SD of the acoustic power strongly correlates with the averaged power.

[2]The deviations for these hours were also presented in [42], but the SDs of the Y- and Z-components were erroneously computed. Nevertheless, only the X-component was used in the analyses carried out in that publication.

Broad-band fluctuation of acoustic power on the frequency range from 1 kHz to 10 kHz was noted by Laine *et al.* [42]. Some of this fluctuation was caused by activities related to the recording session, and corresponding parts of the recording were left out when computing the mean and SD presented in Figure 9.12. Nevertheless, some increased broad-band fluctuation of acoustic power remained within the same frequency range. It was also found that some of the increased power around 1 kHz during the hours starting at 19 UT and 21 UT was caused by birds.

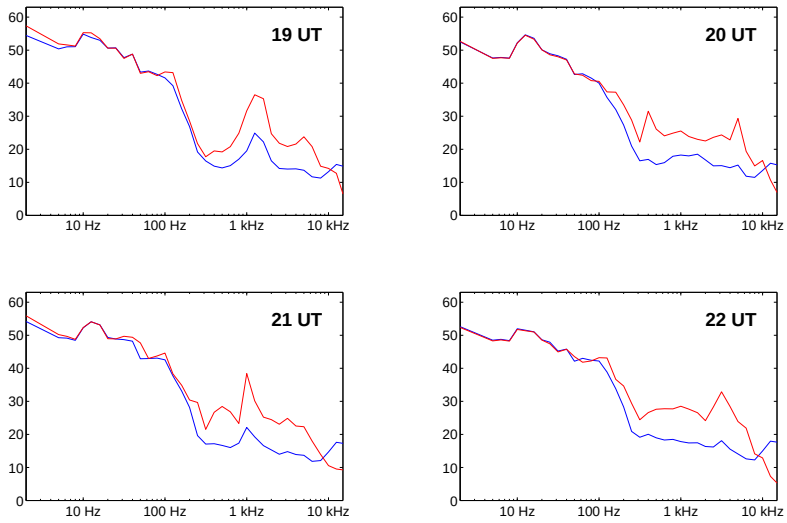

Figure 9.12: 1/3-octave analysis of acoustic power (blue) and its fluctuation (red) in Koli, April 11$^{\mathrm{th}}$, 2001. The scale is an arbitrary dB scale.

The measured SPLs and geomagnetic data between 19 and 23 UT (22–02 LT) are shown on time axis in Figure 9.13. The resultant of the derivatives of the geomagnetic field components (see Figure 9.13c) is now used as the measure of the geomagnetic activity. The geomagnetic activity experiences a peak after 21.30 UT. Clearly, at the moment of the highest geomagnetic activity, the SPL experiences a peak where it rises about 5 dB. The Figure 9.14 shows that the increase of SPL during the peak of geomagnetic activity is due to increased acoustic power in the infrasound region. For practical reasons, we now use acoustic power on an arbitrary scale instead of exact SPLs.

As the Figure 9.14b shows, the increase of acoustic power is most distinct at frequencies below 4.45 Hz. The peak around 21.30 UT diminishes as the frequency grows and is hardly detectable at frequencies of 8.94–11.18 Hz. Before this peak there is some increased noise in the audio frequencies caused by a vehicle. However, the infrasound continues to increase several minutes after the vehicle is no longer detectable in the audio, and therefore we cannot conclude that the infrasound peak is caused by the vehicle. It should also be noted

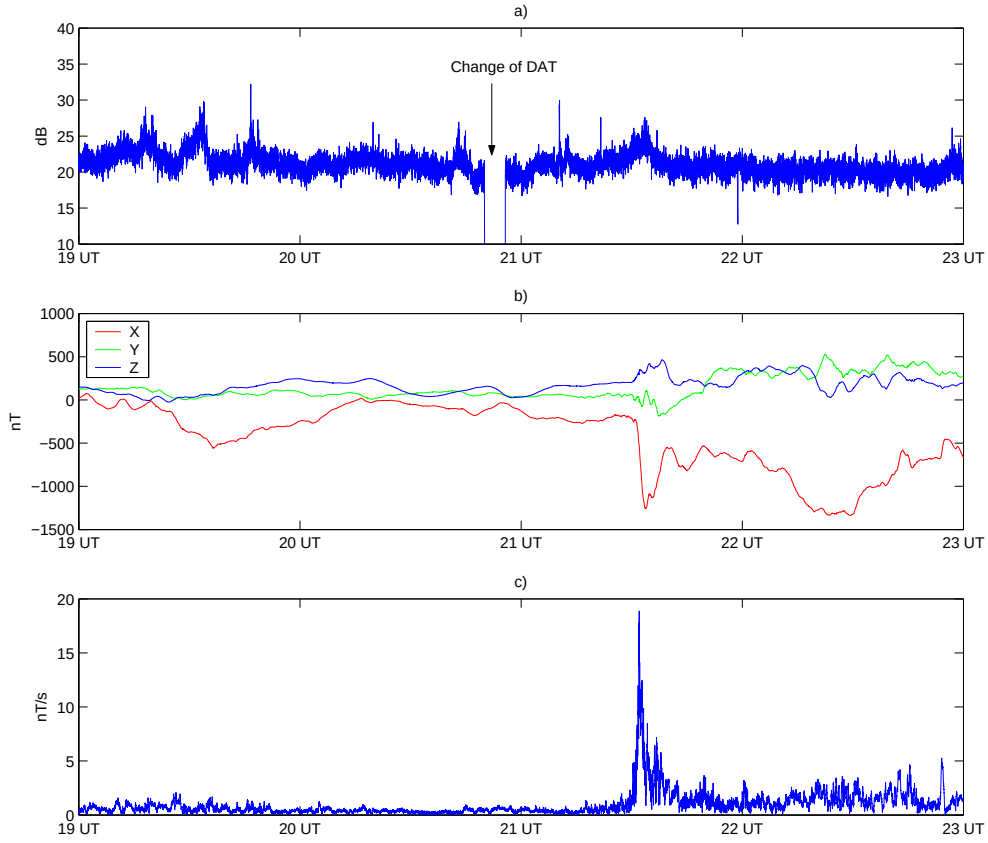

Figure 9.13: The SPLs measured in Koli on April 11$^{\text{th}}$, 2001, are presented in a), the components of dynamic geomagnetic field measured in Hankasalmi in b), and the resultant of the derivates of the geomagnetic field components in c).

that during the peak in infrasound there are many audible sound events, such as cracks, which fit into the characteristics of aurora related sounds.

There is another peak in the infrasound around 19.30 UT. However, the audio signal gives us hints that this may have been produced by a vehicle.

Furthermore, it should be noted that there is no clear correlation between the temperature profile (see Figure 9.10) and the acoustic power.

9.5.2 Correlation with Trend Removal

The correlation analyses are now considered. The Figure 9.13 shows that the time series concerned were nonstationary. For instance, after the peak in geomagnetic activity around 22.30, the geomagnetic activity stabilizes to a higher level than what it had before the peak. The stationarity is increased if the time block (T_b) within which the parameters describing

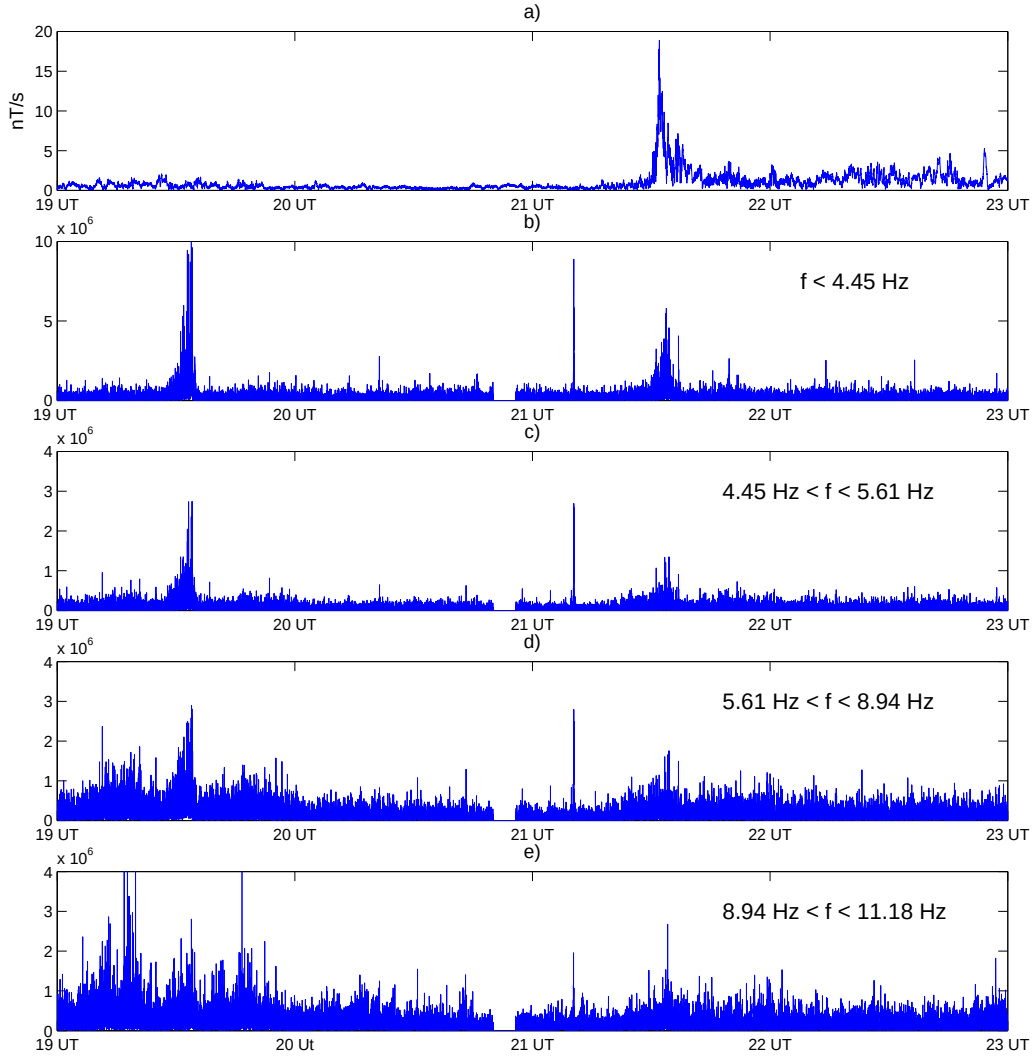

Figure 9.14: Resultant of the derivatives of the geomagnetic field components (a) and acoustic power at different frequencies of infrasound (b–e).

the data are computed is increased. However, the time block should be very large which would result in a small number of samples. Hence, an easier approach to solve the problem of nonstationarity is to remove the nonrandom trend from both data by moving averages and to compute the correlation between the residuals. This allows us to keep the time block relatively short and, correspondingly, to have a relatively large number of samples.

It can be assumed that the background level of acoustic power is primarily determined by ambient noise rather than auroral processes. This level may experience slow diurnal variation and it is desirable to remove it from the series. This is another motivation for us

to remove the trend before computing the correlation.

Since the use of a weighted moving average is likely to strengthen the Slutzky-Yule effect, only simple moving averages were used for detrending.

Outliers were eliminated by rejecting pairs of values that differ from the mean of either (detrended) geomagnetic or (detrended) acoustic data by twice the SD. This criterion was used in all correlation analyses performed in this thesis except one case that is noted separately.

Case 1: Koli; April 11$^{\mathrm{th}}$, 2001; 21.45 to 22.55 UT.

The Pearson correlation coefficients between the geomagnetic activity and acoustic power, and between the geomagnetic activity and fluctuation of acoustic power during geomagnetically the most active part of the Koli measurement are plotted in Figure 9.15 as a function of lag. The lag is now the amount by which the geomagnetic data has been delayed with respect to the acoustic data. The correlation was computed for the time interval 21.45–22.55 UT. There was some noise caused by activities related to the measurement session after 22.55, and therefore data thereafter was not included. If the data before 21.45 had been taken, the peak of geomagnetic activity right after 21.30 would have been included as an outlier, causing some biasing. The block length used was $T_b = 60$ s. Both the geomagnetic and acoustic data were detrended by simple moving averages of five points. Multiple hypothesis, each of which corresponds to a different lag, were tested. The P values are plotted below the correlation coefficients. The P values were computed using the equation 9.11 with the effective sample size given by the equation 9.14.

Both of the correlation coefficient plots experience fluctuation about zero. The maximum correlation coefficient between the geomagnetic activity and acoustic power is 0.36, and it is achieved with a lag of 626 s. The maximum correlation coefficient between the geomagnetic activity and the fluctuation of acoustic power is 0.20 and it is achieved with a lag of 124 s. The behaviour of both coefficients is remarkably similar. The P values are remarkably low at these lags. However, the interpretation of the correlation coefficients is challenging for it is difficult to tie them to some physical model.

The correlation curve in Figure 9.15 is somewhat smooth: correlations at lags close to one another tend to have values close to one another. This is because the block length is $T_b = 60$ s. If the lag is changed by 1 s, only $1/60$ of the geomagnetic data is changed and the acoustic data is kept fixed. As a result, the correlation does not change remarkably. Also, if the correlation truly exists, it is likely that the lag giving the maximum correlation is not stationary. Therefore, if the correlation is computed between relatively long data sequences, surfaces are also smoothed because of this.

An interesting result was obtained when the correlation was repeated using 1/3-octave

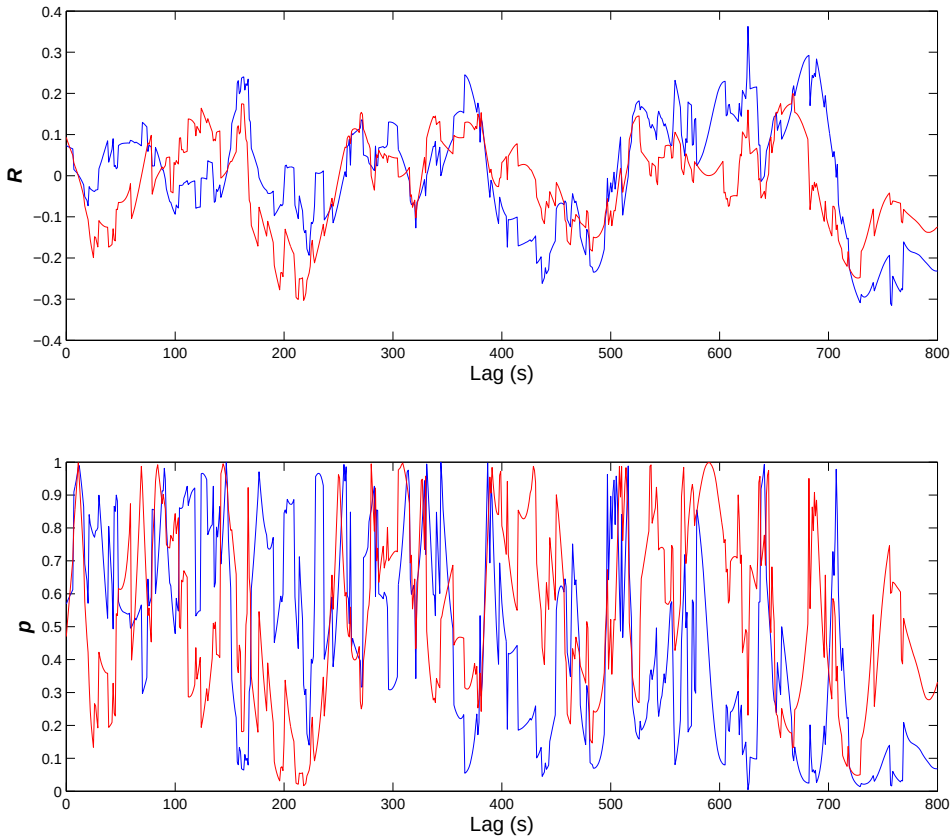

Figure 9.15: Top: The Pearson correlation coefficients between geomagnetic activity and acoustic power (blue line), and between geomagnetic activity and fluctuation of acoustic power (red line) during the geomagnetically most active part of the Koli measurement (21.45–22.55 UT). Bottom: The corresponding P values. The block length used was $T_b = 60$ s. Both the geomagnetic and acoustic data have been detrended with a simple moving average of five points.

bands. The correlation coefficients are now given as a function of lag and frequency. The resulting surfaces are shown in Figure 9.16. If the start time of the time interval is taken even earlier, e.g. from 21 UT, the picture does not change much except that the correlations decrease slightly.

It is seen that there is some increased correlation in the audio frequencies. This occurs in short lags in both correlation surfaces. In the left picture, the greatest correlation coefficient in this fragment of the surface is 0.39, around 8 kHz, and it is obtained with a lag of 29 s. The corresponding P value is 0.0013. Another interesting correlation is found in the infrasound region with a lag of about 380 s. The maximum correlation of this fragment is 0.38, around 6.3 Hz, and it is obtained with a lag of 379 s. The corresponding P value is

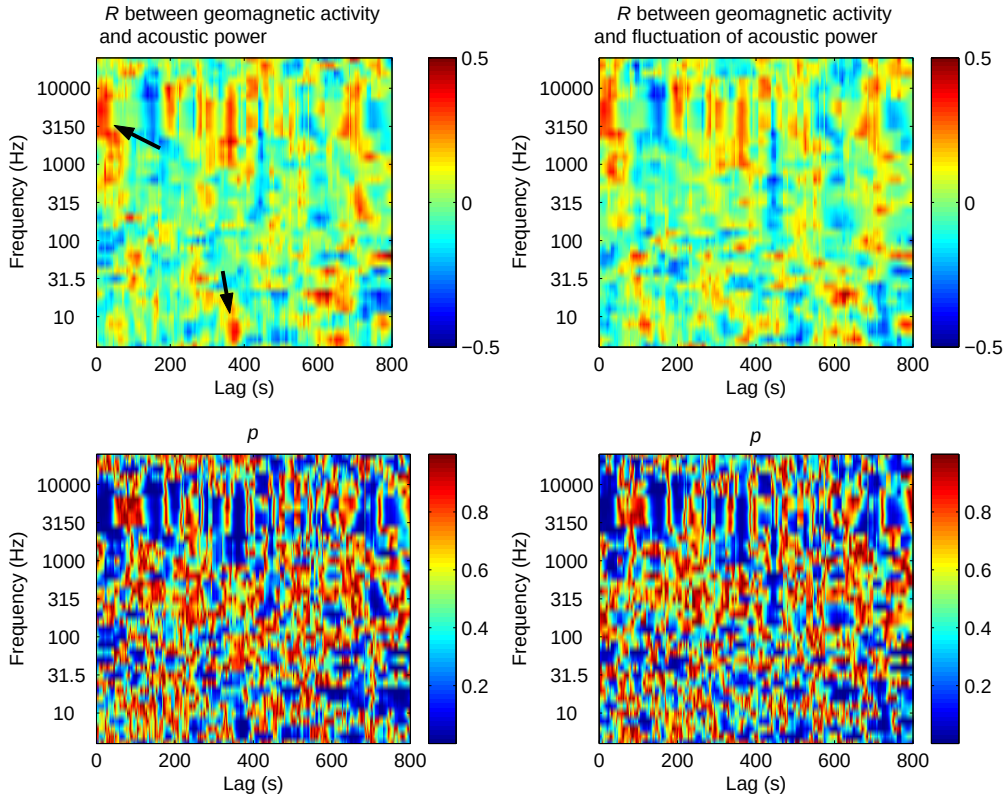

Figure 9.16: The Pearson correlation coefficients between geomagnetic activity and acoustic power within 1/3-octave bands (top left), and between geomagnetic activity and fluctuation of acoustic power within 1/3-octave bands (top right), during the geomagnetically most active part of the Koli measurement (21.45–22.55 UT). The interesting correlations are marked with arrows. The respective P values are shown below the correlation surfaces. The block length was $T_b = 60$ s. Both the geomagnetic and acoustic data have been detrended with a simple moving average of five points.

0.0021. This peak is actually present also in the correlation plot for the total acoustic power (see Figure 9.15), where the correlation is 0.24. This is reasonable because infrasound has a dominant role in the total acoustic power.

Since some hypotheses on sound production mechanisms of aurora related sound state that the sound source is probably located relatively close to the ground, the correlations in the audio range with relatively short lags are interesting. The lag of about 380 s of the infrasound region correlation suggests a distance of about 120 km, which may indicate that the sound source of the infrasound packages is in the heights of the visual aurora — this seems to give support to the work of Procunier [54].

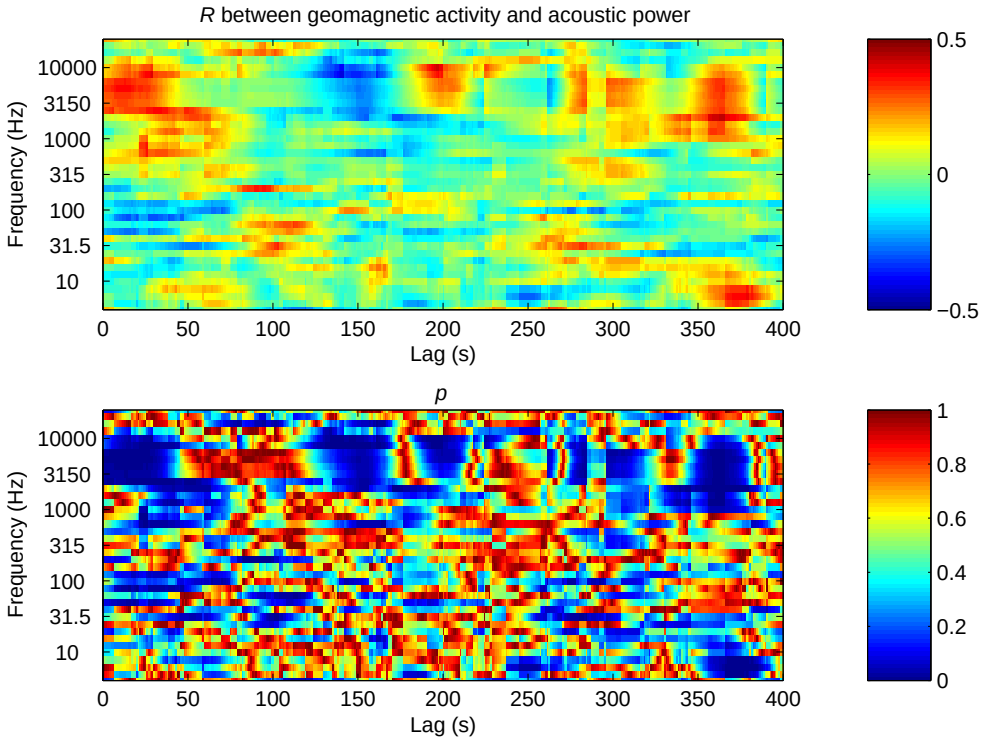

Figure 9.17: Top: The Pearson correlation coefficients between geomagnetic activity and acoustic power during the geomagnetically most active part of the Koli measurement (21.45–22.55 UT). Bottom: The corresponding P values. The block length was $T_b = 60$ s. Both the geomagnetic and acoustic data have been detrended with a simple moving average of five points.

The fluctuation of the acoustic power was intended to characterize the number of individual sound events per time unit. It was perhaps not the best possible measure because acoustic power and its fluctuation are strongly correlated and, therefore, the results obtained with them are remarkably alike. Furthermore, since the infrasound dominates in the fluctuation, too, the fluctuation cannot clearly indicate events that occur in the higher part of the audible frequency range. For these reasons, we leave the fluctuation of acoustic power to lesser notice from now on.

The lefthand surfaces of Figure 9.16 at lags of 0–400 s are now given in Figure 9.17. In the frequency range of 2.5–10 kHz, the lags at which the correlations appear are about 0–40 s. In the range of 630–2000 Hz, the correlations appear more clearly at lags of about 25–70 s.

Some other correlations emerge whose physical interpretation is difficult and may seem confusing. However, since we are dealing with a large number of data points, some “signif-

icant" correlations also arise because of random chance. Another confusing item is that the correlation coefficients in the high-frequency range have somewhat fluctuating behavior. This probably has to do with the Slutzky-Yule effect and biasing caused by some outliers. If the criterion for the outliers is made more strict, it might be assumed that the biasing caused by some single events is smaller. Therefore, the correlation was computed after the elimination of pairs of values that differ from the mean of either detrended acoustic power or detrended geomagnetic activity by once the SD. The result is shown in Figure 9.18. It is seen that the fluctuation of correlation coefficients is decreased.

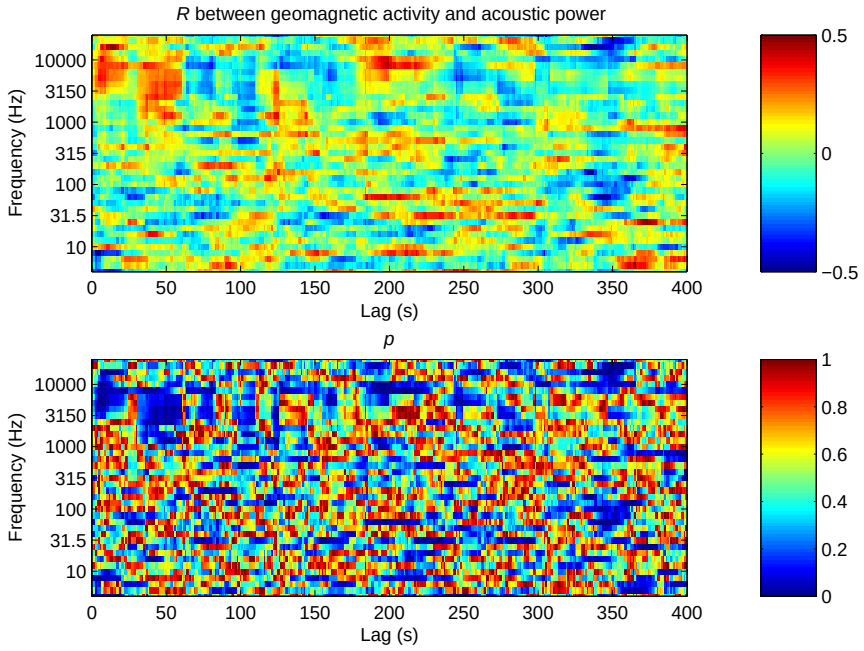

Figure 9.18: The figure was computed with the same principle as the Figure 9.17 with the exception that the criterion for outliers was "mean $\pm 1\times$ SD".

Let us consider the lags between the geomagnetic activity and acoustic data of audio frequencies with the aid of the sound absorption coefficient in air presented in Figure 6.1. The relative humidity is taken to be 85%, according its value at 21 UT. The pressure is estimated by 1 atm. The maximum correlation of Figure 9.17 occurs at 8 kHz with a lag of 29 s, which corresponds to a distance of about 9.5 km. If the attenuation of sound is taken to be 4 dB/100 m, the resulting total attenuation due to absorption alone is as huge as 380 dB. On the other hand, it seems that many maximum correlations in different frequency bands occur more distinctively at lags of 10 s or less. For instance, if we consider a distance of 3 km, corresponding to a sound propagation time of 10 s, the attenuation due to absorption is about 60 dB (2 dB/100 m) for the frequency of 5 kHz. This is already within rational limits.

It should also be noted that the acoustic reflector amplifies the acoustic signal in the most interesting direction even 21 dB, which makes it possible to detect very faint sounds.

As it has already been mentioned, there is no certainty that the hypothetical connection is such that the geomagnetic activity can lead to immediate acoustic response. The lag at which the correlation exists can be interpreted as the maximum possible propagation time of the sound. However, we have no clear understanding of the possible sound production mechanisms involved and the delays involved in these processes.

A question arises as to whether we should be worried about the nonnormality of the variables or the type of the relationship between them. Figure 9.19 shows the corresponding surfaces with Spearman rank correlation coefficients. There is no dramatic difference between the Pearson and Spearman correlation coefficients. In this surface it is, however, noticed more clearly that the maximum delay at which the correlation with short lags is noticeable decreases with increasing frequency. This could be caused by the fact that attenuation of sound increases with frequency if the lag is interpreted as the propagation time of the sound,

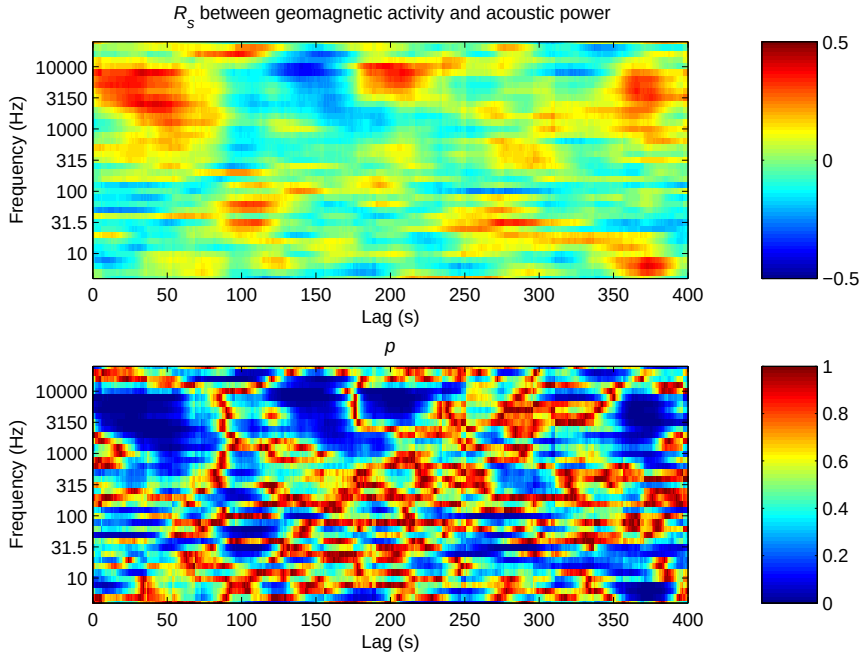

Figure 9.19: The figure has been computed with the same principle as the Figure 9.17 with the exception that the correlation coefficients are now Spearman correlation coefficients.

Case 2: Koli; April 11$^{\text{th}}$, 2001; 19.00 to 20.50 UT

Another interesting result is obtained for the geomagnetically less active part of the Koli measurement, from 19.00 to 20.50 UT. The correlation coefficient between the geomagnetic activity and acoustic power as a function of lag is shown in Figure 9.20. There is a double-peaked correlation maximum around 400 s (0.28 at a lag of 397 s and 0.3 at a lag of 459 s).

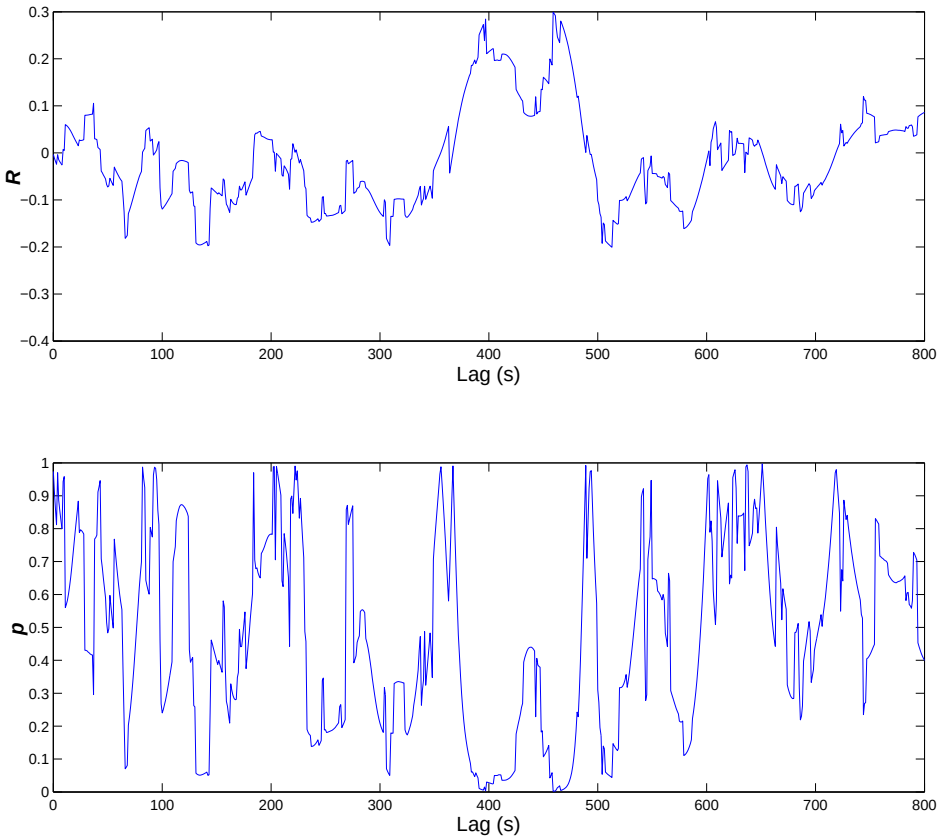

Figure 9.20: Top: The Pearson correlation coefficients between geomagnetic activity and acoustic power of the Koli measurement between 19.00 and 20.50 UT. Bottom: The corresponding P values. The block length was $T_b = 60$ s. Both the geomagnetic and acoustic data have been detrended with a simple moving average of five points.

Figure 9.21 shows that the increased correlation of Figure 9.20 is due to effects in the infrasound region. The maximum correlation coefficient is achieved around 10 Hz with a lag of 398 s. This correlation resembles the infrasound-region correlation of Case 1. However, there was increased infrasound due to distant vehicles during the time period 19.00 to 20.00 UT. Therefore, the reliability of this correlation is lower than that of Case 1.

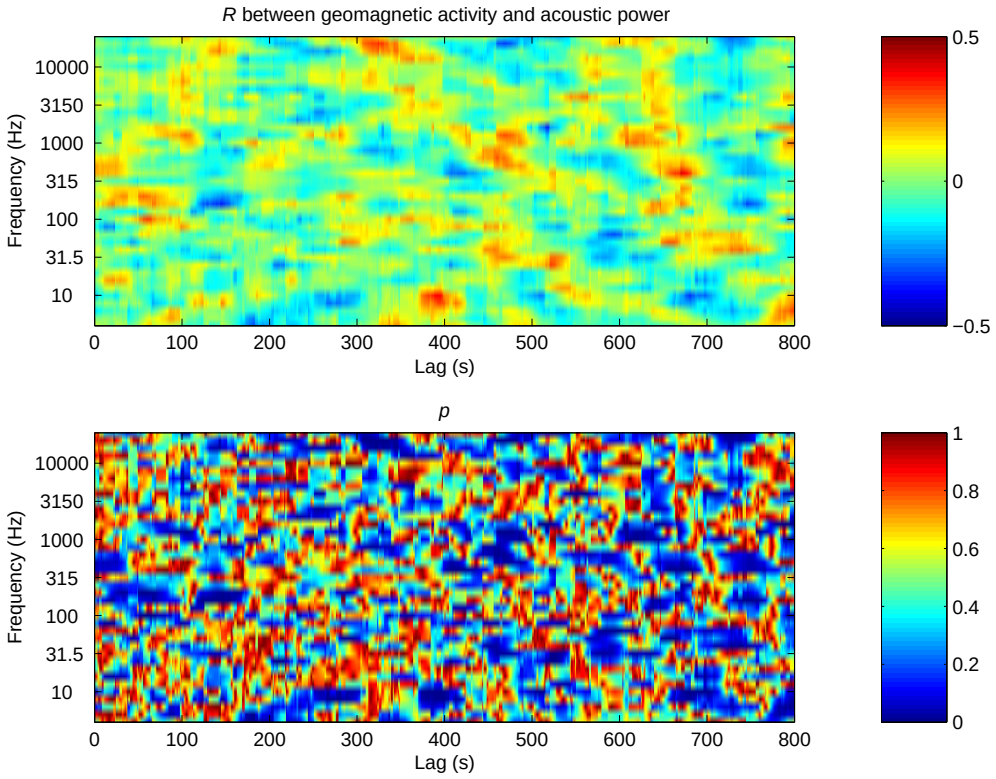

Figure 9.21: The correlation coefficients as in Figure 9.20 given now for every 1/3-octave band separately.

Stationarity of the Correlations

Since we are dealing with time series, the stationarity of the correlations need to be considered. Thus, the time periods were divided into subperiods. The correlation coefficient was computed for each subperiod separately as a function of lag and frequency. At this point it was also necessary to check that there were no known dominating sound sources that could have led to distorted correlation results.

As the data is divided into subperiods, the number of samples is reduced. A general result of this is that the number of correlations caused by a random chance is increased.

Let us first consider Case 1. The period 21.45 to 22.55 UT was divided into subperiods in two different ways and the correlation surfaces were computed for each subperiod. The correlation surfaces are given in Appendix C. It appears that there was some stability both in the correlation of the audio region, with lags of about 0–70 s, and that of the infrasound region, with lags of about 380 s. This was probably the reason why the correlations remained distinct in the “averaged” picture of Figure 9.16, while the more random

correlations noticed in the subperiods tended to vanish.

The period 21.45–22.55 UT was favorable because there was little ambient noise and lots of sound events that could be associated with the descriptions of aurora related sounds. At around 21.58–22.01 there was some disturbance caused by a GSM call but this seemed to cause no distortion to correlations. Nevertheless, the time period from 21.58 to 22.01 is left out from some of the figures of Appendix C. From about 22.22 to 22.25 there was some noise caused by a distant vehicle. This also did not seem to cause any critical distortion to the correlations.

The subperiod correlations of the Case 2 are also given in Appendix C. The infrasound-region correlation is most obvious during the time periods 19.30–19.45 UT and 19.45–20.00 UT.

The Effect of the Block Length on the Correlations

It is now briefly considered to what degree the correlations depend on the length of the block, T_b, in which the mean and SD were computed in subsection 9.4.5.

In Case 1 it was found that the interesting correlations disappear if T_b is made smaller than 60 s. The increase of T_b did not result in a rapid change of correlation coefficients. The correlations in the audio range were still notable with $T_b = 150$ s, but the infrasound region correlations disappeared soon after the T_b was made bigger than 90 s.

In Case 2 the increase of T_b had an effect on the infrasound correlation similar to that in Case 1: the correlation vanished after an increase to 90 s. The decrease of T_b resulted in decreased correlation.

The Effect of the Length of the Simple Moving Average on the Correlations

The increase of the length of the moving average, m, did not have a major influence on the correlations: the correlations were still detectable if moving averages with $m = 19$ were used for detrending both data sets. By contrast, the decrease of the moving average length to three points seemed to make the correlation surfaces rather random.

9.5.3 Correlation without the Trend Removal

As it has been noted, we do not have clear understanding of the phenomenon being studied. Thus, we cannot blindly rely on the correlation coefficients obtained after the detrending procedure. If the time series are not detrended, the problem is that they are clearly nonstationary and the successive samples are correlated — unless the block length T_b is increased dramatically. The increase of T_b has the drawback of decreasing the sample size, making the results less significant. However, the effective sample size tends to stay quite small

regardless of how the T_b is chosen. The decrease of T_b increases the number of samples that are gained for a given time period. Meanwhile, serial correlations are also increased compensating the change of sample size — the effective sample size is therefore kept about the same.

Hereby, it is only mentioned that in Case 1 both the Pearson and Spearman correlations between the geomagnetic activity and acoustic power in audio range were also found without the trend removal. The correlation in the infrasound range was a bit less distinct than with the trend removal. In Case 2, the infrasound correlation also remained.

The peak of the geomagnetic activity (around 21.30 UT) was studied in [42]. The correlation between geomagnetic activity and acoustic power was performed in a slightly different way (the data was downsampled) but the results obtained with the methods of this thesis are essentially similar. However, the correlations in different frequency ranges of the acoustic signal were not considered in [42]. In this thesis, these correlations were considered visually in subsection 9.5.1, where it was found that the correlation was caused by similarities in geomagnetic activity and infrasound. Depending on the way in which the correlation was performed, the maximum seemed to occur when the geomagnetic data was delayed about 50–90 s. This raises a question as to whether this is in contradiction with the other correlations of the infrasound region, which appeared at delays of about 400 s. One possibility is that there is a mechanism producing infrasound in the lower atmosphere. Nevertheless, since it was noticed that there was no certainty that this event, or part of the event, was not caused by some vehicle, further conclusions are not given.

9.6 Analysis of Electric Field Signals

The major motivation for the study of VLF signals comes from the hypothesis that local fluctuations of electric field could in some manner produce sounds (see Chapter 3). Thus, it is desired that we have a way of measuring these fluctuations.

The VLF data embodies strong peaks caused by lightning occuring in different places around the Earth. Figure 9.22 shows a 1-second extract of a VLF signal (f_s = 44.1 kHz) recorded by the SGO. The lightning peaks are seen quite unmistakably from the figure. We may assume that the possible local electric discharges would similarly cause peaks in the data.

Spectrograms of two simultaneous sets of VLF data recorded on October 1$^{\text{st}}$ 2002 are shown in Figure 9.23. One measurement was conducted in Sodankylä by the SGO and the other was conducted in Fiskars by use of the self-constructed VLF antenna of the measurement system. In the VLF signal provided by the SGO, the VLF radio stations in the upper part of the frequency axis have been removed by low-pass filtering. The signal recorded by

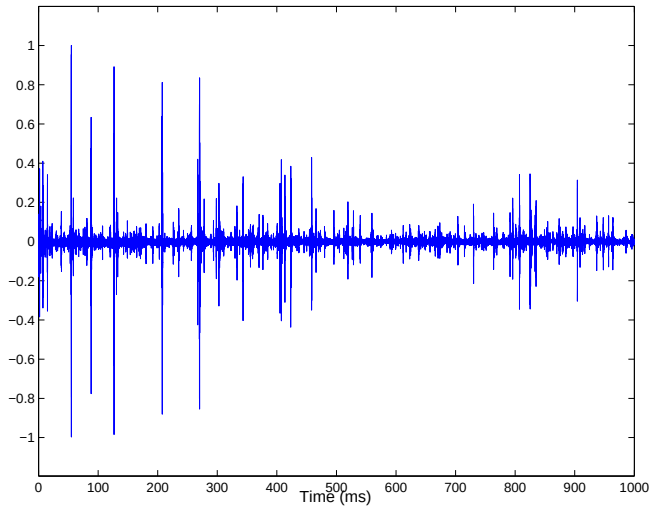

Figure 9.22: A sample of a VLF signal recorded by the SGO.

the self-constructed VLF antenna has a smaller amount of peaks, indicating it is somewhat less sensitive.

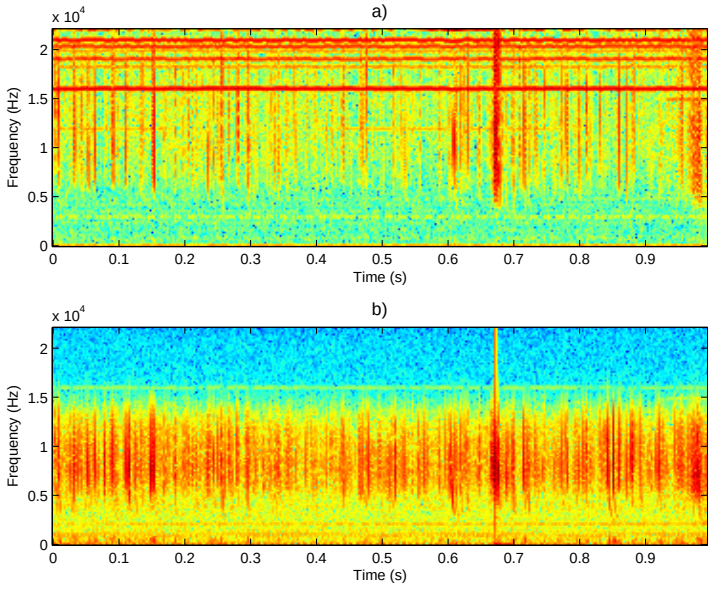

Figure 9.23: An example of spectrograms of VLF signals recorded simultaneously by a) the VLF antenna of the measurement set up, and by the b) SGO .

In order to find indications of local electric discharges, two VLF data may be compared. Some work has already been done on this topic. The hypothesis is: By comparing VLF data sets recorded in locations far enough from each other, events that exist in both data

sets can be classified as “global”, and events that exist only in one of the data as “local”, for the respective data. Thus, it may be assumed that the peaks found in both data sets are global lightning peaks and the peaks found only in one data set are local peaks, potentially corresponding to local electric discharges.

After this procedure it may be studied whether there is a connection between the local peaks of the VLF data and acoustic data. A positive link between these two data would then speak for electric discharge theories.

It was originally intended to pay more attention to the study of VLF signals. However, the analyses of the acoustic and geomagnetic data turned out to require more work than it was expected. The extent of the thesis would have been too large if the VLF data had been analyzed in the same scope. Hereby, we only conclude that the measurement set up has proven appropriate for storing VLF signals, and that attention needs to be paid to the aurora related VLF effects in the future work.

Chapter 10

Conclusions and Future Work

The observational reports collected by Silverman and Tuan [62] and the SGO reveal that quite similar sound effects have been perceived independently of the place of observation and the cultural background and gender of the observer. The observational material supports the reality of auroral sounds. This was also stated by Wang *et al.* [67].

It has sometimes been criticized that many of the aurora related sound reports come from native people who often hold scientifically unfounded beliefs and, thus, could not be reliable. This criticism is in contradiction with the fact that the survival of these people, who spend most of their time outdoors, has always depended on an accurate perception of their environment. In any event, a large number of reports collected by Silverman and Tuan [62] and the SGO come from people whose professional observing skills can in no way be doubted.

The measurement system introduced in this thesis can be used for highly sensitive acoustic measurements. The storage method for electric field signals has also proven competent.

The measurement of aurora related acoustic signals is a difficult process and the success of a measurement depends on many factors. The occurrence of aurora is dependent upon an 11-year long sunspot cycle and the measurements have to be focused on the high-activity point of this cycle.

In the measurement performed on April 11^{th}, 2001, in Koli, a correlation between geomagnetic activity and acoustic power in middle and high frequencies was found with the selected approach. This occured in the geomagnetically most active part of the measurement when the detrended geomagnetic activity was delayed 0–70 s with respect to the detrended acoustic power. The maximum correlation coefficient was 0.39, leading to a coefficient of determination of 15% ($100 \times R^2$). In the infrasound region, there was an increased correlation when the geomagnetic activity was delayed about 380 s. The maximum correlation coefficient obtained was 0.38, leading to a determination of 14%. The infrasound region

correlation was also found in the geomagnetically less active part of the Koli measurement, though the reliability of this result was weaker due to accompanying sound produced by some vehicles. The correlations could not be tracked down to be caused by some known sound source. In addition, they could not be tracked down to some single time period, i.e. there was some stability in the correlations. The correlation found in the infrasound region supports the previous instrumental evidence made by Procunier [54].

The lags at which the correlations were found between the geomagnetic activity and acoustic power of the audio range support the hypotheses that the audible auroral sound is produced relatively close to the ground. However, because of the high absorption of high-frequency sound, it is difficult to interpret all the lags to be directly due to the distance of the sound source. The lag of the infrasound-region correlation is in concordance with the theory that the auroral infrasound is produced at the altitudes of the visual aurora. Although the interpretation of the significance of the results is difficult, the correlation results can be connected, at least to some extent, to a physical model.

Assuming the correlation between the geomagnetic activity and acoustic power truly exists, it is likely that the lag giving the maximum correlation is not stationary in time. This may result in the correlation is not being clearly found at some distinct lag, which makes the interpretation of the results more difficult.

The correlation between the acoustic power in audio frequencies and geomagnetic activity was clearly found only in the geomagnetically most active part of the Koli measurement. Some other measurements with somewhat less geomagnetic activity were also studied but similar correlations were not found. This might suggest that a certain level of geomagnetic activity has to be exceeded before a correlation can exist.

The correlation results should be handled with great care and more study is needed before answers can be given to the primary research problem on the strength of acoustic measurements. Other measurements carried out so far in conditions of high geomagnetic activity should be analyzed more closely. Obviously, even more measurements should be carried out in conditions of high geomagnetic activity and the least amount of ambient noise. However, especially in Southern Finland, it is very difficult to find locations without at least some vehicle traffic noise.

Future work might include automatic detection of potential aurora related sound events. The densities of these events per time unit could then be correlated with geomagnetic activity. Some preliminary work has been done with this by detecting the time indices where the sound power exceeds some threshold level in the high-frequency part of the spectra. These analyses have not been considered in this thesis.

The study of electric field signals has been given less attention. Since some hypotheses, such as brush discharges, suggest that aurora related sounds are produced by electric

discharges, attention needs to be paid to the study of electric field signals. Connections between electric field and acoustic signals should be studied. Furthermore, connections between geomagnetic activity and electric field signals should be considered.

In this thesis, and in the previous work at HUT, geomagnetic data has been used to measure auroral activity. It should be noted that there is no certainty that we have used the appropriate data for the study, or that we have studied the data in the right form. Almost all observations state that there has been a connection between the visual movements of the aurora and the sounds. This suggests that the keogram data (auroral camera) should be reviewed alongside the geomagnetic data. However, this has the difficulty that the optical data is impacted by disturbances such as fog and clouds. Additionally, in terms of computation, the interpretation of optical data is not as straighforward as geomagnetic data.

The measurement set up has had only one microphone to date. This does not enable the determination of the direction of the received sound. Future work might include the use of a microphone antenna which would make directional assessment possible. However, considering the expenses, this may be difficult.

Bibliography

[1] Auroral Acoustics. http://www.acoustics.hut.fi/projects/aurora/index.html.

[2] Answers.com, May 2005. http://www.answers.com/.

[3] Auroras Now!, January 2005. http://aurora.fmi.fi/public_service/.

[4] Christopher Balch. Space Environment Topic, Relationship between Kp and the Aurora, November 2004. http://www.sec.noaa.gov/info/kp-aurora.html.

[5] Christopher Balch. The K-index, November 2004. http://www.sec.noaa.gov/info/Kindex.html.

[6] H. E. Bass, L. C. Sutherland, and A. J. Zuckerwar. Atmospheric Absorption of Sound: Update. *J. of the Acoustical Society of America*, 88(4):2020, October 1990.

[7] C. S. Beals. Audibility of the Aurora and Its Appearance at Low Atmospheric Levels. *Quart. J. Roy. Meteor. Soc.*, 59:71–78, 1933.

[8] C. S. Beals. Low Auroras and Terrestrial Discharges. *Nature*, 132:245, August 1933.

[9] C. S. Beals. The Audibility of the Aurora and Its Appearance at Low Atmospheric Levels. *J. Roy. Astron. Soc. Can.*, 27:184–200, 1933.

[10] Bill Beaty. Taos Hum Homepage, August 2004. http://www.eskimo.com/ billb/hum/hum.html.

[11] The Bible Online, December 2004. http://bible.com/.

[12] James V. Bradley. *Distribution-Free Statistical Tests*. Prentice Hall, Englewood Cliffs, New Jersey, 1968.

[13] Asgeir Brekke and Alv Egeland. *The Northern Light — From Mythology to Space Research*. Springer-Verlag, Berlin Heidelberg, 1983.

[14] W. H. Campbell and J. M. Young. Auroral-Zone Observations of Infrasonic Pressure Waves Related to Ionospheric Disturbances and Geomagnetic Activity. *J. of Geophysical Research*, 68(21):5909–5916, November 1963.

[15] C. A. Chant. Audibility of the Aurora. *J. Roy. Astron. Soc. Can.*, 23:43–44, 1931.

[16] Larry Combs and Rodney Viereck. Space Environment Topic, Aurora, 1996. http://www.sec.noaa.gov/info/Aurora.pdf.

[17] Richard E. Cytowic. Synesthesia: Phenomenology And Neuropsychology, A Review of Current Knowledge. *Psyche*, 2(10), July 1995. http://psyche.cs.monash.edu.au/v2/psyche-2-10-cytowic.html.

[18] D. R. Dawdy and N. C. Matalas. Statistical and Probability Analysis of Hydrologic Data, Part III. Analysis of Variance, Covariance, and Time Series. In Ven Te Chow, editor, *Handbook of Applied Hydrology, A Compendium of Water-Resources Technology*, pages 8.68–8.90. McGraw-Hill, New York, NY, 1964.

[19] John Dawes. The Hum, August 2004. http://homepages.tesco.net/ John.Dawes2/.

[20] Robert H. Eather. *Majestetic Lights — The Aurora in Science, History, and the Arts*. American Geophysical Union, 1980.

[21] European Space Agency (ESA). Coronal Mass Ejections (CMEs), May 2005. http://www.esa-spaceweather.net/spweather/BACKGROUND/PHYS_PROC/SOLAR/cme.html.

[22] Harald Falck-Ytter. *Aurora — The Northern Lights in Mythology, History and Science*. Floris Books, Glasgow, 1999.

[23] Homepage of Finnish Meteorological Institute, November 2004. http://www.fmi.fi/en/index.html.

[24] Allan H. Frey. Human Auditory System Response to Modulated Electromagnetic Energy. *J. Appl. Physiol.*, 17(4):689–692, 1962.

[25] David M. Green and Dennis McFadden. Introduction. In *Encyclopedia of Acoustics*, volume 3, chapter 114, pages 1421–1425. Wiley & Sons, 1997.

[26] W. Lawrence Gulick, George A. Gescheider, and Robert D. Frisina. *Hearing — Physiological acoustics, neural coding, and psychoacoustics*. Oxford University Press, New York, NY, 1989.

[27] Fredric J. Harris. On the Use of Windows for Harmonic Analysis with the Discrete Fourier Transform. In *Proceedings of the IEEE*, volume 66, pages 51–58, January 1978.

[28] Gary Heckman. Space Environment Topic, Solar Maximum, 1999. http://www.sec.noaa.gov/info/SolarMax.pdf.

[29] Matti Karjalainen. *Kommunikaatioakustiikka*. Otamedia Oy, Espoo, Finland, 1999.

[30] Colin S. L. Keay. C.A. Chant and the Mystery of Auroral Sounds. *J. Roy. Astron. Soc. Can.*, 84(6):373–382, December 1990.

[31] Colin S. L. Keay. Electrophonic Sound from Large Meteor Fireballs. *Meteoritics*, 27(2):144–148, June 1992.

[32] Colin S. L. Keay. Audible Fireballs and Geophysical Electrophonics. In *Proc. of Astronomical Society of Australia*, volume 11, pages 12–15, April 1994.

[33] Colin S. L. Keay. Continued Progress in Electrophonic Fireball Investigations. *Earth, Moon, and Planets*, 68:361–368, 1995.

[34] Colin S. L. Keay and Patricia M. Oswald. A Laboratory Test of the Production of Electrophonic Sounds. *J. of the Acoustical Society of America*, 89(4):1823–2824, 1991.

[35] Maurice G. Kendall. *Rank Correlation Methods*. Charles Griffin & Company Limited, London, third edition, 1962.

[36] Maurice G. Kendall. *Time-Series*. Charles Griffin & Company Limited, London, 1973.

[37] Antti Kero. Aine revontuliin liittyvien ääni-ilmiöiden kuulijahavainnoista (An Essay on Aurora Related Sound Reports). University of Oulu, 2003.

[38] W. F. King. Audibility of the Aurora. *J. Roy. Astron. Soc. Can.*, 1:193–194, 1907.

[39] Vern O. Knudsen. The Propagation of Sound in the Atmosphere — Attenuation and Fluctuations. *J. of the Acoustical Society of America*, 18(1):90–96, July 1946.

[40] U. K. Laine. Revontuliäänten taltioinnista ja analyyseistä (On the Recording and Analysis of Auroral Sounds). In *Akustiikkapäivät 8.-9.2001, Espoo*, 2001. http://www.acoustics.hut.fi/asf/publicat/akup01/sivut_119_122.pdf. In Finnish.

[41] U. K. Laine. Denoising and Analysis of Audio Recordings Made during the April 6–7 2000 Geomagnetic Storm by Using a Non-Professional *Ad Hoc* Setup. In *Proc. of Joint Baltic-Nordic Acoustics Meeting 2004*, Mariehamn, Åland, June 2004.

[42] U. K. Laine, E. Turunen, J. Manninen, and H. Nevanlinna. Measurement and Analysis of Sounds During Active Aurorae in Finland 2000–2001. In *URSI General Assembly, Maastricht, the Netherlands August 17–24*, 2002.

[43] U. K. Laine, E. Turunen, and H. Nevanlinna. Revontuliäänet, havaintoja ja mittauksia (Auroral Sounds, Measurements and Analyses). In *XX Geofysiikan päivät 15.–16.5.2001, Helsinki*, pages 101–106, 2001. In Finnish.

[44] J. S. Lamancusa. Outdoor Sound Propagation, May 2000. http://www.mne.psu.edu/lamancusa/me458/10_osp.pdf.

[45] Donald L. Lamar and Mary F. Romig. Anomalous Sounds and Electromagnetic Effects Associated with Fireball Entry. *Meteoritics*, 2(2):127–136, February 1963.

[46] R. S. Little. An Investigation of Acoustic Properties of Parabolic Reflectors, 1963. http://home.att.net/ rsl/APPR2.htm.

[47] R. S. Little. Acoustic Properties of Parabolic Reflectors. *Bio-Acoustics Bulletin*, 4(1):1–3, 1964. http://home.att.net/ rsl/APPR1.htm.

[48] L. H. Martin, R. A. Helliwell, and K. R. Marks. Association Between Aurorae and Very Low-Frequency Hiss Observed At Byrd Station, Antarctica. *Nature*, 187(4739):751–753, 1960.

[49] J. S. Milton and Jesse C. Arnold. *Introduction to Probability and Statistics — Principles and Applications for Engineering and the Computing Sciences*. McGraw-Hill International Editions, New York, NY, 1990.

[50] Sanjit K. Mitra. *Digital Signal Processing — A Computer-Based Approach*. McGraw-Hill, New York, NY, second edition, 2001.

[51] University of Oulu. Space Physics Textbook, November 1998. http://www.oulu.fi/ spaceweb/textbook/.

[52] Donald E. Olson. The Evidence for Auroral Effects on Atmospheric Electricity. *Pure Appl. Geophys.*, 84:118–138, 1971.

[53] Barbara Poppe. A Primer on Space Weather, May 2005. http://www.sec.noaa.gov/primer/primer.html.

[54] R. W. Procunier. Observations of Acoustic Aurora in the 1–16 Hz Range. *Geophys. J. astr. Soc.*, 26:183–189, 1971.

[55] R. W. Procunier and G. W. Sharp. Optimum Frequency for Detection of Acoustic Sources in the Upper Atmosphere. *J. of the Acoustical Society of America*, 49(3):622–626, 1971.

[56] Brüel & Kjær. Battery Driven Power Supply — Type 2804, October 2004. http://www.bksv.com/pdf/Bp0218.pdf.

[57] Brüel & Kjær. Condenser Microphone — Type 4179, Microphone Preamplifier — Type 2660; System for Very-Low-Level Sound Measurements, October 2004. http://www.bksv.com/pdf/Bp0389.pdf.

[58] Uno Ingård. A Review on the Influence of Meteorological Conditions on Sound Propagation. *J. of the Acoustical Society of America*, 25(3), May 1953.

[59] Søren Buus. Auditory Masking. In *Encyclopedia of Acoustics*, volume 3, chapter 115, pages 1427–1445. Wiley & Sons, 1997.

[60] T. S. Jørgensen and E. Ungstrup. Direct Observation of Correlation between Aurorae And Hiss in Greenland. *Nature*, 194(4827):462–463, 1963.

[61] Charles F. Roos. Annual Survey of Statistical Techniques: The Correlation and Analysis of Time Series — Part II. *Econometrica*, 4(4):368–381, October 1936.

[62] S. M. Silverman and T. U. Tuan. Auroral Audibility. In *Adv. Geophysics*, volume 16, pages 155–266. 1973.

[63] David W. Stockburger. Introductory Statistics: Concepts, Models, and Applications, 1996. http://www.psychstat.smsu.edu/introbook/sbk00.htm.

[64] Louis C. Sutherland and Gilles A. Daigle. Atmospheric Sound Propagation. In *Encyclopedia of Acoustics*, volume 1, chapter 32, pages 341–364. Wiley & Sons, 1997.

[65] S. Tromholt. Norwegian Testimony of the Auroral Sounds. *Nature*, 32:499, 1885.

[66] Esa Turunen. Personal communication. SGO.

[67] D. Y. Wang, T. F. Tuan, and S. M. Silverman. A Note on Anomalous Sounds from Meteor Fireballs and Aurorae. *J. Roy. Astron. Soc. Can.*, 78(4):145–149, 1984.

[68] Charles R. Wilson. Infrasonic Pressure Waves from the Aurora: a Shock Wave Model. *Nature*, 216:131–133, 1967.

[69] Charles R. Wilson. Auroral Infrasonic Waves. *J. of Geophysical Research, Space Physics*, 74(7):1812–1836, April 1969.

[70] William A. Yost and Mead C. Killion. Hearing Thresholds. In *Encyclopedia of Acoustics*, volume 3, chapter 123, pages 1545–1554. Wiley & Sons, 1997.

Appendix A

Some Descriptions of Aurora Related Sounds

Some descriptions of aurora related sounds reported in the survey of SGO are given in the following list [66]:

- sound of an electric power house
- hissing noise
- popping sound
- like the whirring of a cannon-shot
- sound of an electric line
- music produced when the strings of a harp are lightly touched
- like the distant stroke of an axe
- loud claps
- swishing noise
- crackling noise
- like a field of ice crackling
- rustling noise
- rumbling noise of distant thunder
- like the brushing/rustling of silk

- like the waving of a large flag in the wind
- sound of welding

Appendix B

1/3-Octave Bands

Table B.1: The Frequency Limits of 1/3-Octave Bands.

nominal center frequency, Hz	upper boundary frequency, Hz
–	4.45
5	5.61
6.3	7.10
8	8.94
10	11.18
12.5	14.14
16	17.89
20	22.36
25	28.06
31.5	35.50
40	44.72
50	56.12
63	70.99
80	89.44
100	111.8
125	141.4
160	178.9
200	223.6
250	280.6
315	355.0
400	447.2
500	561.2
630	710.0

continued on next page

continued from previous page

nominal center frequency, Hz	upper boundary frequency, Hz
800	894.4
1 k	1118
1.25 k	1414
1.6 k	1789
2 k	2236
2.5 k	2806
3.15 k	3550
4 k	4472
5 k	5612
6.3 k	7099
8 k	8944
10 k	11180
12.5 k	14143
16 k	17889
20 k	22449

Appendix C

Correlation Coefficients

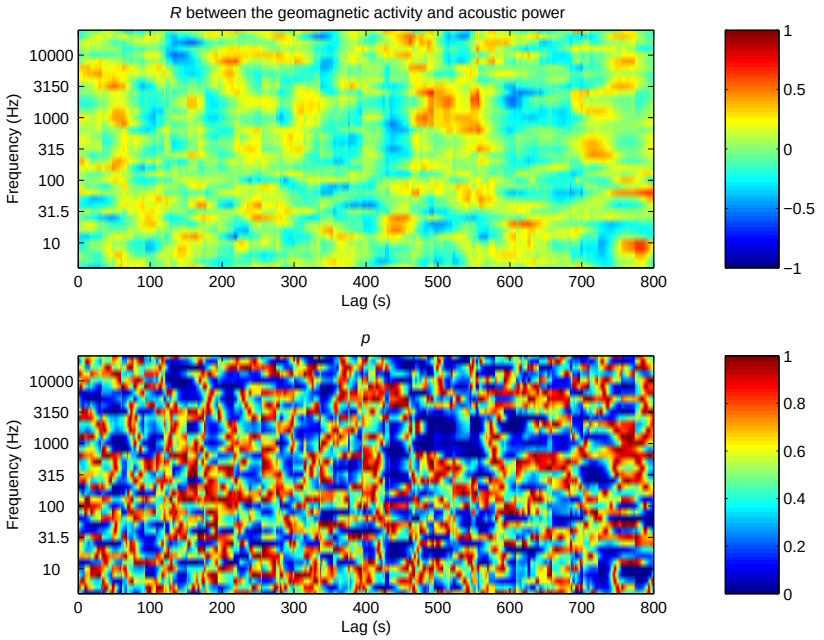

Figure C.1: Top: The Pearson correlation coefficients between geomagnetic activity and acoustic power of the Koli measurement between 21.45 and 22.20 UT. Bottom: The corresponding P values. The block length was $T_b = 60$ s. Both the geomagnetic and acoustic data have been detrended with a simple moving average of five points.

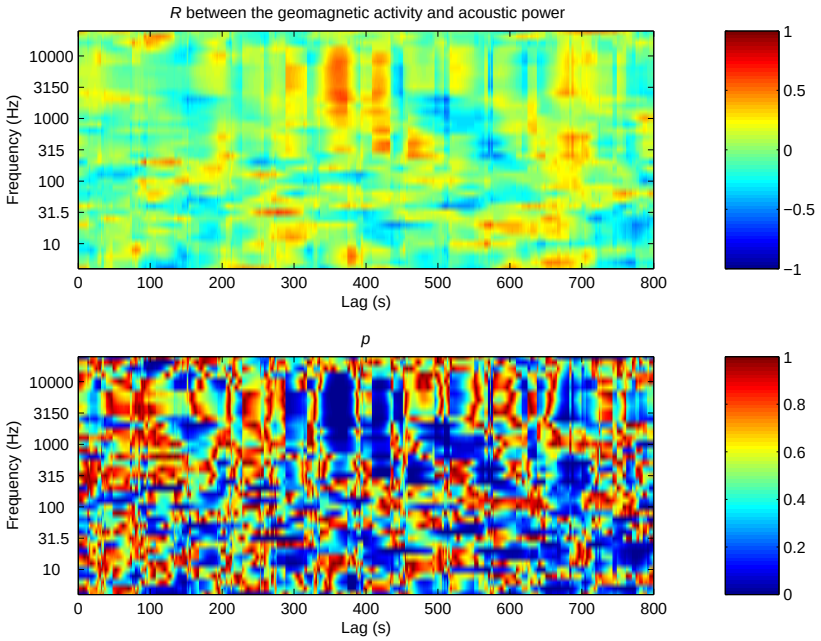

Figure C.2: 22.20–22.55 UT.

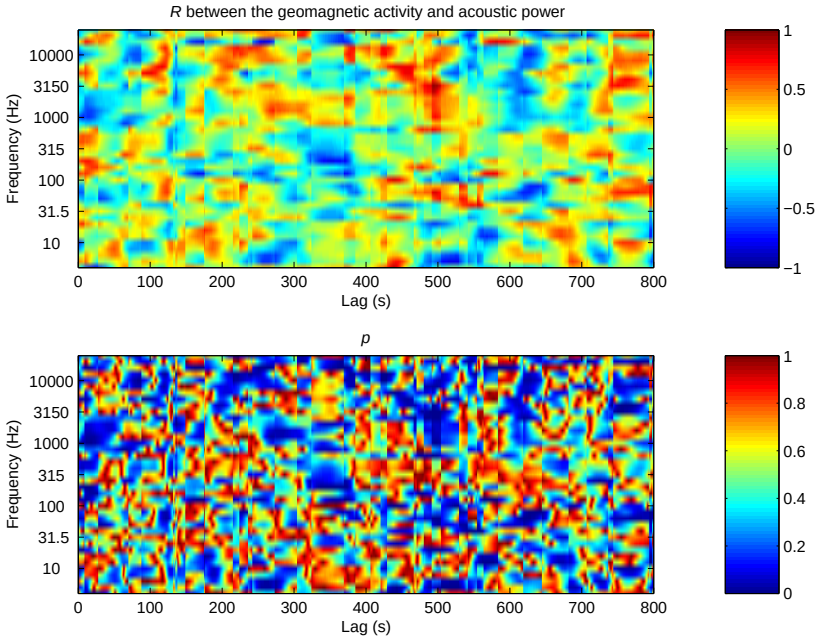

Figure C.3: 21.45–21.58 UT.

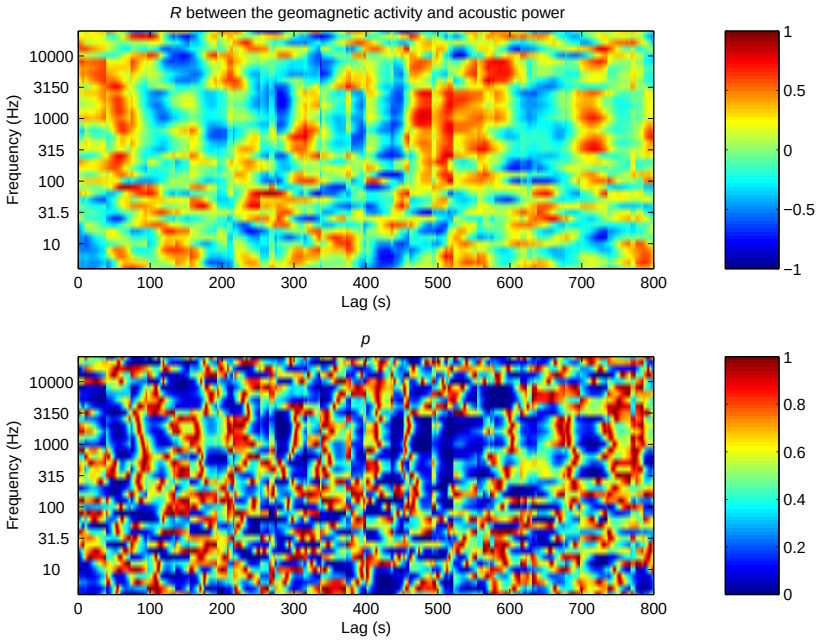

Figure C.4: 22.01–22.15 UT.

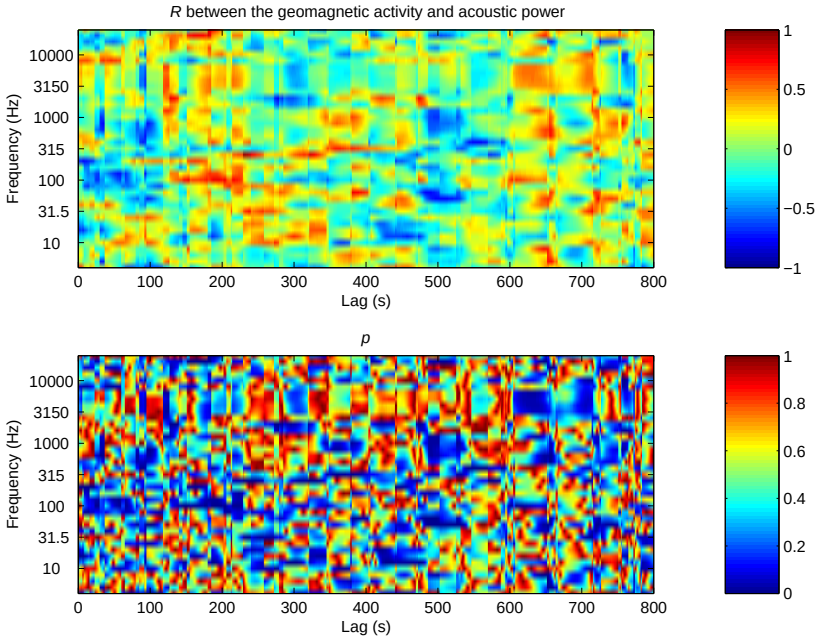

Figure C.5: 22.15–22.30 UT.

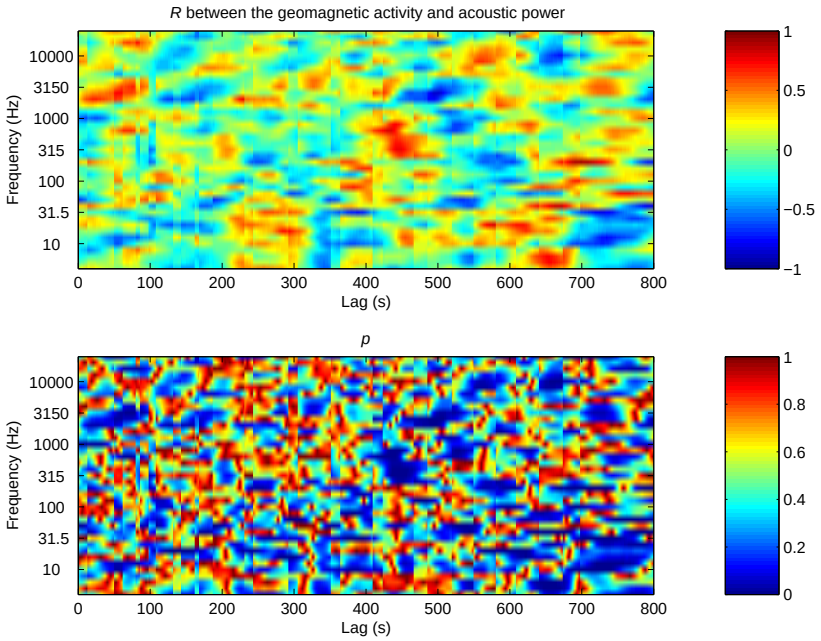

Figure C.6: 22.30–22.45 UT.

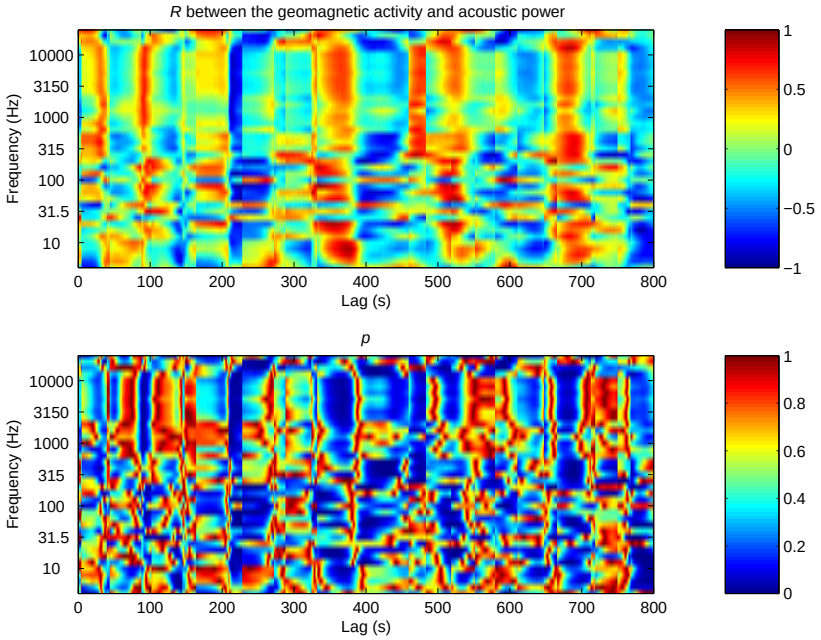

Figure C.7: 22.45–22.55 UT.

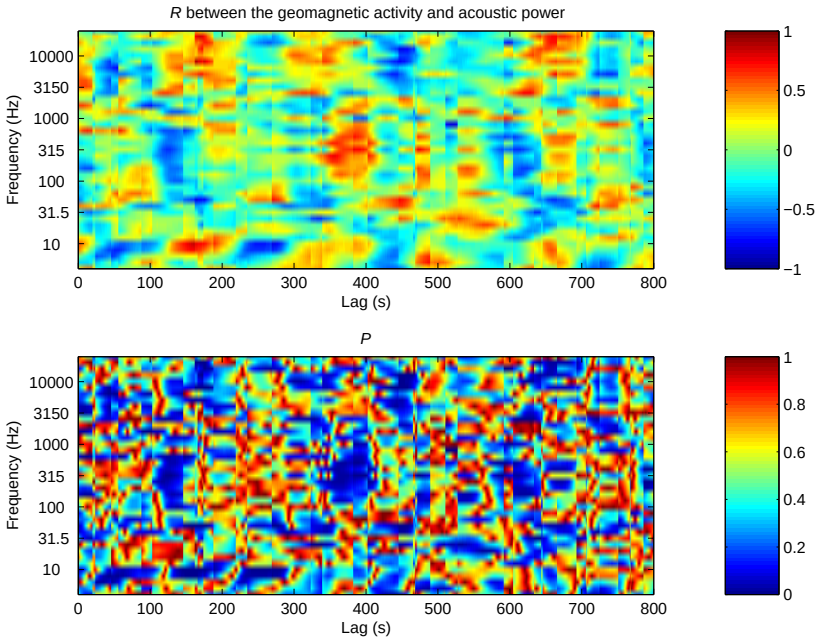

Figure C.8: 19.00–19.15 UT.

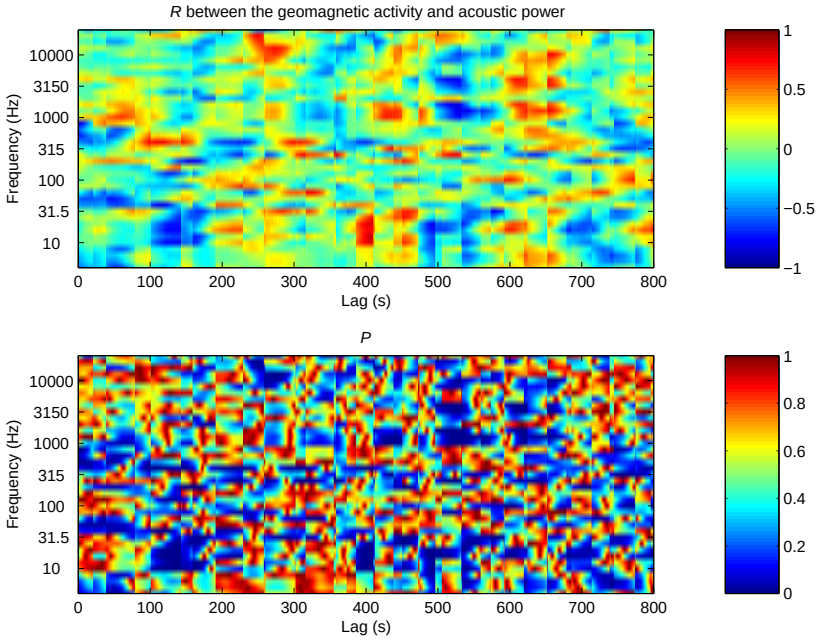

Figure C.9: 19.15–19.30 UT.

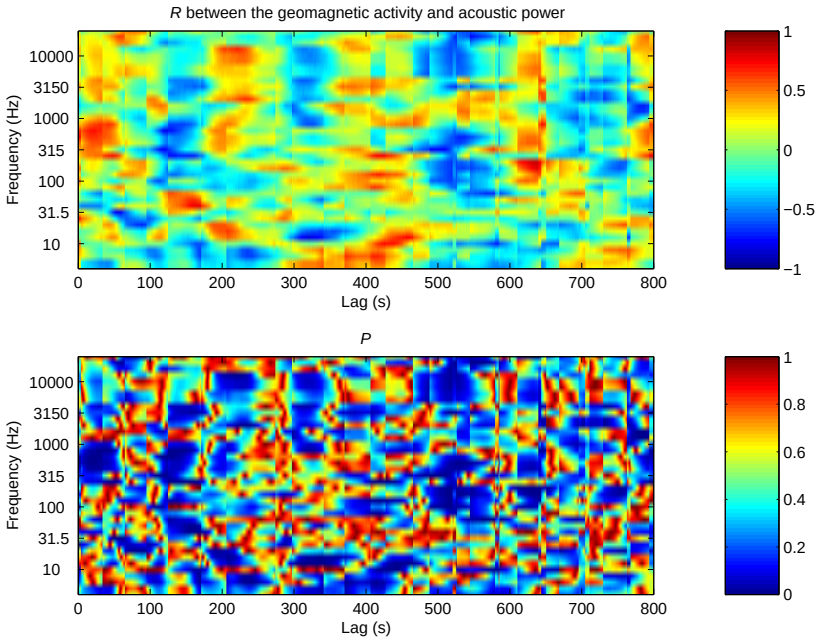

Figure C.10: 19.30–19.45 UT.

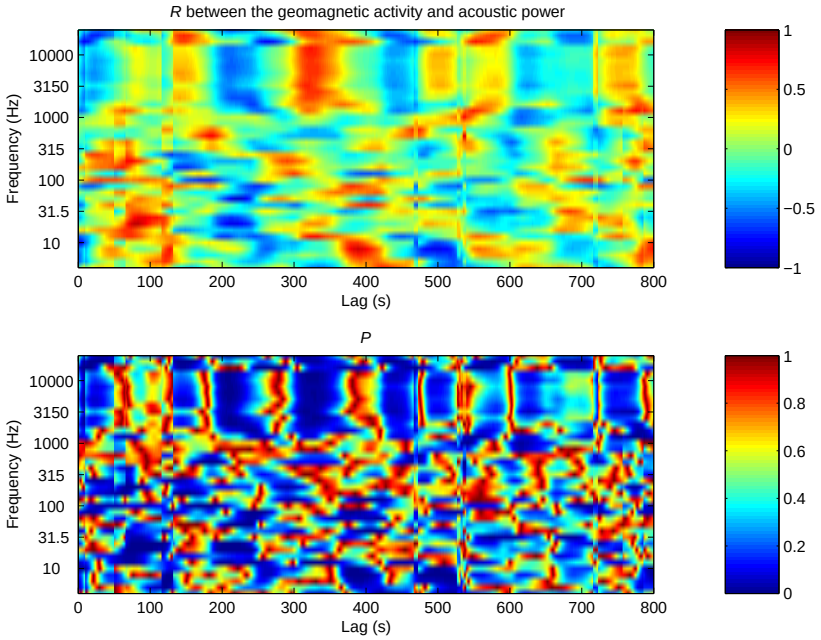

Figure C.11: 19.45–20.00 UT.

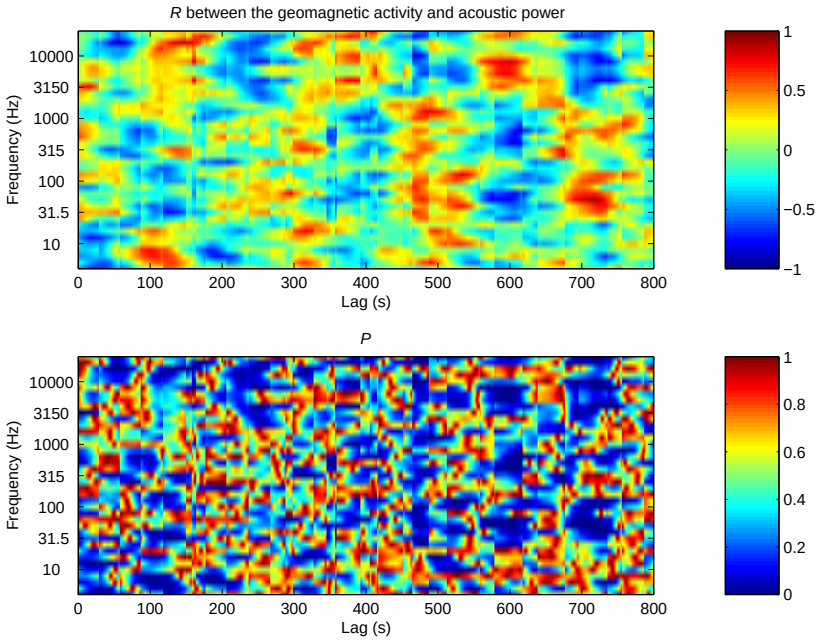

Figure C.12: 20.00–20.15 UT.

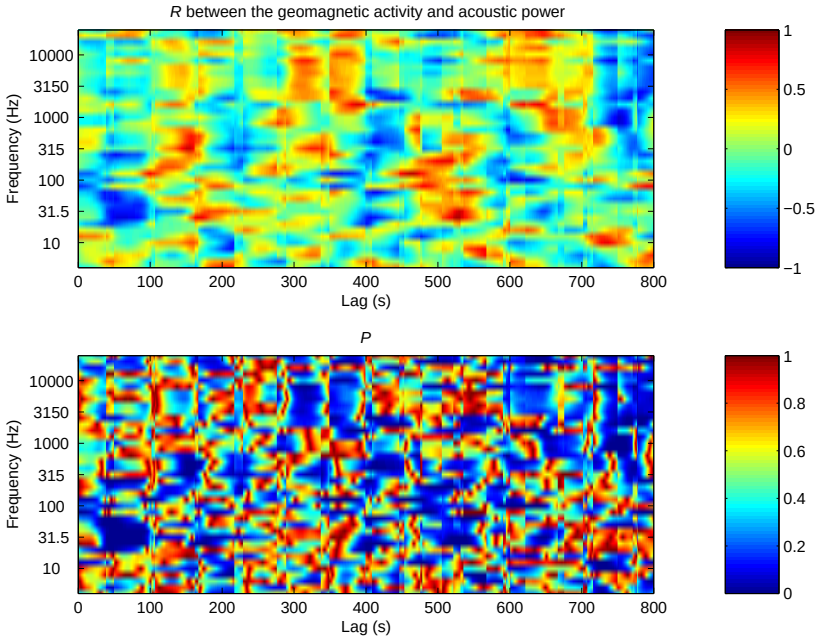

Figure C.13: 20.15–20.30 UT.

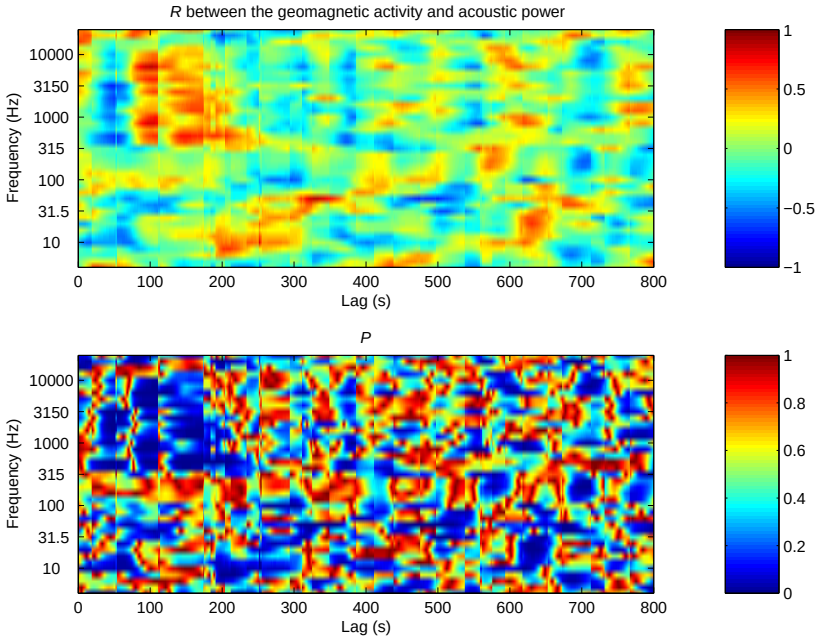

Figure C.14: 20.30–20.50 UT.